

GLOBAL JOURNAL

OF RESEARCHES IN ENGINEERING: F

Electrical and Electronic Engineering

Slot-loaded Microstrip

Green Improving by Autonomous

Highlights

DFIG based Wind Generator

RPAS Communication in Clusters

Discovering Thoughts, Inventing Future

VOLUME 18

ISSUE 1

VERSION 1.0



GLOBAL JOURNAL OF RESEARCHES IN ENGINEERING: F
ELECTRICAL AND ELECTRONICS ENGINEERING



GLOBAL JOURNAL OF RESEARCHES IN ENGINEERING: F
ELECTRICAL AND ELECTRONICS ENGINEERING

VOLUME 18 ISSUE 1 (VER. 1.0)

OPEN ASSOCIATION OF RESEARCH SOCIETY

© Global Journal of
Researches in Engineering.
2018.

All rights reserved.

This is a special issue published in version 1.0
of "Global Journal of Researches in
Engineering." By Global Journals Inc.

All articles are open access articles distributed
under "Global Journal of Researches in
Engineering"

Reading License, which permits restricted use.
Entire contents are copyright by of "Global
Journal of Researches in Engineering" unless
otherwise noted on specific articles.

No part of this publication may be reproduced
or transmitted in any form or by any means,
electronic or mechanical, including
photocopy, recording, or any information
storage and retrieval system, without written
permission.

The opinions and statements made in this
book are those of the authors concerned.
Ultrapublishing has not verified and neither
confirms nor denies any of the foregoing and
no warranty or fitness is implied.

Engage with the contents herein at your own
risk.

The use of this journal, and the terms and
conditions for our providing information, is
governed by our Disclaimer, Terms and
Conditions and Privacy Policy given on our
website [http://globaljournals.us/terms-and-condition/
menu-id-1463/](http://globaljournals.us/terms-and-condition/menu-id-1463/).

By referring / using / reading / any type of
association / referencing this journal, this
signifies and you acknowledge that you have
read them and that you accept and will be
bound by the terms thereof.

All information, journals, this journal,
activities undertaken, materials, services and
our website, terms and conditions, privacy
policy, and this journal is subject to change
anytime without any prior notice.

Incorporation No.: 0423089
License No.: 42125/022010/1186
Registration No.: 430374
Import-Export Code: 1109007027
Employer Identification Number (EIN):
USA Tax ID: 98-0673427

Global Journals Inc.

(A Delaware USA Incorporation with "Good Standing"; Reg. Number: 0423089)

Sponsors: *Open Association of Research Society*
Open Scientific Standards

Publisher's Headquarters office

Global Journals® Headquarters
945th Concord Streets,
Framingham Massachusetts Pin: 01701,
United States of America

USA Toll Free: +001-888-839-7392
USA Toll Free Fax: +001-888-839-7392

Offset Typesetting

Global Journals Incorporated
2nd, Lansdowne, Lansdowne Rd., Croydon-Surrey,
Pin: CR9 2ER, United Kingdom

Packaging & Continental Dispatching

Global Journals Pvt Ltd
E-3130 Sudama Nagar, Near Gopur Square,
Indore, M.P., Pin:452009, India

Find a correspondence nodal officer near you

To find nodal officer of your country, please
email us at local@globaljournals.org

eContacts

Press Inquiries: press@globaljournals.org
Investor Inquiries: investors@globaljournals.org
Technical Support: technology@globaljournals.org
Media & Releases: media@globaljournals.org

Pricing (Excluding Air Parcel Charges):

Yearly Subscription (Personal & Institutional)
250 USD (B/W) & 350 USD (Color)

EDITORIAL BOARD

GLOBAL JOURNAL OF RESEARCH IN ENGINEERING

Dr. Ren-Jye Dzung

Professor
Civil Engineering
National Chiao-Tung University
Taiwan
Dean of General Affairs
Ph.D., Civil & Environmental Engineering
University of Michigan, USA

Dr. Eric M. Lui

Ph.D.,
Structural Engineering
Department of Civil
& Environmental Engineering
Syracuse University, USA

Dr. Ephraim Suhir

Ph.D., Dept. of Mechanics and Mathematics,
Moscow University
Moscow, Russia
Bell Laboratories
Physical Sciences and
Engineering Research Division, USA

Dr. Zhou Yufeng

Ph.D. Mechanical Engineering & Materials Science,
Duke University, US
Assistant Professor College of Engineering,
Nanyang Technological University, Singapore

Dr. Pangil Choi

Ph.D.
Department of Civil, Environmental, and Construction
Engineering
Texas Tech University, US

Dr. Pallav Purohit

Ph.D. Energy Policy and Planning
Indian Institute of Technology (IIT), Delhi
Research Scientist,
International Institute for Applied Systems Analysis
(IIASA), Austria

Dr. Iman Hajirasouliha

Ph.D. in Structural Engineering
Associate Professor,
Department of Civil and Structural Engineering,
University of Sheffield, UK

Dr. Zi Chen

Ph.D. Department of Mechanical & Aerospace
Engineering,
Princeton University, US
Assistant Professor, Thayer School of Engineering,
Dartmouth College, Hanover, US

Dr. Wenfang Xie

Ph.D., Department of Electrical Engineering,
Hong Kong Polytechnic University,
Department of Automatic Control,
Beijing University of Aeronautics and Astronautics, China

Dr. Giacomo Risitano,

Ph.D., Industrial Engineering at University of Perugia
(Italy)
"Automotive Design" at Engineering Department of
Messina University (Messina) Italy.

Dr. Joaquim Carneiro

Ph.D. in Mechanical Engineering,
Faculty of Engineering,
University of Porto(FEUP),
University of Minho,
Department of Physics, Portugal

Dr. Hai-Wen Li

Ph.D., Materials Engineering
Kyushu University
Fukuoka
Guest Professor at Aarhus University, Japan

Dr. Wei-Hsin Chen

Ph.D., National Cheng Kung University
Department of Aeronautics
and Astronautics, Taiwan

Dr. Saeed Chehreh Chelgani

Ph.D. in Mineral Processing
University of Western Ontario,
Adjunct professor,
Mining engineering and Mineral processing
University of Michigan

Belen Riveiro

Ph.D.,
School of Industrial Engineering
University of Vigo, Spain

Dr. Bin Chen

B.Sc., M.Sc., Ph.D., Xi'an Jiaotong University, China.
State Key Laboratory of Multiphase Flow in Power
Engineering
Xi'an Jiaotong University, China

Dr. Maurizio Palesi

Ph.D. in Computer Engineering,
University of Catania
Faculty of Engineering and Architecture
Italy

Dr. Cesar M. A. Vasques

Ph.D., Mechanical Engineering
Department of Mechanical Engineering
School of Engineering, Polytechnic of Porto
Porto, Portugal

Dr. Stefano Invernizzi

Ph.D. in Structural Engineering
Technical University of Turin,
Department of Structural,
Geotechnical and Building Engineering, Italy

Dr. T.S. Jang

Ph.D. Naval Architecture and Ocean Engineering
Seoul National University, Korea
Director, Arctic Engineering Research Center,
The Korea Ship and Offshore Research Institute,
Pusan National University, South Korea

Dr. Jun Wang

Ph.D. in Architecture, University of Hong Kong, China
Urban Studies
City University of Hong Kong, China

Dr. Salvatore Brischetto

Ph.D. in Aerospace Engineering, Polytechnic University of
Turin and
in Mechanics, Paris West University Nanterre La Défense
Department of Mechanical and Aerospace Engineering,
Polytechnic University of Turin, Italy

Dr. Francesco Tornabene

Ph.D. in Structural Mechanics, University of Bologna
Professor Department of Civil, Chemical, Environmental
and Materials Engineering
University of Bologna, Italy

Dr. Togay Ozbakkaloglu

B.Sc. in Civil Engineering
Ph.D. in Structural Engineering, University of Ottawa,
Canada
Senior Lecturer University of Adelaide, Australia

Dr. Paolo Veronesi

Ph.D., Materials Engineering
Institute of Electronics, Italy
President of the master Degree in Materials Engineering
Dept. of Engineering, Italy

Dr. Maria Daniela

Ph.D. in Aerospace Science and Technologies
Second University of Naples
Research Fellow University of Naples "Federico II", Italy

Dr. Charles-Darwin Annan

Ph.D.,
Professor Civil and Water Engineering University Laval,
Canada

Dr. Stefano Mariani

Associate Professor
Structural Mechanics
Department of Civil
and Environmental Engineering,
Ph.D., in Structural Engineering
Polytechnic University of Milan, Italy

Dr. Wesam S. Alaloul

B.Sc., M.Sc.,
Ph.D. in Civil and Environmental Engineering,
University Technology Petronas, Malaysia

Dr. Sofoklis S. Makridis

B.Sc(Hons), M.Eng, Ph.D.
Professor Department of Mechanical Engineering
University of Western Macedonia, Greece

Dr. Ananda Kumar Palaniappan

B.Sc., MBA, MED, Ph.D. in Civil and Environmental
Engineering,
Ph.D. University of Malaya, Malaysia
University of Malaya, Malaysia

Dr. Zhen Yuan

B.E., Ph.D. in Mechanical Engineering
University of Sciences and Technology of China, China
Professor, Faculty of Health Sciences, University of Macau,
China

Dr. Hugo Silva

Associate Professor
University of Minho
Department of Civil Engineering
Ph.D., Civil Engineering
University of Minho, Portugal

Dr. Jui-Sheng Chou

Ph.D. University of Texas at Austin, U.S.A.
Department of Civil and Construction Engineering
National Taiwan University of Science and Technology
(Taiwan Tech)

Dr. Shaoping Xiao

BS, MS
Ph.D. Mechanical Engineering, Northwestern University
The University of Iowa
Department of Mechanical and Industrial Engineering
Center for Computer-Aided Design

Dr. Vladimir Gurao

Associate Professor
Ph.D. in Mechanical /
Aerospace Engineering
University of Miami
Engineering Technology

Dr. Adel Al Jumaily

Ph.D. Electrical Engineering (AI)
Faculty of Engineering and IT
University of Technology, Sydney

Dr. A. Stegou-Sagia

Ph.D. Mechanical Engineering, Environmental
Engineering School of Mechanical Engineering
National Technical University of Athens

Dr. Jalal Kafashan

Mechanical Engineering
Division of Mechatronics
KU Leuven, BELGIUM

Dr. Fausto Gallucci

Associate Professor
Chemical Process Intensification (SPI)
Faculty of Chemical
Engineering and Chemistry
Assistant Editor
International J. Hydrogen Energy, Netherlands

Prof. (LU) Prof. (UoS) Dr. Miklas Scholz

Cand Ing, BEng (equiv), PgC, MSc, Ph.D., CWEM, CEnv,
CSci, CEng,
FHEA, FIEMA, FCIWEM, FICE, Fellow of IWA,
VINNOVA Fellow, Marie Curie Senior Fellow,
Chair in Civil Engineering (UoS)
Wetland systems, sustainable drainage, and water quality

Dr. Houfa Shen

Ph.D. Manufacturing Engineering, Mechanical Engineering,
Structural Engineering
Department of Mechanical Engineering
Tsinghua University, China

Dr. Kitipong Jaojaruek

B. Eng, M. Eng
D. Eng (Energy Technology, Asian Institute of
Technology).
Kasetsart University Kamphaeng Saen (KPS) Campus
Energy Research Laboratory of Mechanical Engineering

Dr. Haijian Shi

Ph.D. Civil Engineering
Structural Engineering
Oakland, CA, United States

Dr. Omid Gohardani

Ph.D. Senior Aerospace/Mechanical/
Aeronautical Engineering professional
M.Sc. Mechanical Engineering
M.Sc. Aeronautical Engineering
B.Sc. Vehicle Engineering
Orange County, California, US

Dr. Maciej Gucma

Asistant Professor, Maritime Univeristy of Szczecin
Szczecin, Poland
Ph.D.. Eng. Master Mariner
Web: www.mendeley.com/profiles/maciej-gucma/

Dr. Ye Tian

Ph.D. Electrical Engineering
The Pennsylvania State University
121 Electrical Engineering East
University Park, PA 16802, US

Dr. Alex W. Dawotola

Hydraulic Engineering Section,
Delft University of Technology,
Stevinweg, Delft, Netherlands

Dr. M. Meguellati

Department of Electronics,
University of Batna, Batna 05000, Algeria

Dr. Burcin Becerik-Gerber

University of Southern Californi
Ph.D. in Civil Engineering
DDes from Harvard University
M.S. from University of California, Berkeley
M.S. from Istanbul Technical University
Web: i-lab.usc.edu

Dr. Balasubramani R

Ph.D., (IT) in Faculty of Engg. & Tech.
Professor & Head, Dept. of ISE at NMAM Institute of
Technology

Dr. Minghua He

Department of Civil Engineering
Tsinghua University
Beijing, 100084, China

Dr. Diego González-Aguilera

Ph.D. Dep. Cartographic and Land Engineering,
University of Salamanca, Ávila, Spain

Dr. Fentahun Moges Kasie

Department of mechanical & Industrial Engineering,
Institute of technology
Hawassa University Hawassa, Ethiopia

Dr. Ciprian LĂPUȘAN

Ph. D in Mechanical Engineering
Technical University of Cluj-Napoca
Cluj-Napoca (Romania)

Dr. Zhibin Lin

Center for Infrastructure Engineering Studies
Missouri University of Science and Technology
ERL, 500 W. 16th St. Rolla,
Missouri 65409, US

Dr. Shun-Chung Lee

Department of Resources Engineering,
National Cheng Kung University, Taiwan

Dr. Philip T Moore

Ph.D., Graduate
Master Supervisor
School of Information
Science and engineering
Lanzhou University, China

Dr. Gordana Colovic

B.Sc Textile Technology, M.Sc. Technical Science
Ph.D. in Industrial management.
The College of Textile – Design, Technology and
Management, Belgrade, Serbia

Dr. Xianbo Zhao

Ph.D. Department of Building,
National University of Singapore, Singapore,
Senior Lecturer, Central Queensland University, Australia

Dr. Chao Wang

Ph.D. in Computational Mechanics
Rosharon, TX,
US

Hiroshi Sekimoto

Professor Emeritus
Tokyo Institute of Technology, Japan
Ph.D., University of California, Berkeley

Dr. Steffen Lehmann

Faculty of Creative and
Cultural Industries
PhD, AA Dip
University of Portsmouth, UK

Dr. Yudong Zhang

B.S., M.S., Ph.D. Signal and Information Processing,
Southeast University
Professor School of Information Science and Technology at
Nanjing Normal University, China

Dr. Philip G. Moscoso

Technology and Operations Management
IESE Business School, University of Navarra
Ph.D in Industrial Engineering and Management, ETH
Zurich
M.Sc. in Chemical Engineering, ETH Zurich
Link: [Philip G. Moscoso personal webpage](#)

Dr. Sam-Ang Keo

Materials and Structural Engineering, Non-Destructive
Testing (NDT), Infrared Thermography, Mechanic of
Materials, Finite Element Method, Thermal, Laser,
Microwave, Signal Processing

CONTENTS OF THE ISSUE

- i. Copyright Notice
 - ii. Editorial Board Members
 - iii. Chief Author and Dean
 - iv. Contents of the Issue
-
1. The Issue of Control Cables Selection for HEMP-Protected Electric Facilities. *1-4*
 2. Nonlinearities Impact on Satellite RPAS Communication in Cluters. *5-12*
 3. Review on Characteristic Modeling of Electric Arc Furnace and its Effects. *13-21*
 4. Resonance Characteristics Enhancement of Slot-loaded Microstrip Patch Antenna for GPS Application. *23-29*
 5. Design and Manufacturing of an Array an Single Microstrip Patch Antenna to Transmit and Receive by using Same Patch Shape. *31-38*
 6. Transient Stability Enhancement of DFIG based Wind Generator by Switching Frequency Control Strategy with Parallel Resonance Fault Current Limiter. *39-48*
 7. Green Improving by Autonomous PV Mini-Grid Model in Central Myanmar. *49-64*
-
- v. Fellows
 - vi. Auxiliary Memberships
 - vii. Preferred Author Guidelines
 - viii. Index



GLOBAL JOURNAL OF RESEARCHES IN ENGINEERING: F
ELECTRICAL AND ELECTRONICS ENGINEERING
Volume 18 Issue 1 Version 1.0 Year 2018
Type: Double Blind Peer Reviewed International Research Journal
Publisher: Global Journals
Online ISSN: 2249-4596 & Print ISSN: 0975-5861

The Issue of Control Cables Selection for HEMP-Protected Electric Facilities

By Vladimir Gurevich

Abstract- The article addresses two methods of evaluation of control cables for electric utilities that need to be protected from High Altitude Electromagnetic Pulse (HEMP): the first, based on accurate measurements of the cable's shielding effectiveness using special equipment; and the second, based on information about the cables' design and marking given in this article. A conclusion is made that the second method does not require significant investments in special equipment and allows evaluation and correct choice of a cable.

Keywords: HEMP, control cables, screening effectiveness.

GJRE-F Classification: FOR Code: 290901



Strictly as per the compliance and regulations of:



© 2018. Vladimir Gurevich. This is a research/review paper, distributed under the terms of the Creative Commons Attribution-Noncommercial 3.0 Unported License <http://creativecommons.org/licenses/by-nc/3.0/>, permitting all non commercial use, distribution, and reproduction in any medium, provided the original work is properly cited.

The Issue of Control Cables Selection for HEMP-Protected Electric Facilities

Vladimir Gurevich

Abstract- The article addresses two methods of evaluation of control cables for electric utilities that need to be protected from High Altitude Electromagnetic Pulse (HEMP): the first, based on accurate measurements of the cable's shielding effectiveness using special equipment; and the second, based on information about the cables' design and marking given in this article. A conclusion is made that the second method does not require significant investments in special equipment and allows evaluation and correct choice of a cable.

Keywords: HEMP, control cables, screening effectiveness.

I. INTRODUCTION

Protection of electronic equipment of control, automation, and relay protection, installed at electric power facilities from an electromagnetic pulse of high altitude (30 - 400 km) nuclear explosion (HEMP), which creates electric field density about 50 kV/m at the ground surface, has recently become very relevant. Nowadays, there are technical solutions including special shielded cabinets, filters, arresters, etc., which provide HEMP protection for highly sensitive electronic equipment of power plants and substations, [1, 2]. However, local protection of this equipment at a level of an individual cabinet or even a room is facing a serious problem, evolving in wasted efforts. This this problem is called control cables. They run over long distances and act as huge antennas absorbing HEMP energy from a large area and deliver it to an interior space of protected rooms and cabinets, directly to inputs of sensitive electronic equipment. Thus, only exceptional cables should be used for HEMP-protected facilities, as otherwise all the efforts will be wasted.

II. DESIGN AND FEATURES OF SHIELDED CONTROL CABLES

The fact that low-voltage low-frequency control cables used in this application (also preferable power cables) should be shielded is obvious and does not require additional explanations. Indeed, there are various designs of shielded cables and not all of them provide the best protection against HEMP. So, it is appropriate to address different designs of low-voltage shielded cables and their features.

But first of all it should be noted that there are two kinds of screens used for shielding of cables:

1. *Foil:* screens made of thin (30 - 100 μm) copper or aluminum foil or made of metal-coated (usually aluminum) plastic strip – single strip wrapped around the cable, or consisting of several separate overlaying strips.
2. *Braid:* screens made of interlaced (usually in the way of a “French braid”) thin copper (usually tinned) wires, which look like a solid flexible hose, put onto a cable, Fig. 1. This screen is much thicker than that made of foil.

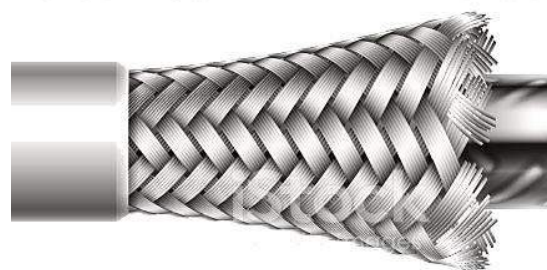


Fig. 1: A braided screen of a cable – “French braid”.

The specifications of these two kinds of screens are different, Fig. 2.

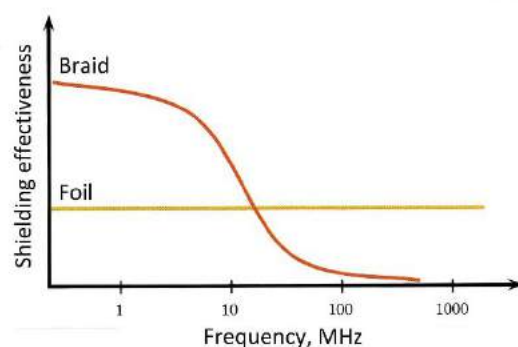


Fig. 2: Shielding effectiveness of two kinds of screens.

For example, a foil screen will hardly be efficient at low frequencies as electromagnetic wave penetrates much deeper into metal than the foil thickness. Whereas at higher frequencies, foil screens are much more effective than braid screens, as the surface resistance of the latter is too high for high frequency.

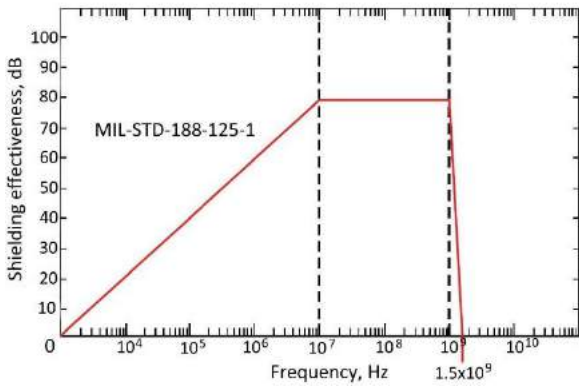


Fig. 3: Required shielding effectiveness of HEMP-protected equipment according to MIL-STD-188-125-1 [3].

Since STD-188-125-1 [3] (Fig. 3) requires effective shielding of HEMP-protected equipment in a quite broad range of frequencies, it is obvious that none of the above-mentioned kinds of screens meets these requirements.

Fortunately, there are many compound screens, which combine advantages of both types (Fig. 4).

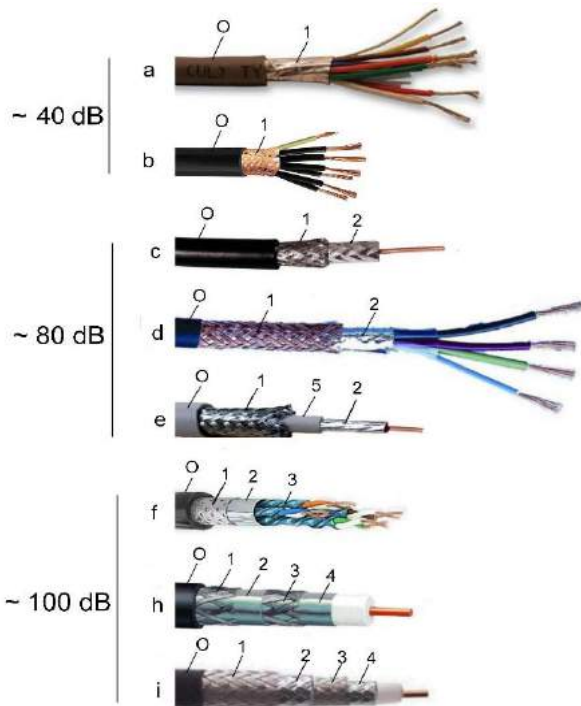


Fig. 4: Different designs of shielded low-voltage cables and approximate averaged and generalized values of shielding effectiveness.

a, b – with a single-layer screen (1); c, d, e – with double-layer compound screen: with foil (2) and braid (1); f – with triple-layer and (h) – with four-layer compound screens; i - with four-layer braid; 0 – outer casing of a cable, 5 – internal inter-screen insulation.

Apart from design differences, they also differ in the way of placement of individual insulated cores inside the cable, as this can also affect the cable's protection from electromagnetic interference.



Fig. 5: Shielded control cable with twisted pairs.

To enhance protection, individual pairs of cables are twisted with each other many times along the whole length of the cable (Fig. 5).

The above-mentioned design features of cables are often reflected in their marking:

- UTP - Unshielded Twisted Pair;
- F (Foiled) – a cable with common outer foil screen;
- F/UTP (Foiled/ Unshielded Twisted Pair) – a cable with common outer foil screen and unshielded twisted pairs;
- FTP (Foiled Twisted Pair) – a cable without outer screen, but with foiled twisted pair;
- U/FTP (Unshielded overall/ Foiled Twisted Pair) – same as above;
- STP (Shielded Twisted Pair) – a cable without the outer screen, but with braid shielded twisted pairs;
- S/FTP (Screened overall/ Foiled Twisted Pair) – a cable with common outer braid screen and with twisted pairs with individual foiled screens;
- F/FTP (Foiled/ Foiled Twisted Pair) – a cable with common outer foiled screen and with twisted pairs with individual foiled screens;
- SF/FTP (Screened Foiled/ Foiled Twisted Pair) – a cable with a double screen (braid + foil) and with foiled twisted pairs.
- SF/UTP (Screened Foiled/Unshielded Twisted Pair) – a cable with a double outer screen (braid + foil) and with unshielded twisted pairs.
- SF (Screened Foiled) same as above.

Other designs are very rare; they do not control cables, but rather coaxial high-frequency cables.

There are two other design features of shielded control cables, applying to the quality of the outer braid, which can be more or less filling (Fig. 6).



Fig. 6: Outer cable braids with different filling thickness (in percent).

Apparently, the higher the braid thickness, the better the shielding capacity. The maximum thickness of braid filling is 95%.

The second design feature of the braid is related to its surface resistance: the lower the resistance, the higher the shielding capacity. This is the reason why high-quality braids are made of tinned copper, which is distinguished (tin color) from non-tinned copper (copper color).

Due to high diversity of designs and because different types of cables are used at electric power facilities, a question arises if shielding effectiveness can be measured.

III. MEASURING SHIELDING EFFECTIVENESS OF CONTROL CABLES

The method of measurement of shielding effectiveness is described in IEC 62153-4-4 [4]. It is based on measuring the correlation between the power of a high-frequency signal delivered from an external generator to a conductive core of a cable, and the power of a signal emitted from the outer surface of the cable's screen to a special enclosed chamber.

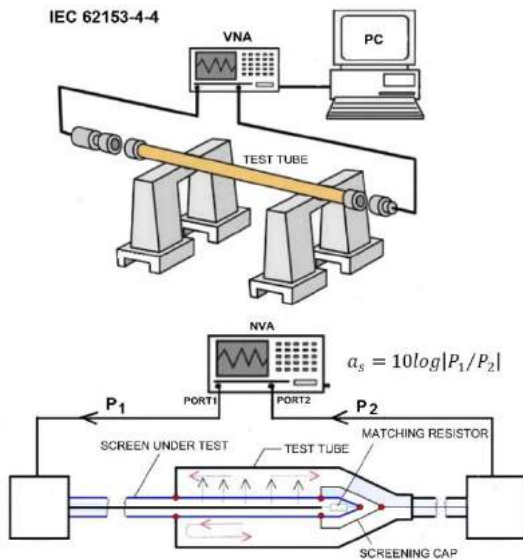


Fig. 7: Layout for testing effectiveness of cable shielding according to IEC 62153-4-4 standard.

The Vector Network Analyzer (VNA), which consists of a high-frequency signal generator (port 1) and a receiver (port 2) of a signal weakened by the screen, is very convenient to measure the correlation between delivered (on to a cable) and measured emitted signals (Fig. 7).

The cost of one of the cheapest VNAs (type Planar TR 1300/1) which works with an external PC (it is

necessary to work both with VNA and with special software calculating attenuation caused by the cable's screen based on data transferred from VNA) is \$ 2,900.

Based on the layout of the testing bench shown in Figure 7 (indeed, this is a metal tube with two special locks and connectors at both ends), its cost should not be significant.



Fig. 8: A kit of testing tubes (type CoMeT 90/1) with a kit of locks and connectors manufactured by the Bedea (Rosenberger) company to test cable shielding effectiveness with an outside diameter from 6 through 22 millimeters.

But the reality turned out to be different. A kit of tubes of various lengths, along with a kit of connectors (Fig. 8) and PC software to calculate attenuation imposed by the screen is sold at \$ 20,000. Apparently, this high cost results from the lack of competitors in the market, as this measuring kit is manufactured exclusively by the Bedea company (Germany) in cooperation with the Rosenberger company (also Germany). There is something similar promoted by the Japanese company Keycom (SEM03 trademark), but they don't reply to requests for information regarding this equipment.

Thus, the total price of the testing kit (with VNA and PC) makes the feasibility of this purchase very questionable. Is it so important to know the effectiveness of cable shielding, provided that the standard measuring method and the formulas used for it stipulate testing of a symmetric coaxial cable with a single conductive core with one screen? What will be the accuracy of measurement of a compound cable, which contains the screens of twisted pairs in addition to the outer screen?

Thus, considering all the above mentioned would suggest to use an approximate estimating of cable shielding efficiency based on cable designs and their features described earlier.

IV. CHOOSING OF CONTROL CABLES

It is obvious that facilities being designed should employ exceptionally new cables with double (at least) shielding capacity, such as *S/FTP*, *SF/FTP*, *SF/UTP* or *SF* with the filling thickness of outer braid (compulsory tinned!) of not less than 85%. Cables of such kind are manufactured by many large companies, such as Belden, Hosiwell, DDA, Helukabel, Elettrotekkabel, Huanghe Cable Group and many others. In addition to that, many cable companies offer customized cable production. If it was impossible to pick up a cable from one of the manufacturers mentioned above (with the required section and the number of cores), it is possible to have this cable individually produced.

For old facilities with existing old cables that are not planned to be replaced, the approximate estimating of shielding effectiveness of these old cables can be taken into account. This estimation may be based on the above-mentioned criteria (for critical sites with critical equipment only). Additional protection means will be planned, taking into consideration the estimation of existing shielding effectiveness of these cables.

At the same time, it is unacceptable to use both protected and unprotected cables connected to different input terminals of the same piece of equipment or lead into the same control cabinet.

Another important parameter, which is not connected with shielding effectiveness, but which is one of the important indicators of the cable's reliability, (needs to be considered during cable selection) is the electric strength of the cable's insulation. For HEMP-protected electric facilities, insulation of a cable should sustain one-minute test voltage of not less than 2 kV AC between conductive cores, and between them and the common outer screen. As a rule, this insulation sustains short pulses of less than 1 μ sec and the amplitude of up to 8 kV (such as HEMP's pulse) without any damage.

According to IEC 61000-4-25 [5] requirements, a pulse voltage of this amplitude should be used for testing equipment located inside ordinary reinforced concrete production facilities upon HEMP impact.

V. CONCLUSION

Use of shielded control cables in electric units, which need to be protected from HEMP, is very

important. Due to a high diversity of shielded cables available in the market, the problem of proper cable selection becomes very relevant. The choice can be based either on accurate measurements of shielding effectiveness of various cable samples, (use of special measurement tools) or an approximate evaluation based on information regarding unique features of different cable designs. Due to the high cost of tools and devices measuring shielding effectiveness and imperfect correspondence of the standard measurement method to some important cable designs, the second method of evaluation is preferable. Information regarding shielded cables' designs, their features, marking and estimated screens' efficiency provided in this article allows a customer to browse through the diversity of types and kinds of control cables available in the market and to make a correct choice.

REFERENCES RÉFÉRENCES REFERENCIAS

1. Gurevich V. *Cyber and Electromagnetic Threats in Modern Relay Protection.*– Taylor & Francis Group, Boca Raton, 2015, 205 p.
2. Gurevich V. *Protection of Substation Critical Equipment against Intentional Electromagnetic Threats.* – Wiley, London, 2017, 240 pp.
3. MIL-STD-188-125-1 High-Altitude Electromagnetic Pulse (HEMP) Protection for Ground Based C41 Facilities Performing Critical. Time-Urgent Mission. Part 1 Fixed Facilities, 2005.
4. IEC 62153-4-4 Metallic communication cable test methods–Part 4-4: Electromagnetic compatibility (EMC)– Shielded screening attenuation, test method for measuring of the screening attenuation as up to and above 3 GHz.
5. IEC 61000-4-25 Electromagnetic compatibility (EMC) - Part 4-25: Testing and measurement techniques - HEMP immunity test methods for equipment and systems.



GLOBAL JOURNAL OF RESEARCHES IN ENGINEERING: F
ELECTRICAL AND ELECTRONICS ENGINEERING
Volume 18 Issue 1 Version 1.0 Year 2018
Type: Double Blind Peer Reviewed International Research Journal
Publisher: Global Journals
Online ISSN: 2249-4596 & Print ISSN: 0975-5861

Nonlinearities Impact on Satellite RPAS Communication in Clusters

By A. Grekhov, V. Kondratiuk & S. Ilnytska

National Aviation University

Abstract- For modeling of data transmission from Remotely Piloted Air System (RPAS) clusters (or swarms), the original models of communication channels with Radio Line of Sight (RLOS) and Beyond Radio Line of Sight (BRLOS) were built using MATLAB Simulink. Models comprise of “Base Station Transmitter”; RLOS channel: “Uplink Path”, “RPAS Receiver”; BRLOS channel: “Uplink Path”, “Satellite Transponder”, “Downlink Path”; “RPAS Receiver”. Dependences of the Bit Error Rate (BER) on the Signal-to-Noise Ratio (SNR) for different levels of the Base Station (BS) transmitter nonlinearity, its gain, the BS antenna and Satellite Transponder antennas diameters were received.

Keywords: *RPAS clusters, swarms, satellite links, data transmission; transmitter nonlinearity.*

GJRE-F Classification: *FOR Code: 100508*



Strictly as per the compliance and regulations of:



Nonlinearities Impact on Satellite RPAS Communication in Clusters

A. Grekhov^α, V. Kondratiuk^σ & S. Ilnytska^ρ

Abstract- For modeling of data transmission from Remotely Piloted Air System (RPAS) clusters (or swarms), the original models of communication channels with Radio Line of Sight (RLOS) and Beyond Radio Line of Sight (BRLOS) were built using MATLAB Simulink. Models comprise of "Base Station Transmitter"; RLOS channel: "Uplink Path", "RPAS Receiver"; BRLOS channel: "Uplink Path", "Satellite Transponder", "Downlink Path"; "RPAS Receiver". Dependences of the Bit Error Rate (BER) on the Signal-to-Noise Ratio (SNR) for different levels of the Base Station (BS) transmitter nonlinearity, its gain, the BS antenna and Satellite Transponder antennas diameters were received.

Keywords: RPAS clusters, swarms, satellite links, data transmission; transmitter nonlinearity.

I. PROBLEM STATEMENT

The importance of Remotely Piloted Air Systems (RPASs) or Unmanned Aerial Vehicles (UAVs) networks is continuously growing, as they are new technologies for civilian and military purposes. Common use of RPASs is carried out by state bodies, police, transport management systems, medical personnel and used to warn about natural disasters and to promote the acceleration of rescue operations in absence of public communication networks. Military use of RPAS consists of border surveillance, reconnaissance, and strikes [1].

The Federal Aviation Administration guidelines allow the use of RPAS up to 4.4 pounds within the operator's visibility during the day at heights of up to 400 feet above ground in Class G airspace and beyond 5 miles from any airport[2].

RPAS technologies are improving and expanding the amount of memory, onboard data processing capabilities, information storage and communication. For widespread use in commercial, military, civil, agricultural and environmental purposes, RPASs should be able effectively to communicate with each other and with existing network infrastructures[3].

The registered number of RPASs in use in the U.S. exceed 200 thousand just in the first 20 days of January 2016 [4]. However, the deployment of a considerable number of RPASs leads to substantial problems. It is necessary to ensure collision-free and

seamless operation of RPASs in the conventional airspace to maintain standard levels of safety.

In the review[5] RPAS's classification, possible cluster architectures, RPAS-based services, obstacle detection techniques, RPAS's networks, RPAS equipment, data collection methods, communication technologies, processing of collected data, use of clouds for computational unloading of an RPAS resource are considered.

The cluster has several RPASs working synchronously to solve a single task [6]. Swarm Coordination refers to communication with individual RPAS, regardless of the ground control station and information exchange between RPASs. Cluster members report their position and other useful information at predetermined intervals. To ensure such coordination, members of the RPASs swarm should communicate with each other [6]. In the case of a dedicated communication infrastructure, the hive itself establishes and maintains a specific communication network. Communication in the Flying Ad-hoc Network (FANET) includes UAV-UAV (U2U) and UAV-Infrastructure (U2I) communications [1]. Thus, the mobility of nodes is higher than the Mobile Ad-hoc network (MANET) and the Vehicular Ad-hoc network (VANET) [6]. The topology often changes (it requires a peer-to-peer network). The communication range should be bigger than in other systems [7].

Collaborative mission planning for UAV cluster to optimize relay distance is considered in a paper [8]. The concept of RPAS Required Communication Performance Methodology for the Command, Control, and Communication Link is given in [9].

Requirements for RPAS data rate indicated in the NATO standards [10-12].

In connection with the need to evaluate the parameters of aeronautical satellite communication channels, methods have been developed by us that makes it possible to predict the behavior of the communication channel with sufficient accuracy under different conditions.

The original model for Iridium satellite communication channel "Aircraft-Satellite-Ground Station" was built using MATLAB Simulink software [13, 14]. Dependencies of the BER on free space path losses, antennas diameter, phase/frequency offsets, satellite transponder linear gain, aircraft and satellite

Author ^α: Department of Air Navigation Systems.

e-mail: grekhovam@gmail.com

Author ^{σ ρ}: Research Training Center "Aerospace Center" National Aviation University Kyiv, Ukraine.

e-mails: kon_ym@ukr.net, ilnytskasv84@gmail.com

transponder high power amplifier back off level, and phase noise were received and analyzed.

Automatic Dependent Surveillance-Broadcast (ADS-B) message traveling time and average downlink utilization for different Iridium link architectures were estimated in the paper [15]. The delay is about 1.4-1.5 seconds, which agrees well with the experimental data recently obtained in the USA and Canada. Dependences of message travelling time on the different number of satellites ($N = 1-10$) for several aircraft ($n = 1-3$) were obtained on the base of original models.

A modeling of "Satellite-to-Aircraft" link for self-separation was provided in an article [16].

A simulation of satellite communication links operation with orthogonal frequency-division multiplexing was done in papers [17-19].

An impact of transmitter nonlinearity on satellite channel parameters was studied in articles [19-21].

Nevertheless, now in the literature, there are no studies devoted to the calculation of satellite communication channels characteristics in RPAS clusters, taking into account the nonlinearities of the transmitter.

II. AIM OF THE WORK

Transmitter nonlinearities are critical for wireless communications systems and have a significant impact on the transmission of RPAS's data.

The purpose of this work is: 1) to build models of RPAS clusters, including both transmission within the Radio Line of Sight (RLOS), and through the satellite using Beyond Radio Line of Sight (BRLOS); 2) to investigate and compare the features of data transmission on both channels; 3) to obtain the dependences of the BER on the SNR for different levels of transmitter nonlinearity of the Base Station (BS), on the BS transmitter gain, on the BS antenna diameter for different levels of the BS transmitter nonlinearity, on the diameter of the satellite transponder antennas.

III. MODELS FOR RPAS COMMUNICATION CHANNELS IN CLUSTERS

Clusters of RPASs can have a wide variety of architecture and organization, depending on the tasks assigned to perform. The main difference is the nature of communication with the BS - RLOS or BRLOS. Figure 1 shows, as an example, a cluster of five RPASs with RLOS and five RPASs with BRLOS communicating with the BS via a satellite.

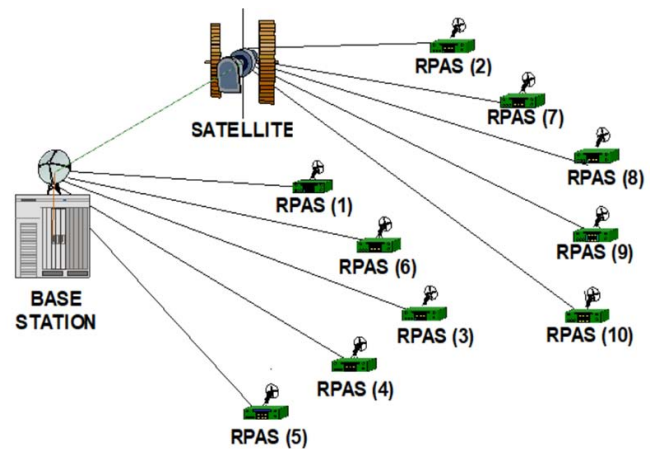


Fig. 1: RPAS Clusters with RLOS and BRLOS

The original models were built, containing up to 30 RPASs with different types of communication channels - Additive White Gaussian Noise (AWGN), Free Space Path Loss, Rician Frequency-Flat and Frequency-Selective Fading. A cycle of calculations with different number of RPASs, different types of modulation (BPSK, QPSK, 16QAM, 64QAM), with and without Doppler shift, is performed.

In this paper, we present only results obtained for QPSK1/2 modulation on the model shown in Fig. 2. This model contains one RPAS with RLOS and one with BRLOS. As our calculations have shown, the addition of any number of RPASs to the base station directly or to the satellite results in the same BER values that are typical for specific type of communication.

A model (Fig. 2) comprises of "Base Station Transmitter" (Bernoulli Random Binary Generator, Convolutional Encoder, QPSK Baseband Modulator, High Power Amplifier with a memoryless nonlinearity, Transmitter Dish Antenna Gain); RLOS channel: "Uplink Path" (AWGN), "RPAS Receiver" (Receiver Dish Antenna Gain, RPAS Receiver System Temperature, Viterbi Decoder), "Error Rate Calculation" block and "Display"; BLOS channel: "Uplink Path" (AWGN), "Satellite Transponder" (Receiver Dish Antenna Gain, Satellite Receiver System Temperature, Complex Baseband Amplifier, Phase Noise, Transmitter Dish Antenna Gain), "Downlink Path" (AWGN); "RPAS Receiver".

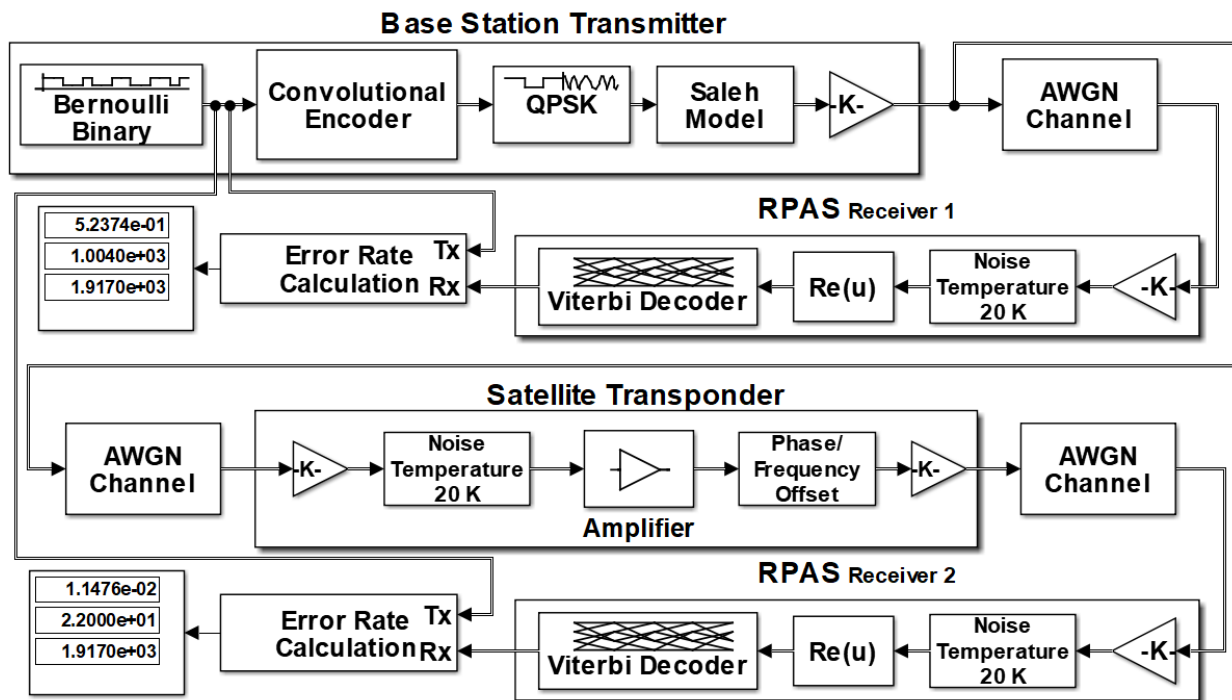


Fig. 2: Communication Links in RPAS Cluster

In the “Base Station Transmitter”, the Bernoulli Binary Generator block generates random binary numbers using a Bernoulli distribution with parameter p , produces “zero” with probability p and “one” with probability $1-p$ (here the value $p=0,5$).

A model employs forward error correction coding in the form of convolutional encoding with Viterbi decoding [22]. A model uses a rate $3/4$, constraint length 7 , ($r=3/4$; $K=7$) convolutional code on both transmission and reception. The Convolutional Encoder block is using the poly2trellis (7 , [171 133], 171) function with a constraint length of 7 , code generator polynomials of 171 and 133 (in octal numbers), and a feedback connection of 171 (in octal). The puncture vector is $[1; 1; 0; 1; 1; 0]$.

The QPSK1/2 Baseband Modulator block modulates a signal using the binary phase shift keying method.

The High Power Amplifier block applies memoryless nonlinearity to a complex baseband signal and provides five different methods for modeling the nonlinearity. In this paper results for Saleh model with standard AM/AM and AM/PM parameters [23] and linear amplifier gain are given. An HPA backoff level determines how close the satellite high power amplifier is to the saturation. When the backoff is 30 dB the average input power is 30 decibels below the input power that causes amplifier saturation and, in this case, AM/AM and AM/PM conversion is negligible. For the backoff ≈ 7 dB - moderate nonlinearity exists and for the backoff ≈ 1 dB - severe nonlinearity takes place.

The Transmitter (Receiver) Dish Antenna Gain block multiplies the input by a constant value (gain). The relationship between the antenna gain and the antenna diameter and the wavelength is the following:

$$G = \eta(\pi D/\lambda)^2,$$

Where η is the antenna efficiency. For calculations (here $\eta = 1$), the following parameters in the model were set up: RPAS antenna gain ≈ 1.55 (an antenna diameter ≈ 0.12 m at 1 GHz), Base Station antenna gain ≈ 7.8 and Satellite Transponder antennas gains ≈ 7.8 (an antenna diameter ≈ 0.28 m at 1 GHz),

In the “Uplink (Downlink) Path” the AWGN block add white Gaussian noise to the input signal.

IV. RPAS COMMUNICATION CHANNELS SIMULATION

From dependences of the BER on the SNR for different levels of BS transmitter nonlinearity (Fig. 3) it follows that, a transmission with increasing nonlinearity requires an increase in the SNR. The transmission of data through the satellite and directly has significant differences (dotted and solid curves). Interestingly, with negligible nonlinearity (crosses) of the BS transmitter amplifier, transmission through the satellite gives fewer errors than for direct transmission. However, with moderate and severe non-linearity, everything happens in reverse. All the graphs have a rapid decline with the growth of the SNR.

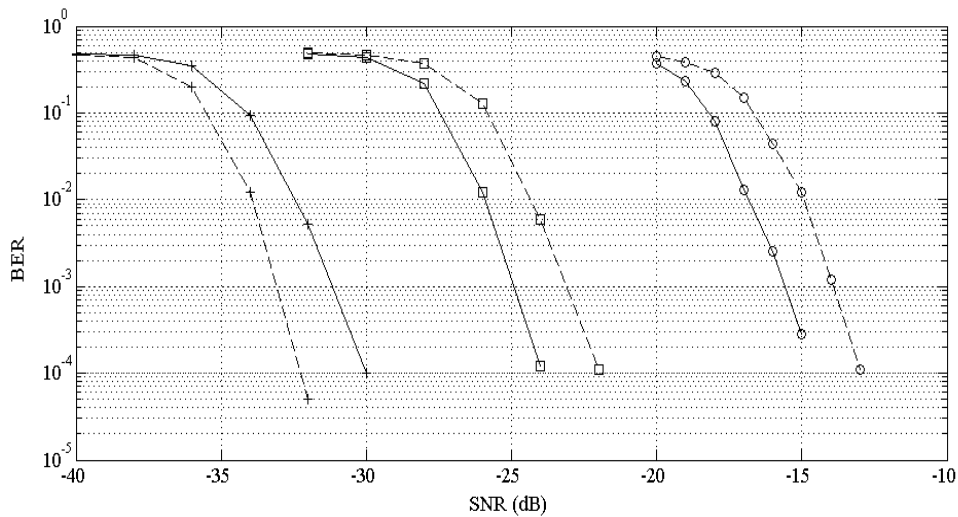


Fig. 3: Dependencies of the BER on the SNR for different levels of BS transmitter nonlinearity: solid lines - RLOS, dashed lines - BRLOS; crosses - negligible nonlinearity, squares - moderate nonlinearity, circles - severe nonlinearity; modulation QPSK1/2; noise temperature 20 K; BS antenna diameter ≈ 0.28 m, satellite transponder antennas diameters ≈ 0.28 m, RPAS antenna diameter ≈ 0.12 m; satellite transponder amplifier linear gain 10 dB

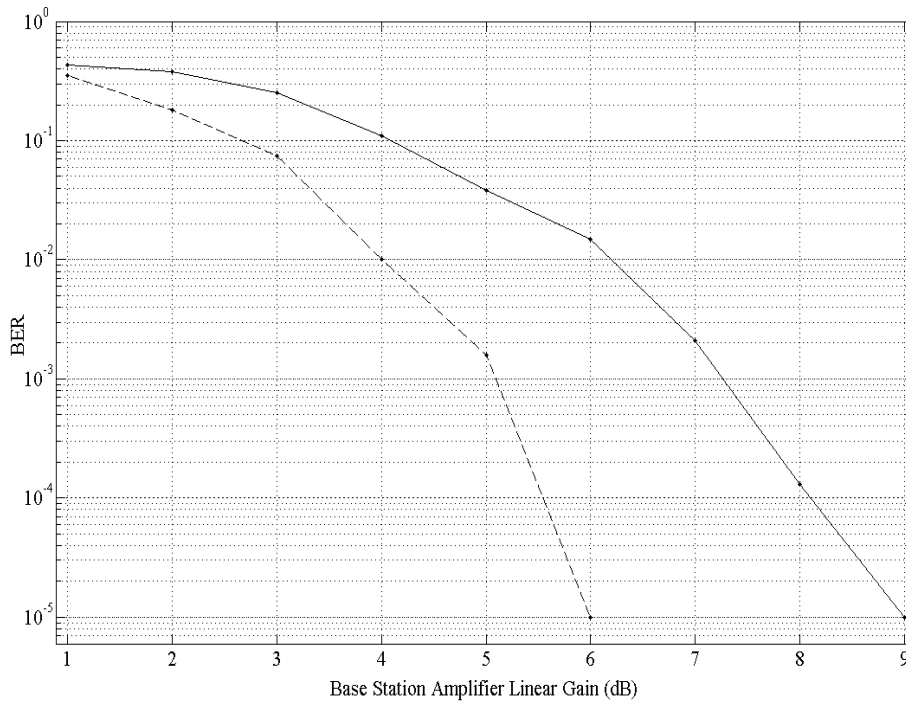


Fig. 4: Dependencies of the BER on the linear gain of BS amplifier linear gain: solid line - RLOS, dashed line - BRLOS; SNR = -20 dB; modulation QPSK1/2; noise temperature 20 K; BS antenna diameter ≈ 0.28 m, satellite transponder antennas diameters ≈ 0.28 m, RPAS antenna diameter ≈ 0.12 m; satellite transponder amplifier linear gain 10 dB

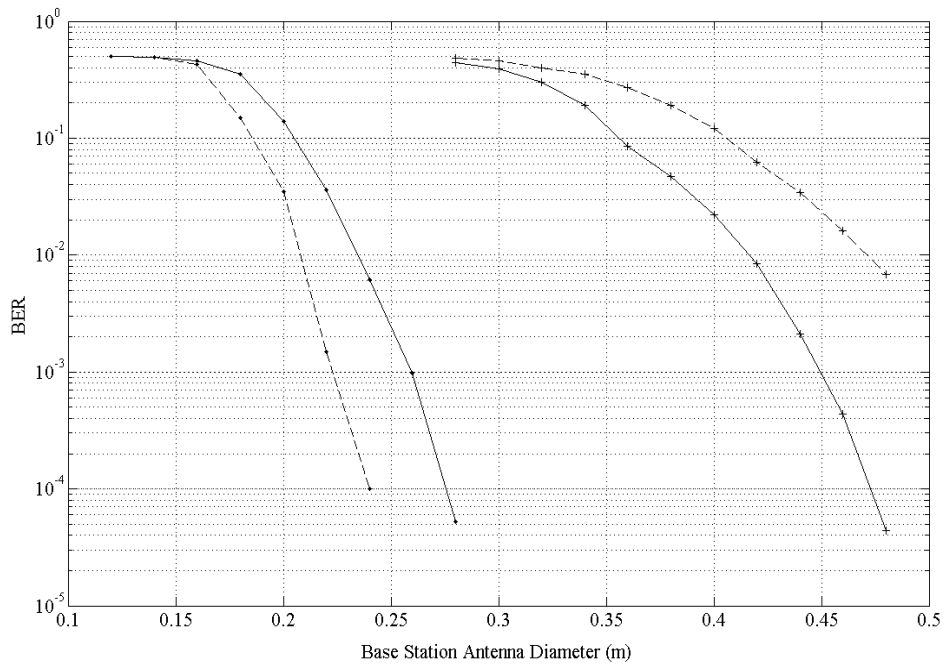


Fig. 5: Dependencies of the BER on BS antenna diameter for different levels of nonlinearity of the BS transmitter amplifier: solid lines - RLOS, dashed lines- BRLOS; points- negligible nonlinearity, crosses - moderate nonlinearity; SNR= -30 dB; modulation QPSK1/2; noise temperature 20 K; diameters of antennas: satellite transponder ≈ 0.28 m, RPAS ≈ 0.12 m; satellite transponder amplifier linear gain 10 dB

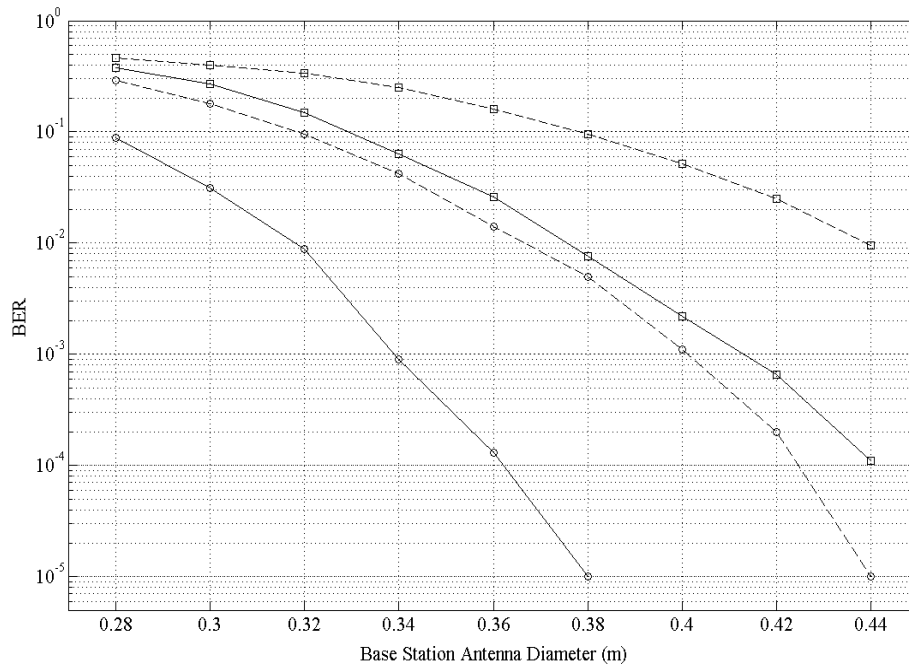


Fig. 6: Dependencies of the BER on BS antenna diameter for the severe nonlinearity of BS transmitter amplifier: solid lines - RLOS, dashed lines - BRLOS; circles: SNR = -18 dB; squares: SNR = -20 dB; modulation QPSK1/2; noise temperature 20 K; diameters of antennas: satellite transponder ≈ 0.28 m, RPAS ≈ 0.12 m; satellite transponder amplifier linear gain 10 dB

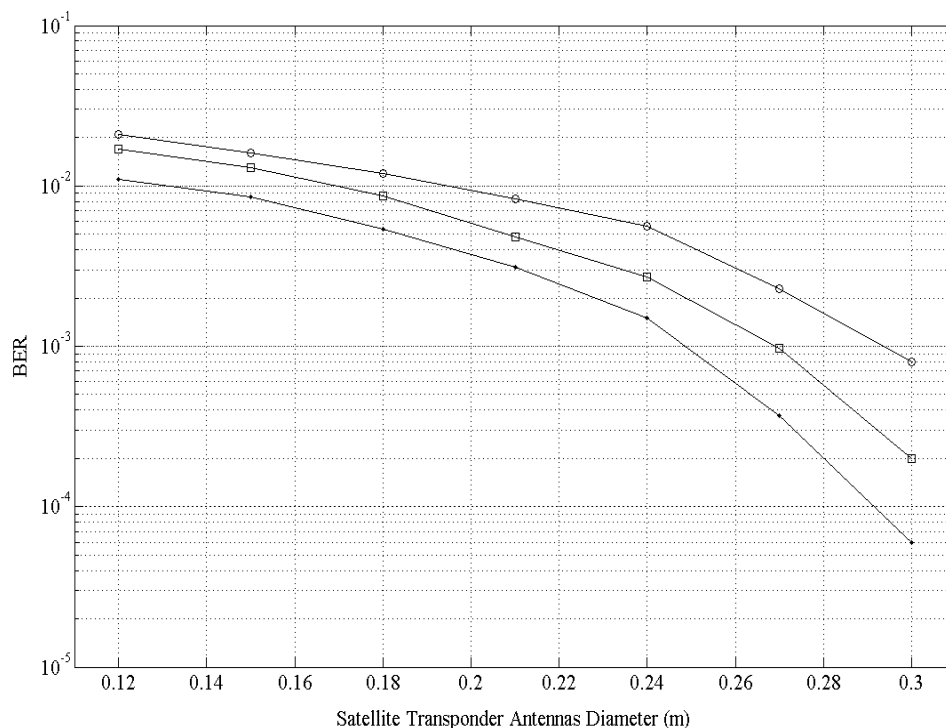


Fig. 7: Dependencies of the BER on diameters of satellite transponder antennas: dots - negligible nonlinearity of BS transmitter amplifier, SNR = -33 dB; squares - moderate nonlinearity, SNR = -23 dB; circles - severe nonlinearity, SNR = -14 dB; modulation QPSK1/2; noise temperature 20 K; BS antenna diameter ≈ 0.28 m; RPAS ≈ 0.12 m; satellite transponder amplifier linear gain 10 dB

We draw attention to the fact that here we are talking about the transmission, in which the SNR is the same for RLOS and BRLOS. Upon obtaining the dependencies, we consciously changed the SNR in all channels shown in Fig. 2 in the same way. BRLOS signal path is, of course, longer and in a real situation, the SNR for BRLOS will be lower in comparison with RLOS.

As follows from dependencies of the BER on the linear gain of BS amplifier (Fig. 4) the BER is lower when transmitting data through the satellite with the selected values of SNR = -20 dB and nonlinearity absence (since the BS amplifier has the linear gain). It is so due to the additional amplification of the signal by antennas of the satellite transponder and its power amplifier. It would be so if the SNR in RLOS and BRLOS were equal.

Fig. 5 shows dependencies of the BER on BS antenna diameter for different levels of BS transmitter amplifier nonlinearity. All curves use the same value SNR = -30 dB. RLOS and BRLOS channels for a negligible nonlinearity (points) can operate when BS antenna diameter is ≈ 0.28 m (with satellite transponder antennas ≈ 0.28 m and the RPAS antenna diameter ≈ 0.12 m). However, the BER is higher with moderate nonlinearity (crosses), and the BS antenna diameter is required ≈ 0.5 m for an operation of channels.

For a severe nonlinearity, we need bigger values of the SNR, and Fig. 6 shows how the BER changes in dependence on BS antenna diameter for different levels of nonlinearity. For negligible and moderate nonlinearities the channel can operate at SNR = -30 dB, but for a severe nonlinearity we need a much bigger value of the SNR. In this case, the following BS antenna diameters are required for the channel operation: at SNR = -18 dB (circles) a diameter ≈ 0.38 m is required for RLOS and ≈ 0.5 m for BRLOS. A slight decrease in the SNR to -20 dB (squares) requires a significant increase in BS antenna diameter. That is, for a severe nonlinearity the "sensitivity" of the BER to the value of the antenna diameter is much higher than for negligible and moderate nonlinearities.

Dependencies of the BER on satellite transponder antennas diameters for different levels of BS station amplifier nonlinearity (Fig. 7) show less influence of nonlinearity. In contrast to the curves in Fig. 5, 6 dependencies for all levels of nonlinearity change ("fall") more slowly with an increase in satellite antennas diameters (with constant diameters of BS and RPAS antennas). Therefore, the effect of transponder antennas diameters is not very noticeable, and the data for all levels of nonlinearity are close.

V. CONCLUSION

This work is the first calculation of RPAS data links characteristics in clusters with satellite (BRLOS) and direct (RLOS) connections. It is a way for estimating the parameters of such channels using the MATLAB Simulink package.

The task of the RPAS is to collect data using embedded devices and programs and to transmit them over communication channels. The centralized communication includes a topology with the BS as the central node to which all RPASs of clusters with RLOS and BRLOS are connected. In this architecture, RPAS are not directly connected, and the connection between the two RPASs is realized via the BS.

The direct connection between the RPAS and the BS is the simplest one. In this study, we also consider the architecture with satellite exchange, which exists at different levels of RPASs interaction. The development of a fully autonomous and cooperative RPAS cluster system requires reliable communication. At present, there is insufficient research in this area.

The development of theoretical bases for the construction of aeronautical satellite data transmission systems and obtaining of numerical information about RPAS digital channel characteristics in clusters is necessary for predicting the behavior of such systems. To achieve this goal, it is necessary to solve the following main tasks:

1. To create RPAS cluster models for the digital data transmission via satellite.
2. To develop a method for RPAS channel parameters estimation based on the MATLAB Simulink software package.
3. To investigate RPAS transmission system in dependence of a SNR, transmitter nonlinearity levels, the type of signal modulation, RPAS and satellite antenna diameters, the nonlinearity of the amplifier and the noise temperature of the satellite transponder.

Nonlinear distortions are the reason for a degradation. The primary source of nonlinear distortions is the transmitter power amplifier. Nonlinear power amplifiers for wireless communications were modeled [24], and nonlinear power amplifier effects in multi-antenna OFDM systems were analyzed [25]. The influence of aircraft transmitter nonlinearity for different types of fading in the channel (Rayleigh and Rician) was studied, and the possibility of correcting nonlinearity by using pre-distortion was revealed in a paper [26].

Channel nonlinearity is critical for wireless communications systems. Therefore here models of RPAS clusters were constructed for the first time, including both RLOS and BRLOS (Fig. 2). The obtained

data (Fig. 3-7) allow comparing quantitatively data transmission on both channels. The dependencies of the BER on the SNR (Fig. 3) for different nonlinearity levels of BS transmitter show that data transfer with increasing nonlinearity requires an increase in the SNR on average by ≈ 10 dB in the transition from negligible to moderate nonlinearity and from moderate to severe nonlinearity. The BER dependencies on BS transmitter gain (Fig. 4), on BS antenna diameter for different nonlinearity levels of the BS transmitter (Fig. 5, 6) and on the satellite transponder antennas diameters (Fig. 7) allow analyzing and predicting the behavior of communication channels for various conditions of data transmission.

The significance of the obtained results consists in the fact that calculations and modeling of the dependencies presented above can not only reveal problems in the early stages of RPAS channels designing, but also minimize errors, reduce time and cost, and provide scalability for future needs. As a result, such calculations quickly become a necessary tool for the researcher and developer of RPAS communication systems in clusters.

REFERENCES RÉFÉRENCES REFERENCIAS

1. L. Gupta, R. Jain, G. Vaszkun. Survey of Important Issues in UAV Communication Networks. Published in IEEE Communications Surveys and Tutorials, vol. PP, no.99, pp. 1-32, 2015.
2. US Department of Transportation Federal Aviation Authority, "Integration of Civil Unmanned Aircraft Systems (UAS) in the National Airspace System (NAS) Roadmap," First Edition, 2013, http://www.faa.gov/uas/media/uas_roadmap_2013.pdf.
3. I. Jawhara, N. Mohamed, J. Al-Jaroodi, D. Agrawal, S. Zhange. Communication and Networking of UAV-based Systems: Classification and Associated Architectures. Journal of Network and Computer Applications, vol. 84, pp. 93-108, 2017.
4. A Hanscom, M. Bedford. Unmanned Aircraft System (UAS) Service Demand 2015–2035, Literature Review & Projections of Future Usage. Res. Innov. Technol. Admin., U.S. Dept. Transp., Washington, DC, USA, Tech. Rep. DOT-VNTSC-DoD-13-01, 2016.
5. N. Motlagh, T. Taleb, O. Arouk. Low-Altitude Unmanned Aerial Vehicles-Based Internet of Things Services: Comprehensive Survey and Future Perspectives. IEEE Internet of Things Journal, vol. 3, no. 6, pp. 899-922, 2016.
6. D. Vikranth. UAV Swarm Co-Ordination and Control Using Grossberg Neural Network. International

- Journal of Computer Science Trends and Technology (JCST), vol. 5, no. 4, pp 1-7, 2017.
7. R. Szabolcsi. Establishment of the Unmanned Aerial Vehicle System Cluster: Mission, Motivation, Vision, Goals. Review of the Air Force Academy, vol. 28, no. 1, pp. 27-30, 2015.
 8. Ç. Tanil, C. Warty, E. Obiedat. Collaborative Mission Planning for UAV Cluster to Optimize Relay Distance. IEEE Aerospace Conference, pp. 2-9, March 2013.
 9. EUROCAE WG73 UAS - Concept of RPAS Required Communication Performance Methodology for the Command, Control and Communication Link. Available from Internet: https://www.uavdach.org/News/WG73_CCLink_RRCPDraftforWG73Comm entV0%2010.pdf.
 10. STANAG 4609/AEDP-8. NATO Digital Motion Imagery Format. http://www.gwg.nga.mil/misb/docs/nato_docs/STANAG_4609_Ed3.pdf.
 11. STANAG 7023/AEDP-9 NATO Primary Image Format. <https://booksmovie.org/similar-pdf-stanag-7023-nato.html>.
 12. STANAG 4607/AEDP-7. NATO Ground Moving Target Indicator Format. (GMTIF). <http://standards.globalspec.com/std/1300603/nato-stanag-4607>.
 13. Kharchenko, Y. Barabanov, A. Grekhov. Modelling of Aviation Telecommunications. Proceedings of the National Aviation University, vol. 16, no. 1, pp. 5-13, 2012.
 14. V. Kharchenko, Y. Barabanov, A. Grekhov. Modelling of ADS-B Data Transmission via Satellite. Aviation, vol. 17, no. 3, pp. 119-127, 2013.
 15. V. Kharchenko, W. Bo, A. Grekhov, M. Kovalenko. Investigation of ADS-B Messages Traffic via Satellite Communication Channel. Proceedings of the National Aviation University, vol. 61, no. 4, pp. 7-13, 2014.
 16. V. Kharchenko, Y Barabanov, A Grekhov. Modelling of 'Satellite-to-Aircraft' Link for Self-separation. Transport, vol. 28, no. 4, pp. 361-367, 2013.
 17. V. Kharchenko, W. Bo, A. Grekhov, A. Leschenko. Modelling the Satellite Communication Links with Orthogonal Frequency-Division Multiplexing. Transport, vol. 31, no. 1, pp. 22-28, 2016.
 18. V. Kharchenko, A, Grekhov, I. Ali, Y. Udod. Effects of Rician Fading on the Operation of Aeronautical Satellite OFDM Channel. Proceedings of the National Aviation University, vol.67, no. 2, pp. 7-16, 2016.
 19. V. Kharchenko, W. Bo, A. Grekhov, D. Bezsmertna. Investigation of Modulation Scheme and Transmitter Nonlinearity Impact on ADS-B Messages Transmission via OFDM Satellite Link. Proceedings of the National Aviation University, vol. 61, no. 1, pp.7-14, 2014.
 20. V. Kharchenko, A. Grekhov, I. Ali. Influence of Nonlinearity on Aviation Satellite Communication Channel Parameters. Proceedings of the National Aviation University, vol. 65, no. 4, pp. 12-21, 2016.
 21. A. Grekhov, V. Kondratiuk, A. Ermakov, E. Chernyuk. Influence of Transmitter Nonlinearities on Data Transmission from Remotely Piloted Air System. Proceedings of the National Aviation University, vol. 72, no. 3, pp. 33-41, 2017.
 22. I. Viterbi. Convolutional Codes and Their Performance in Communications Systems. IEEE Trans. Commun. Technol., vol. COM-19, no. 5, pp. 751-772, 1971.
 23. Saleh. Frequency-Independent and Frequency-Dependent Nonlinear Models of TWT Amplifiers. IEEE Trans. Communications, vol. 29, no. 11, pp. 1715-1720, 1981.
 24. P.Jantunen. Modeling of Nonlinear Power Amplifiers for Wireless Communications. The thesis for the degree of Master of Science. Finland.138 p., 2004. Available from Internet: <http://www.researchgate.net/publication/224263342_Nonlinear_RF_power_amplifier_behavioural_analysis_of_wireless_OFDM_systems>.
 25. F. Gregorio. Analysis and Compensation of Nonlinear Power Amplifier Effects in Multi-Antenna OFDM Systems. Dissertation for the degree of Doctor of Science in Technology. 133 p., 2007.
 26. V. Kharchenko, A. Grekhov, V. Kondratiuk, K. Nagorna. ADS-B Satellite Communication Channel Based on IEEE 802.16 Standard. Transport and Aerospace Engineering, vol. 5, pp. 18-27, 2017.



GLOBAL JOURNAL OF RESEARCHES IN ENGINEERING: F
ELECTRICAL AND ELECTRONICS ENGINEERING
Volume 18 Issue 1 Version 1.0 Year 2018
Type: Double Blind Peer Reviewed International Research Journal
Publisher: Global Journals
Online ISSN: 2249-4596 & Print ISSN: 0975-5861

Review on Characteristic Modeling of Electric Arc Furnace and its Effects

By Vinayaka K.U & Dr. P.S. Puttaswamy

Siddaganga Institute of Technology

Abstract- Development on a country is based on its industrialization and infrastructure; steel is used as a vital part of any building infrastructure, the process of steel manufacturing using electric arc furnace (EAF) introduces several power quality disturbances, in this paper, characteristic modeling of electric arc furnace and its effects on power quality is investigated. Several EAF models are modeled and reviewed from power quality assessment. Voltage flicker, Harmonics and Inter harmonics arises in an electrical network due to the non-linear nature of EAF operation. Time-domain modeling and frequency domain modeling of an EAF is simulated using MATLAB/ SIMULINK and PSCAD simulation software.

Keywords: *electric arc furnace (EAF); powerquality (PQ); voltage-current (V-I); voltage current characteristics (VIC).*

GJRE-F Classification: FOR Code: 090699



Strictly as per the compliance and regulations of:



Review on Characteristic Modeling of Electric Arc Furnace and its Effects

Vinayaka K.U^α & Dr. P.S. Puttaswamy^σ

Abstract - Development on a country is based on its industrialization and infrastructure; steel is used as a vital part of any building infrastructure, the process of steel manufacturing using electric arc furnace (EAF) introduces several power quality disturbances, in this paper, characteristic modeling of electric arc furnace and its effects on power quality is investigated. Several EAF models are modeled and reviewed from power quality assessment. Voltage flicker, Harmonics and Inter harmonics arises in an electrical network due to the non-linear nature of EAF operation. Time-domain modeling and frequency domain modeling of an EAF is simulated using MATLAB/ SIMULINK and PSCAD simulation software.

Keywords: electric arc furnace (EAF); powerquality (PQ); voltage-current (V-I); voltage current characteristics (VIC).

I. INTRODUCTION TO POWER QUALITY

The modern-day equipment is automatic and semiautomatic in nature and is expensive too, which are vulnerable to the changes in the input power supply. As these machines are the workhorse of any industry, the productivity and economics are dependent on these machines. The malfunctioning/damage to this sensitive equipment puts the work into the halt. In this regard, it is essential to provide the quality input to the machines for stable and reliable operation.

The term "Power Quality" deals with the quality of the power distributed and delivered to the end users, there are many factors that disturb the quality of the power delivered commonly called as power quality disturbances. Generally the power quality refers to the voltage quality and the current quality, as an end user we cannot ensure the current quality as it depends on the type of the load connected to the system, so as to improve the overall power quality it is the need of the hour to maintain a proper voltage quality so as to uplift the overall power quality.

The major threats to the power quality are the long and short duration voltage variations, harmonics, inter-harmonics etc.

Author α: Dept. of Electrical and Electronics Engineering SIT, Tumakuru Tumakuru, India. e-mail: vinay.ene@gmail.com

Author σ: Professor and Head, Dept. of Electrical and Electronics Engineering PESCE, Mandya Mandya, India. e-mail: Psputtaswamy_ee@yahoo.com

A Phenomenon associated with light intensity caused due to the non-linear and stochastic behavior of EAF is commonly termed as voltage flickers. Flicker causes the voltage fluctuations at PCC and disturbs consumers by causing flicker of bulbs and lamps.

Voltage flicker is characterized by fluctuations of voltage below 0.5% in the frequency range of 5-10Hz.

An Unbalanced and periodically varying load such as EAF disturbs the quality of power system; the operation of an EAF introduces voltage flicker, unbalance, characteristic and noncharacteristic harmonics to the system thereby degrading the quality of the power delivered at the consumer end.

To investigate the voltage flicker and harmonics introduced by an EAF, the characteristics of EAF operation is to be understood. Therefore an attempt is made to model different kinds of EAF models and study its behavior.

Figure 1 display the typical line-voltage fluctuations introduced due to the stochastic behavior of EAF. The flicker curve showing the human perception is shown below.

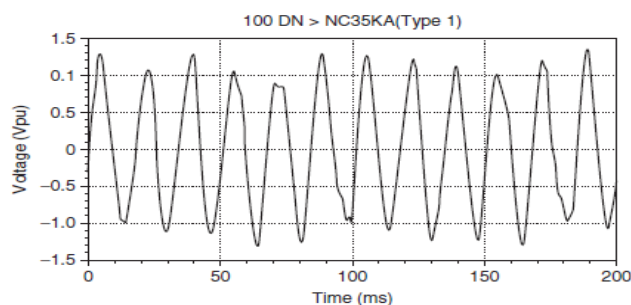


Figure 1: Voltage Flicker curve

Since the electrical networks are interconnected, the current harmonics and voltage flicker due to EAF operation will affect the other users of the same system. For technological reasons the new age EAF's are operated at very reduced power factor, from the EAF operation it can be observed that, the current distortion level is high during the melting stage and comparatively lower during other stages of operation. A sample harmonic spectrum of current in different stages of EAF operation is shown below in Figure 2.

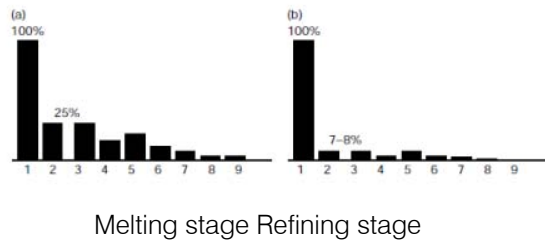


Figure 2: Current distortion of EAF

The harmonic spectrum exhibits the characteristics and non-characteristics harmonics under different stages of operation, the total harmonic distortion during the melting stage is comparatively higher than during the refining stage.

II. ELECTRIC ARC FURNACE

The EAF is used in Steelmaking has emerged as an important steelmaking process in recent years. One of the methods is through production of electric arc which gives an arc temperature between 3000C to 3500C. Arc is the flow of current through an air gap between two electrodes.

In brief, when an AC Current is applied through the electrodes, an arc gets struck between the Graphite electrode and metal scrap, thereby inducing a very high temperature heat to melt the scrap /charge into molten metal, the electrical energy required during the process of steel making is tremendously large and is dependent on the quantity of the charge to be melted.

The process of steel making is very chaotic in nature characterized by large and sudden variations in currents and voltages disturbing the power grids.

The disturbances due to high nonlinearity of the EAF load affects the Sub transmission and transmission of overall power system network.

The variations of voltage both with respect to magnitude and frequency are the characteristics of voltage flicker, and the injection of integral and fractional multiples of fundamental frequency components of supply voltage is termed as voltage harmonics and voltage inter harmonics.

The arc resistance of an EAF is highly variable making The V-I characteristic be non-linear, thereby introducing harmonic currents, resulting in voltage harmonics due to circulation of harmonic currents in an electrical network.

III. MODELING OF ELECTRIC ARC FURNACE

a) Introduction to Modeling of Electric Arc Furnace

An unbalanced and periodically varying load such as EAF injects disturbances to the system leading to degradation of the quality of power system.

To understand the randomness in operation of an EAF it is essential to build the characteristic model of an electric arc furnace.

The process of arc melting is stochastic and is hard to realize an accurate model for EAF load.

Stages of steel making process, the position of the electrodes, nature of the supply voltage, and system impedance are the critical parameters to be considered for modeling of an EAF with regards to electrical power quality.

Also For any characteristic model the accuracy of the characteristics model depends on the least assumptions made during modeling process, lesser the number of assumption closer will be the model with the actual characteristics of EAF.

Thus, the description of an arc furnace load depends on the following items: arc voltage, arc current and arc length (which is determined by the the position of electrode).

In general the models can be classified into,

- Time domain analysis methods
- Frequency domain analysis methods and
- Power balance method

IV. MODELING OF ARC FURNACE ON SIMULATORS

a) Introduction to modeling of Electric Arc Furnace on Simulators

Detailed electrical operations of an EAF have been outlined in the preceding sections. As evident, the EAF is unbalanced, highly nonlinear, periodically varying load. Since such random behavior is difficult to be realized on a simulator, many researchers have published various models that can be used to simulate the characteristics.

The models may be classified as:

- Based on the V-I characteristics.
- Based on the time domain nonlinear equivalent circuit
- Based on the harmonic voltage source method.
- Based on the Harmonic domain solution of a nonlinear differential equation.
- Based on the Random process.

The V-I characteristic models are derived from the relation between arc voltage and arc current using the V-I characteristics. The static and dynamic operation of an EAF is usually realized using VIC.

The time domain equivalent circuit model is also based on the V-I characteristics. The approximation made in this type of modeling is more than that made in the previous type and hence this is very simple model.

Both model 3 and 4 use a harmonic voltage source to model the arc furnace. While the harmonic voltage source does not work under maximum power transfer condition, the harmonic domain model solution

is derived from experimental formula. This method is highly dependent on the system parameters and operating conditions.

The random process model reflects the model of arc furnace during the early stage of meltdown period. It has been mainly used for voltage flicker analysis

b) Model based on the V-I characteristic

The model based on the solution of nonlinear differential equation closely approximates a practical arc furnace, hence this is chosen for the simulation studies. This is justified in the following subsections where a comparison is made between the practical EAF and V-I characteristics of the same.

The real time V-I characteristics and linearized model of an EAF is as shown below. The arc length in the furnace operation determines the ignition and extinction voltage of an EAF.

Various time domain models can be derived by approximating the voltage-current characteristics of an EAF.

Figure 3 shows the actual V-I characteristics and its piecewise linear model an arc furnace. The arc ignition voltage and the arc extinction voltage are determined by the arc length during arc furnace operation. Ignition Voltage (V_{ig}) and Extinction voltage (V_{ex}) are determined by the arc length during arc furnace operation.

By approximating the actual V-I characteristics of an arc furnace, different time domain models has been derived as follow:

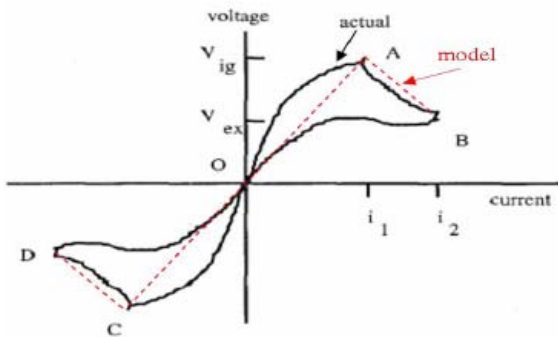


Figure 3: Actual and piece-wise linear approximation of V-I characteristic of an Arc Furnace Load

Model 1

The EAF model analysis is approximated considering two linear equations on VI-characteristics of the EAF. The two linear equations are shown below, arc voltage as a function of currents for one cycle in this model is represented as,

$$V = \begin{cases} R1 * i & -i1 \leq i < i1 \\ R2 * i + Vig \left(1 - \frac{R2}{R1}\right) & i1 < i < i2 \\ R2 * i - Vig \left(1 - \frac{R2}{R1}\right) & -i2 \leq i < -i1 \end{cases} \quad (1)$$

$$i1 = \frac{Vig}{R1} \quad (2)$$

$$i2 = \frac{Vex}{R1} - Vig \left(\frac{1}{R2} - \frac{1}{R1}\right) \quad (3)$$

R_1 : linear slope obtained when the V-I characteristic approximation is between the limits $(-i_1, i_1)$

R_2 : linear slope obtained when the V-I characteristic approximation is between the limits $[-i_2, -i_1]$ or $[i_1, i_2]$

i_1 : arc current reached at the ignition voltage of the electric arc (V_{ig})

i_2 : arc current reached at the extinction voltage of the electric arc (V_{ex}).

Model 2

Further precise model can be achieved by reducing the number of approximations and considering the detailed variations of V-I characteristics

EAF acts as a pure resistor, in the first stage where magnitude of the voltage rises from extinction voltage to ignition voltage. During this stage the polarity of an arc current change from $-i_3$ to i_1 .

Initiation of melting process is considered as second stage of EAF operation, characterized by an exponential drop in voltage across the electrode leading to drop of arc voltage from V_{ig} to V_{st} followed by an increase in arc current i_1 to i_2 .

Normal arc melting process is regarded as third stage of EAF operation; here arc voltage tends to drop in a line of slope gradually from V_{st} to V_{ex} .

$$v = \begin{cases} R1 & (-i3 \leq i < i1, inc) \text{ or } (-i1 \leq i < i3, dec) \\ Vst + (Vig - Vst) \exp\left(\frac{i1 - i}{iT}\right) & i1 \leq i < i2, inc \\ Vst + (i1 - i2)R2 & i \geq i2, inc \\ Vex + (i - i3)R3 & i \geq i3, dec \\ -Vst + (Vst - Vig) \exp\left(\frac{i1 + i}{iT}\right) & -i2 \leq i < -i1, dec \\ -Vst + (i + i2)R2 & i < -i2, dec \\ -Vex + (i + i3)R3 & i < -i3, dec \end{cases} \quad (4)$$

$$i1 = \frac{Vig}{R1}$$

$$iT = 1.5i1 \quad (5)$$

$$i2 = 3i1 \quad (6)$$

$$i3 = \frac{Vex}{R1} \quad (7)$$

Model 3

Hyperbolic Model:

Here, the V-I characteristics of EAF is Considered as

$$V = \left\{ VT + \frac{Ci, d}{Di, d} \right\} sign(I) \tag{8}$$

Where, I: Arc current

V: Arc voltage

VT: Threshold voltage

Model 4

Exponential Model:

The VI-characteristics of the arc voltage is expressed as an exponential function given by,

$$V = VT \left(1 - e^{-\frac{|I|}{I_0}} \right) sign(I) \tag{9}$$

I₀: current constant is employed to realize the slope of positive and negative currents.

Model 5

Arc Resistance Model:

The non-linear resistance of an EAF is expressed as function of current source The V-I characteristics is shown. The equations pertaining to the operation of an EAF is as expressed below.

$$Ra = \left\{ \begin{array}{ll} R1 & , 0 \leq I < i_{ig} , \frac{dI}{dt} > 0 \\ \frac{Vd + (Vig - Vd) \exp\left(-\frac{I - i_{ig}}{\tau1}\right)}{I} & , I \leq i_{ig} , \frac{dI}{dt} > 0 \\ \frac{Vt + (Vig - Vt) \exp\left(-\frac{I}{\tau2}\right)}{I + i_{ig}} & , \frac{dI}{dt} > 0 \end{array} \right\} \tag{10}$$

$$I = |i(t)| \tag{11}$$

$$Vig = 1.15Vd \tag{12}$$

$$i_{ig} = \frac{vig}{R1} \tag{13}$$

Model 6

Exponential-Hyperbolic Model:

In this model, the combination of Hyperbolic and exponential is presented, the V-I Characteristics of this model is expressed by

$$V = \left\{ \begin{array}{l} VT + \frac{C}{D + I} \frac{dI}{dt} \geq 0, I > 0 \\ VT * \left(1 - e^{-\frac{|I|}{I_0}} \right) \frac{dI}{dt} < 0, I > 0 \end{array} \right\} \tag{14}$$

In this model, hyperbolic function describes the increase of the current and the exponential function describes the decrease of the current. The relation between arc length (l) and threshold voltage (V_T) is explained by the given below expression.

$$V_T = A + B * l \tag{15}$$

A: constant evaluated as the sum of voltage sag for anode and cathode and is approximately 40 Volts.

B: voltage sag depended on the arc length and empirically is acceptable as B=10 V/cm and: arc length.

V. RESULTS AND DISCUSSION

The characteristics of various arc models can be studied by considering a simple EAF in single phase. The EAF system configuration is shown below.

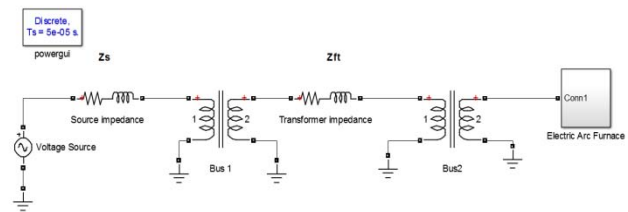


Figure 4: Single Phase Test circuit of EAF

In the figure4, the source impedance is represented as Zs and the source side transformer represents PCC and the EAF bus represents the secondary side of transformer having impedance as Zt. The system specifications and parameters of various models are as presented in the below table 1.

Table 1: System and model specifications

Items	Parameters
System	V=566V , f=50Hz Zs=0.0568+j0.468mΩ Zt=0.3366+j3.22mΩ
Model 1	Vig=350.75V R1=0.05Ω I1=7015A Vex=289.75V R2= -0.76mΩ I2=87278A
Model 2	Vig=350.75V R1=0.05Ω Vex=289.75V R2= -0.76mΩ Vst=320.75V R3=-0.39mΩ
Model 3, 6	Vt=200V, Ci=190kW, Cd=39kW Di=Dd=5000A
Model 4	Vt=200V, I0=1000A
Model 5	Vig=350.75V Imax=100kA τ1=0.01sec τ2=0.02sec

a) Static Characteristics

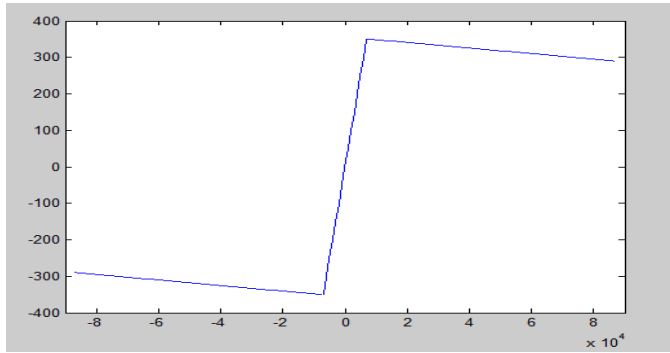


Figure 5: VI-characteristics of model1 in static state

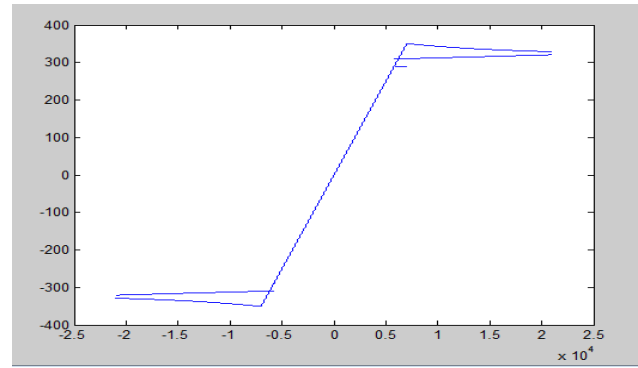


Figure 7: VI-characteristics of model2 in static state

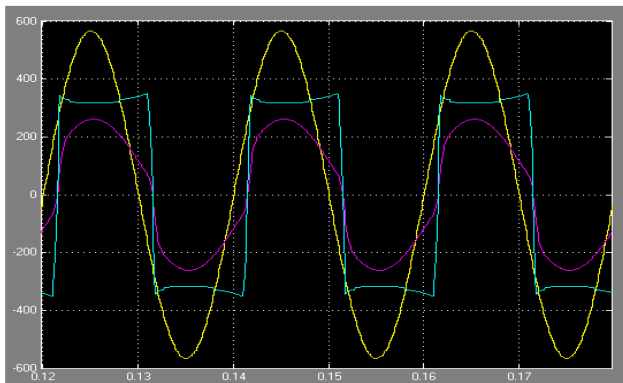


Figure 6: Arc voltage & current of model1 in static state

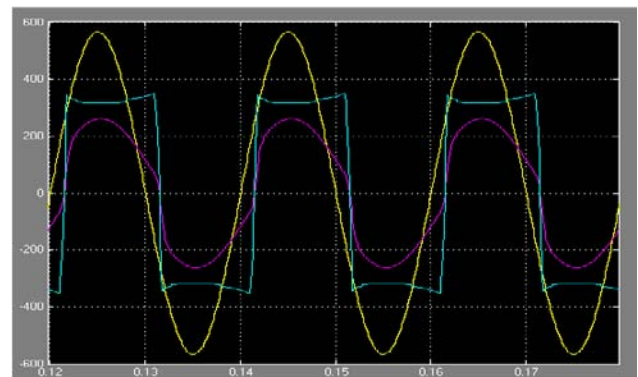


Figure 8: Arc voltage & current of model2 in static state

The static V-I characteristics of model-1 as shown in the Figure 5 is based on the real voltage current characteristics approximation.

It is observed that the V-I characteristics comprises of the linear region where the arc resistance remains constant between the ignition voltages, and arc resistances varies between the ignition and extinction voltages.

Model 1 represents the linearized characteristics of the actual EAF model; hence the accuracy of the model is far from the actual characteristics.

The corresponding Arc voltage and Arc current are shown in figure 6, it is observed that the arc voltage is distorted in nature, hence signifies the non-linearity in the system.

The Static V-I Characteristics and corresponding Arc voltage and Arc current of model-2 are shown in figure 7 and figure 8 respectively. Model-2 approximates more accurately, the typical voltage-current characteristic of an electric arc. When the electric arc voltage reaches the extinction voltage value, V_{ex} , arc voltage continues its variation for a moment of time and will not change it immediately.

As compared to the previous model, the differences are:

A different electric arc functioning zone is defined;

In the case the value of the current is below $-i_2$ or above than i_2 , one can notice that the voltage variation is constant, maintained at the extinction voltage value of the electric arc;

The range in which the dynamic voltage-current characteristic can vary is larger.

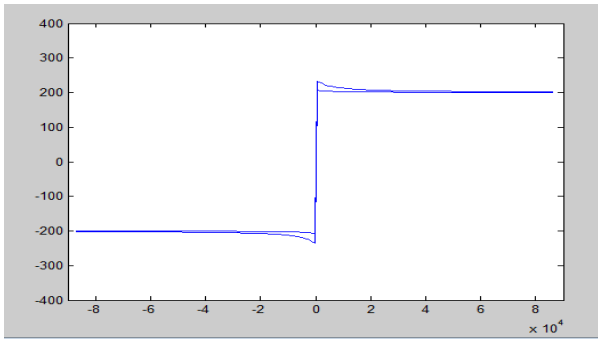


Figure 9: VI-characteristics of model3 in static state

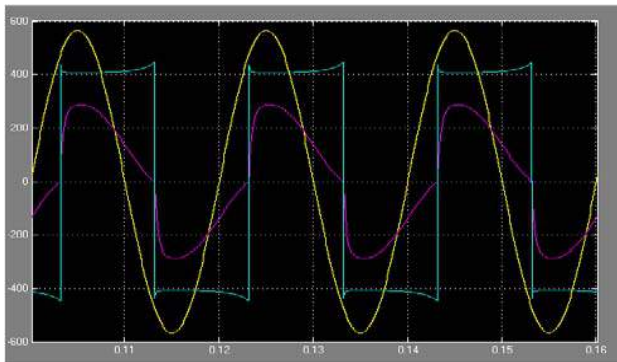


Figure 10: Arc voltage & current of model3 in static state

The static V-I Characteristics and Arc voltage and Arc current of model 3 is as shown in the figure 9 and figure 10 respectively.

From the characteristic curve it is observed that the arc voltage is a hyperbolic function of an arc current and the characteristic curve has two curves forming the three zones of operation of an EAF, the curves for increasing and decreasing values of arc current with different constants under various operating conditions are simulated.

This model nearly resembles the actual V-I Characteristics of an EAF model, here it is also observed that, the arc voltage is far from sinusoidal similar to the previous models, hence higher order of harmonics.

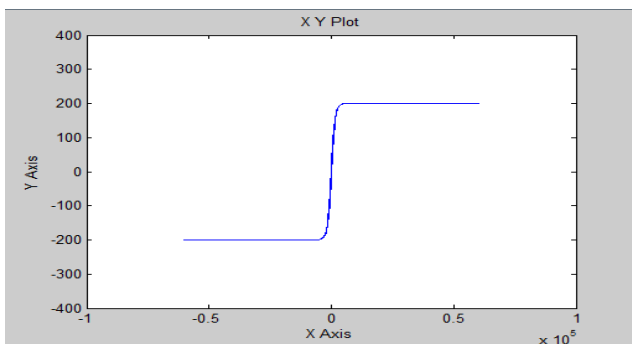


Figure 11: VI-characteristics of model4 in static state

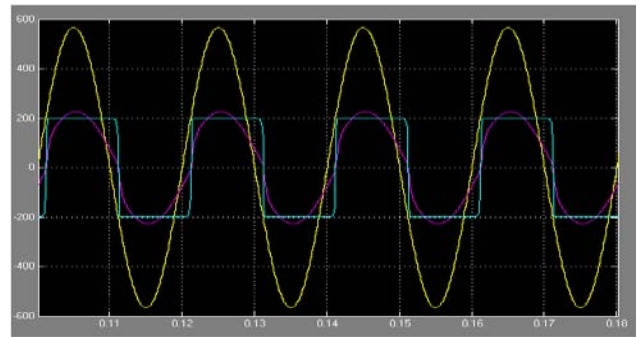


Figure 12: Arc voltage & current of model4 in static state

The static V-I Characteristics and Arc voltage and Arc current of model 4 is as displayed in the figure 11 and figure 12 respectively. The characteristic curve shows the exponential behavior of the arc voltage with respect to the arc current and the characteristic curve has two regions consisting of a linear and exponential regions, as the approximations are more, the accuracy of model with respect to actual characteristic is poor. The arc voltage curve has higher distortion, hence the presence of harmonics is considered to be high.

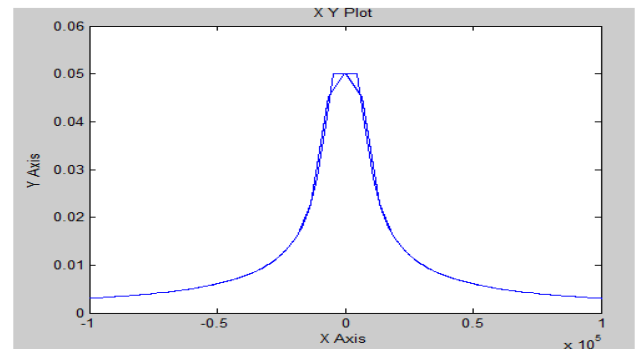


Figure 13: Arc current-resistance curve of model5

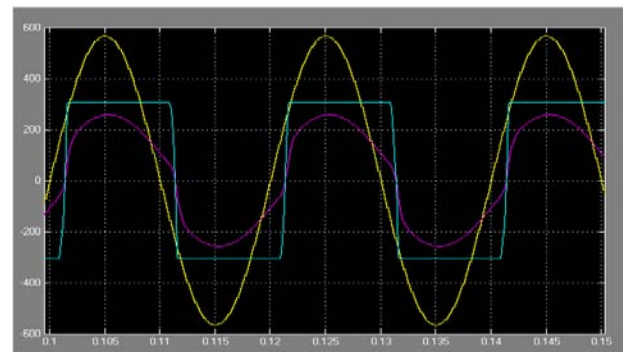


Figure 14: Arc voltage & current of model5 in static state

The Arc current-resistance curve and Arc voltage & current of model 5 in static state are as shown in figure 13 and figure 14 respectively, in model-5 there are three working phases of the electric arc.

In the first one, the electric arc voltage increases to the ignition voltage of the electric arc, so the electric arc reignites. Hereby, the other phase can take place.

In the second phase, the electric arc voltage has an exponentially drop from the ignition voltage of the electric arc to the Vex voltage. In this phase take place the melting process of the metals, electric arc voltage being stable. This segment is approximated with an exponential function with time constant $\tau 1$.

In the third phase of the electric arc working zone, the arc begins to be extinct; its voltage keeps dropping, process which can also be assumed to be represented by an exponential function with the time constant $\tau 2$.

Here it is observed that, the arc voltage is less distorted to the previous models.

Since all the regions of operation are considered for modeling, model-5 presents almost actual characteristics of an EAF.

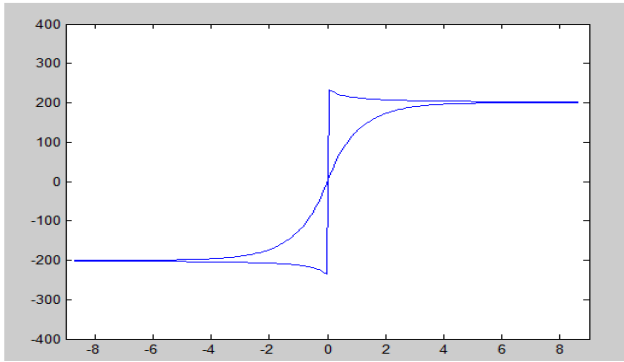


Figure 15: VI-characteristics of model6 in static state

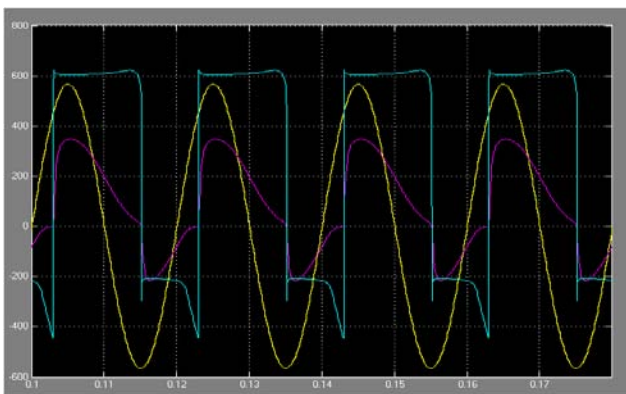


Figure 16: Arc voltage & current of model6 in static state

The static V-I Characteristics and Arc voltage and Arc current of model 6 is as displayed in the figure 15 and figure 16 respectively. The characteristic curve displays both the exponential and hyperbolic nature of

the arc voltage with respect to variation in arc current and the characteristic curve has three working phase.

The accuracy of model with respect to actual characteristic is high.

b) *Dynamic Characteristics of Arc Models*

Dynamic model of an EAF is required for the Flicker analysis in an EAF. The dynamic behavior of an EAF is obtained for different models by replacing the static V-I characteristics by sinusoidal functions. Dynamic models are characterized by either periodic or random change of arc resistance about a value of R_a for each model.

Sinusoidal variations of arc resistance is given by

$$Ra(t) = Ra(1 + m \sin(\omega_f * t))$$

Where R_a : static arc resistance

m : modulation index

ω_f : Frequency in the flickering range

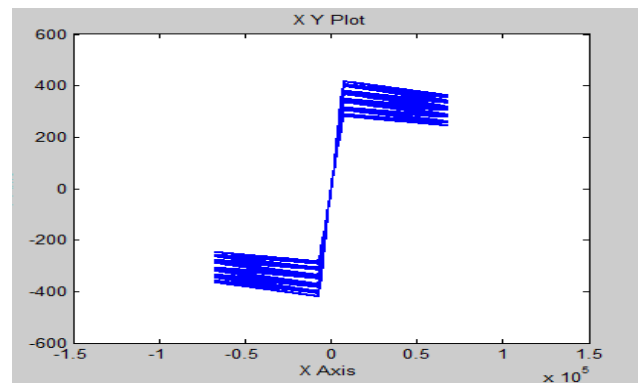


Figure 17: VI-characteristics of model1 in Dynamic state with $m=0.2$.

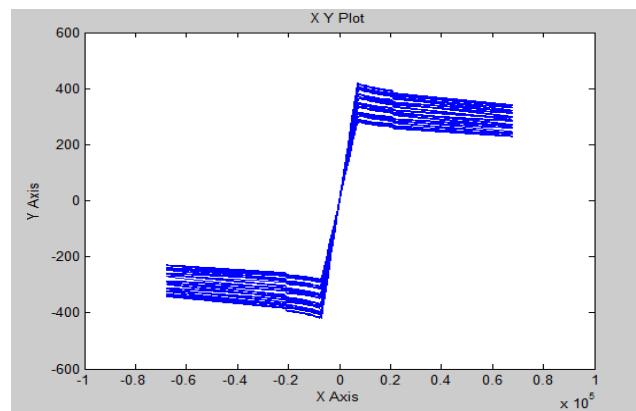


Figure 18: VI-characteristics of model2 in Dynamic state with $m=0.2$.

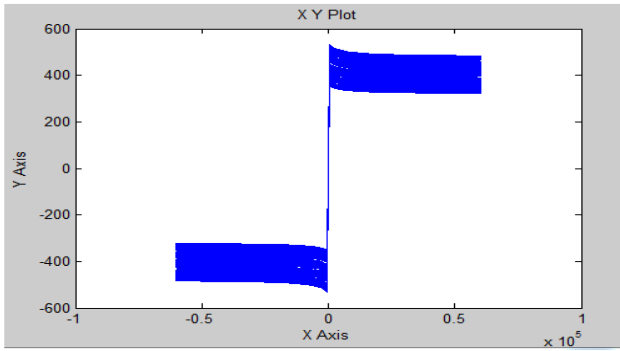


Figure 19: VI-characteristics of model3 in Dynamic state with $m=0.2$

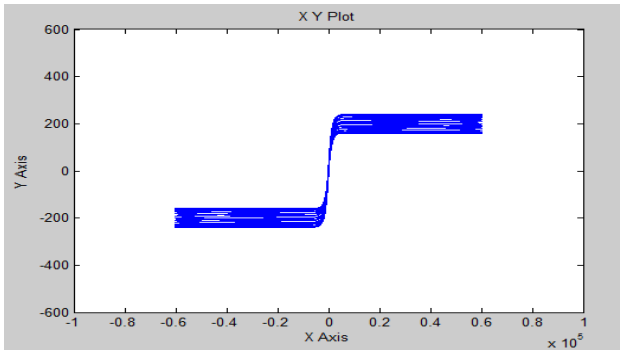


Figure 20: VI-characteristics of model4 in Dynamic state with $m=0.2$

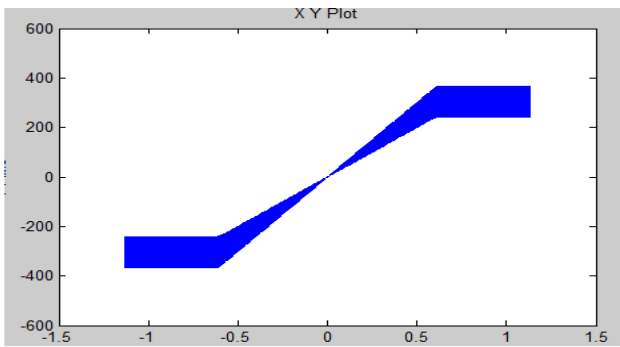


Figure 21: VI-characteristics of model5 in Dynamic state with $m=0.2$

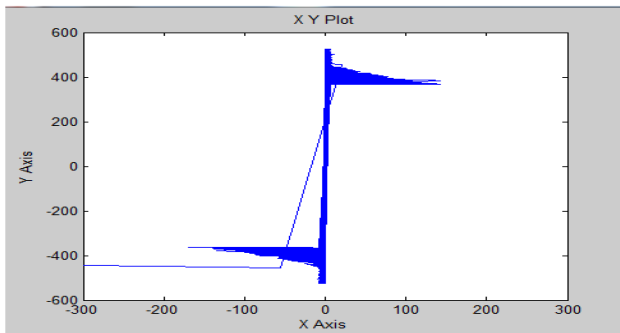


Figure 22: VI-characteristics of model6 in Dynamic state with $m=0.2$

The dynamic characteristics of the Models 1,2,3,4,5 and 6 are represented in figure 17,18,19,20,21 and 22 respectively, the dynamic characteristics of the models are observed for constant modulation index with constant sinusoidal variation, the random flicker can be observed for random variation in the modulation index for the same characteristic model.

c) Harmonic Behavior of EAF system

The Three phase Test circuit of EAF connected supply system developed in Simulink is shown in Figure 23.

A controlled voltage source with resistive and inductive network is used to couple the generated flicker disturbance to a given phase of the power system line. For a three-phase system, three sets of controlled voltage source and resistive and inductive networks are required.

The electric arc furnace model can be implemented using the MATLAB function block and a sinusoidal block.

Each electric arc furnace MATLAB Function block represent each electrode at each phase; therefore, three MATLAB function blocks are required for each phase. The sinusoidal is used to model the flicker frequency and magnitude variation

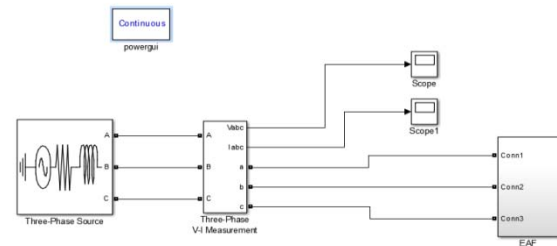


Figure 23: three phases Test circuit of EAF connected supply system.

The arc voltage and Arc current at the point of common coupling (Measurement block) can be visualized in the figure 24 and 25 respectively.

It is observed from the below figures that due to the nonlinear nature of an EAF load the Arc current is flickering and resulting in flickering of the voltage, these flickers are dynamic in nature, random flicker at the initial stage of EAF can be observed by variation of modulation index.

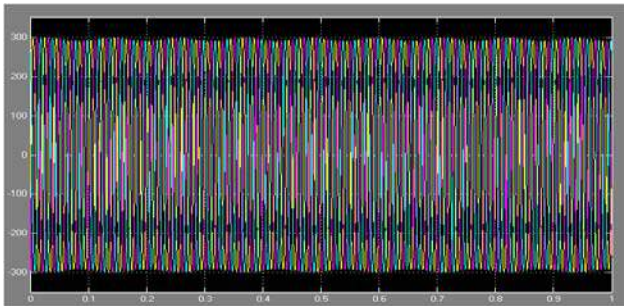


Figure 24: Three phase Voltage flicker curve

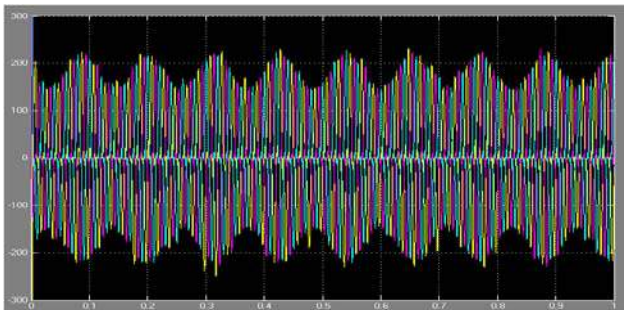


Figure 25: Three phase Arc current curve

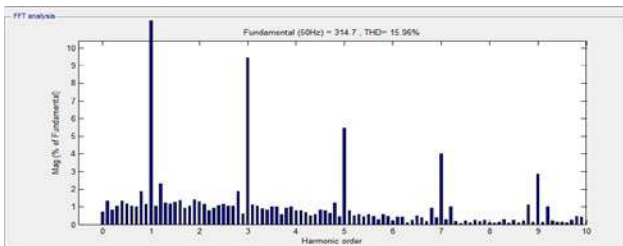


Figure 26: Harmonic spectrum of an arc furnace current during melting

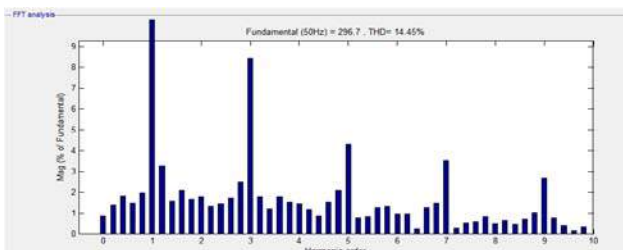


Figure 27: Harmonic spectrum of an arc furnace current during refining

The harmonics introduced in the system can be studied by carrying out FFT analysis. Figure 26 and figure 27 shows the harmonic spectrum of Arc voltage during smelting and refining process,

It is observed that these results resembles the theoretical studies of an EAF, the harmonic spectrum consists of both the characteristic and non-characteristic harmonics and inter-harmonics.

It is observed that due to high non linearity at the melting stage of an arc furnace the Total harmonic

distortion is high and the THD reduces during the refining stage.

VI. CONCLUSIONS

EAF is a highly nonlinear, timely varying load with stochastic behavior introducing several power quality disturbances to the system.

Several models based on Voltage current characteristics and few current source models are modeled to investigate the voltage flicker and harmonics introduced into an electrical network by an EAF.

The static and dynamic behavior of the arc furnace models are studied and the results obtained indicates the existence of voltage flicker in the system, harmonic analysis is carried out to determine the current harmonics under different stages of EAF operation.

Various models of Electric Arc furnace resembles the actual characteristics of an EAF, out of the various models model 5 puts forward the précised result.

REFERENCES RÉFÉRENCES REFERENCIAS

1. Tongxin Zheng, Elham B.Makram, Adly A.Girgis. "Effect of Different Arc Furnace Models on Voltage Distortion", IEEE 1998.
2. C.Sharmeela, G.uma, M.R.Mohan, K.Karthikeyan, "Voltage Flicker Analysis and Mitigation Case Study in an Electric Arc Furnace Using PSCAD/EMTDC", international conference on power system technology, IEEE 2004.
3. Golkar, M.A., Meschi, S., "MATLAB modeling of arc furnace for flicker study", IEEE International Conference on Industrial Technology, 2008. ICIT 2008. , 21-24 April 2008, pp. 1-6.
4. K. Anuradha, B. P. Muni and A. D. Raj Kumar, "Modeling of Electric Arc Furnace & Control Algorithms for voltage flicker mitigation using DSTATCOM", IPEMC, 1123-1129, 2009 .
5. S. Varadan, E.B. Makram, A.A. Girgis, "A new time domain voltage source model for an arc furnace using EMTP," *IEEE Trans. on Power Del.*, vol. 11, no. 3, pp. 1685–1690, July 1996.
6. G.C.Maontanari, M.loggini, A.carallini, L.pitti, "Flicker and distortion compensation in electrical plants supplying arc furnace", IEEE 1994.
7. "Modeling of three phase electric arc furnace" by Manuela panoiu, caiuspanoiu and ionasora, ACTA ELECTROTECHNICA, Volume 48,number 2,2007
8. Ana Tomasovic´ Teklic´, Bozidar Filipovic-Gr´ c´ c´, IvicaPavic´ "Modelling of three-phase electric arc furnace for estimation of voltage flicker in power transmission network" *Electric Power Systems Research* 146 (2017) 218–227

This page is intentionally left blank



GLOBAL JOURNAL OF RESEARCHES IN ENGINEERING: F
ELECTRICAL AND ELECTRONICS ENGINEERING
Volume 18 Issue 1 Version 1.0 Year 2018
Type: Double Blind Peer Reviewed International Research Journal
Publisher: Global Journals
Online ISSN: 2249-4596 & Print ISSN: 0975-5861

Resonance Characteristics Enhancement of Slot-loaded Microstrip Patch Antenna for GPS Application

By Rakib Hasan, Mustakim Ahmed Rahat, Sakhawat Hussain & Anis Ahmed

University of Dhaka

Abstract- For GPS application, a rectangular microstrip patch antenna has been designed and fabricated focusing on single resonant frequency at 1.575 GHz of the L-1 band. Slots are incorporated into the patch to fine-tune the resonant frequency, decrease the return loss, and increase the directivity and bandwidth. The proposed antenna has four rectangular slots of different sizes on the patch. The antenna is designed by commercially available simulation software. The simulation result shows that it resonates at 1.536 GHz with a return loss value of -50.72 dB having a bandwidth of 48.5 MHz and directivity of 7.13 dBi and the fabricated antenna has a resonant frequency of 1.5 GHz with return loss and bandwidth of -25 dB and 30 MHz, respectively. It is found that the proposed antenna perform much better than a conventional microstrip patch antenna.

Keywords: GPS, L-1 band, rectangular slot-loaded patch antenna.

GJRE-F Classification: FOR Code: 090609



RESONANCE CHARACTERISTICS ENHANCEMENT OF SLOT-LOADED MICROSTRIP PATCH ANTENNA FOR GPS APPLICATION

Strictly as per the compliance and regulations of:



© 2018. Rakib Hasan, Mustakim Ahmed Rahat, Sakhawat Hussain & Anis Ahmed. This is a research/review paper, distributed under the terms of the Creative Commons Attribution-Noncommercial 3.0 Unported License <http://creativecommons.org/licenses/by-nc/3.0/>), permitting all non commercial use, distribution, and reproduction in any medium, provided the original work is properly cited.

Resonance Characteristics Enhancement of Slot-loaded Microstrip Patch Antenna for GPS Application

Rakib Hasan^α, Mustakim Ahmed Rahat^σ, Sakhawat Hussain^ρ & Anis Ahmed^ω

Abstract- For GPS application, a rectangular microstrip patch antenna has been designed and fabricated focusing on single resonant frequency at 1.575 GHz of the L-1 band. Slots are incorporated into the patch to fine-tune the resonant frequency, decrease the return loss, and increase the directivity and bandwidth. The proposed antenna has four rectangular slots of different sizes on the patch. The antenna is designed by commercially available simulation software. The simulation result shows that it resonates at 1.536 GHz with a return loss value of -50.72 dB having a bandwidth of 48.5 MHz and directivity of 7.13 dBi and the fabricated antenna has a resonant frequency of 1.5 GHz with return loss and bandwidth of -25 dB and 30 MHz, respectively. It is found that the proposed antenna perform much better than a conventional microstrip patch antenna.

Keywords: GPS, L-1 band, rectangular slot-loaded patch antenna.

I. INTRODUCTION

Global Positioning System (GPS) is a well-known technology to determine the exact position and provide navigation functionality to connected-devices. A GPS antenna uses signals from multiple satellites to identify the three-dimensional location. To achieve accurate positioning, the radiation characteristics of GPS antennas should be circularly polarized and have broad beam width. These attributes can be attained mainly by two types of antennas such as quadrifilar helix and microstrip patch antenna (MPA) [1]. However, small size, mechanical robustness, low fabrication cost and easy installation process have made microstrip patch antennas more favorable than quadrifilar helix antennas for GPS navigation. Moreover, microstrip patch antennas have applications in cellular communication, satellite communication, medical sector, etc. [2, 3]. Despite the advantages, MPAs have some drawbacks such as low gain, narrow bandwidth, multiple resonances, less efficiency and low power handling capability [4-7]. Researchers have been working on MPAs to overcome all these flaws. For

instance, the return loss characteristics, bandwidth, and gain are improved by designing MPAs of rectangular [7], circular [8], and E-shaped patches [9]. Slot-loaded MPAs have also been made to enhance the performance furthermore [10]. Different feeding techniques with various substrate materials are also examined to overcome the limitations of the MPAs [11,12].

In this paper, we have proposed a new structure of a microstrip patch antenna which is designed for a single resonant frequency of 1.575 GHz. It is found that the resonance characteristics of the proposed antenna can be improved by using four rectangular slots of different sizes placed symmetrically into the patch. The return loss (S_{11}) and bandwidth of the tetra-slotted rectangular MPA are increased remarkably in comparison with that of the conventional slot-less patch antenna. All the antennas are optimized and designed using CST Microwave Studio software for a various number of rectangular slots. The radiation pattern and S_{11} of the proposed patch antenna are measured using Vector Network Analyzer or VNA (Rohde & Schwarz-ZVH8) and Wave and Antenna Training System (Man & Tel Co.). The antennas are fabricated on 1.6 mm thick FR-4 substrate. The S_{11} of the proposed tetra-slotted patch antenna are found -50.72 dB and -25 dB from simulation and measurement, respectively. Moreover, the measured values of other parameters such as resonant frequency, bandwidth, VSWR, and directivity allow us to conclude that the proposed antenna is well suited for the L-1 frequency band application.

In Section II the design procedure of optimization of tetra slotted MPA is described. The simulated and measured results of the proposed antenna are presented in Section III and IV, respectively. And finally, in Section V, we conclude by mentioning the research findings.

II. DESIGN OF THE PROPOSED MICROSTRIP PATCH ANTENNA

The schematic diagram of the proposed MPA and the dimensions of the incorporated slots have been shown in Fig. 1. The length and width of the patch are

Author ^{α σ ρ ω}: Department of Electrical and Electronic Engineering, University of Dhaka, Bangladesh. e-mail: rakib.hasan@eee.du.ac.bd

denoted by L and W , respectively. The signal is applied to the patch through an inset feed transmission line having a length of L_f and a width of W_f . The feed line inset distance is represented by F_i and is separated from the patch by a distance G_f . The substrate is symmetrically divided into four quadrants by vertical and horizontal dashed lines as shown in Fig. 1. The patch has been placed in the middle of the substrate.

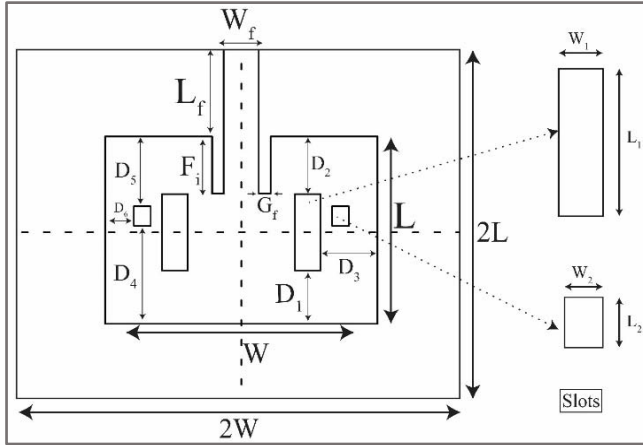


Fig. 1: Proposed structure of tetra-slotted microstrip patch antenna with slot dimensions

To design both slot-less (conventional) as well as slot-loaded (proposed) MPAs we have assumed FR-4 substrate whose dielectric constant (ϵ_r) and height (h) are 4.3 and 1.6 mm, respectively [13]. For GPS application, the resonant frequency (f_r) of our proposed antenna is chosen at 1.575 GHz. With the aforementioned known parameters, the other unknown parameters such as patch length (L), patch width (W) and effective dielectric constant ($\epsilon_{r_{eff}}$) are to be calculated by using the following equations [14].

The patch width, W is expressed as

$$W = \frac{v_0}{2f_r} \sqrt{\frac{2}{\epsilon_r + 1}} \quad (1)$$

where v_0 is the free-space light velocity.

The expression for effective dielectric constant, $\epsilon_{r_{eff}}$ is

$$\epsilon_{r_{eff}} = \frac{\epsilon_r + 1}{2} + \left[\frac{\epsilon_r - 1}{2} \right] \left[\left(1 + \frac{12h}{W} \right)^{-1/2} \right] \quad (2)$$

For $W/h > 1$, which is satisfied for our chosen parameters given in Table-1, the length of the metallic patch, L is determined using the following equation:

$$L = L_{eff} - 2\Delta L \quad (3)$$

where L_{eff} is the effective length of the patch and ΔL is the extended length due to field fringing. The effective length L_{eff} is determined from the following equation:

$$L_{eff} = \frac{v_0}{2f_r \sqrt{\epsilon_{r_{eff}}}} \quad (4)$$

The extended length of the patch is determined from the following expression:

$$\Delta L = 0.412 h \times \frac{(\epsilon_{r_{eff}} + 0.3) \left(\frac{W}{h} + 0.264 \right)}{(\epsilon_{r_{eff}} - 0.258) \left(\frac{W}{h} + 0.8 \right)} \quad (5)$$

The expression for microstrip feed-line length (L_f) is

$$L_f = \frac{v_0}{4f_r \sqrt{\epsilon_r}} \quad (6)$$

The value of the width of the microstrip feed-line W_f is found from the results of best fit. By varying W_f from $W/10$ to $W/5$, the best fit has been found at 7.5 mm (see Table-1).

The gap between the patch and the feed line is often called the notch width. We have denoted this notch width by G_f and taken its value to be of 0.6 mm. For an inset feed MPA, it is also customary to define the distance by how much the microstrip feed-line will insert into the patch. We have denoted this distance by F_i and the equation to determine this distance is mentioned below [15]:

$$F_i = 10^{-4} \{ F_{c7} \epsilon_r^7 + F_{c6} \epsilon_r^6 - F_{c5} \epsilon_r^5 + F_{c4} \epsilon_r^4 - F_{c3} \epsilon_r^3 + F_{c2} \epsilon_r^2 - F_{c1} \epsilon_r^1 + F_{c0} \} \frac{L}{2} \quad (7)$$

where $F_{c7} = 0.001699$, $F_{c6} = 0.13761$, $F_{c5} = 6.1783$, $F_{c4} = 93.187$, $F_{c3} = 682.93$, $F_{c2} = 2561.9$, $F_{c1} = 4043$, and $F_{c0} = 6697$.

The design of our proposed MPA starts by observing the characteristics of a conventional MPA (without slots). Keeping all the structural parameters same, a conventional MPA is first simulated. According to calculation, the antenna has a dimension of 91.2 mm by 117.0 mm. To improve the attributes of the conventional MPA, we have introduced few slots of different sizes placed symmetrically on the patch as shown in Fig. 1. After several attempts of optimization, we have found that the characteristics of the MPA are remarkably enhanced by two pairs of slots having different dimensions; one pair of slots is 18.66 mm \times 5.22 mm ($L_1 \times W_1$; large-slot), and the other pair is 4.79 mm \times 3.61 mm ($L_2 \times W_2$; small-slot).

The placement of the slots on the patch also plays a vital role in the overall performance of the antenna. The large- and small- slot pairs are described by the distances (D_1, D_2, D_3) and (D_4, D_5, D_6), respectively from the edges of the patch (see Fig. 1.) For achieving a satisfactory result, the large-slot pair should be at a distance of $D_1 = 12.94$ mm, $D_2 = 14.00$ mm and

$D_3 = 12.23$ mm. Similarly, the small-slot pair should be placed at a distance of $D_4 = 23.83$ mm, $D_5 = 16.98$ mm and $D_6 = 6.15$ mm. The optimized values of the structural parameters which give best simulation results are shown in Table-1. The results of simulation and measurements of different MPAs are discussed in the following sections.

Table 1: Parameters of MPA Obtained from Calculation

Parameters	Optimized Value	Parameters	Optimized Value
Frequency, f_r (GHz)	1.575	Thickness of Copper Layer, M_t (mm)	0.1
Wavelength, λ (mm)	190.476	L_1 (mm)	18.66 ($\cong 0.1\lambda$)
Dielectric constant, ϵ_r	4.3	W_1 (mm)	5.22 ($\cong 0.027\lambda$)
Substrate Height, h (mm)	1.6	L_2 (mm)	4.79 ($\cong 0.025\lambda$)
Patch Width, W (mm)	58.5 ($\cong 0.3\lambda$)	W_2 (mm)	3.61 ($\cong 0.018\lambda$)
Patch Length, L (mm)	45.6 ($\cong 0.23\lambda$)	D_1 (mm)	12.94 ($\cong 0.067\lambda$)
Substrate Width, $2W$ (mm)	117.0 ($\cong 0.61\lambda$)	D_2 (mm)	14.00 ($\cong 0.07\lambda$)
Substrate Length, $2L$ (mm)	91.2 ($\cong 0.47\lambda$)	D_3 (mm)	12.23 ($\cong 0.064\lambda$)
Microstrip Transmission Line Length, L_f (mm)	22.96 ($\cong 0.12\lambda$)	D_4 (mm)	23.83 ($\cong 0.125\lambda$)
Microstrip Transmission Line Width, W_f (mm)	7.5 ($\cong 0.039\lambda$)	D_5 (mm)	16.98 ($\cong 0.089\lambda$)
Microstrip Line Inset Feed Length, F_i (mm)	13.9 ($\cong 0.07\lambda$)	D_6 (mm)	6.15 ($\cong 0.032\lambda$)
Gap between patch and feed line, G_f (mm)	0.6 ($\cong 0.003\lambda$)		

III. SIMULATION RESULTS

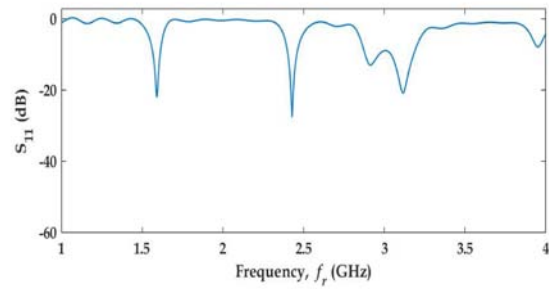
For the structural optimization and analysis of MPA, we have used CST Microwave Studio software. Simulation results of the resonant frequency, return loss, bandwidth, radiation pattern and directivity of MPA are presented in the following sections.

a) Return Loss

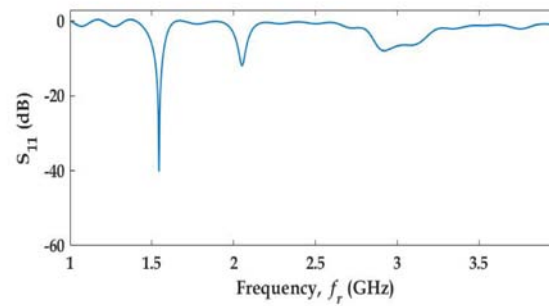
Figure 2 shows the return loss (S_{11}) of conventional (without slot) as well as proposed (with slot) MPA. Even though the designed parameters are set to have a resonant frequency of 1.575 GHz, we have found the main return loss peak at (1.575+0.015) GHz for the conventional (Fig. 2(a)) and at (1.575-0.039) GHz for proposed antennas (Fig. 2(b,c)). Several other return loss peaks appear at resonant frequencies of 2.42 GHz, 2.90 GHz and 3.11 GHz for the conventional MPA. By introducing slots, these other return loss peaks are completely suppressed as shown in Fig. 2(b) and 2(c).

In Fig. 2(b) and 2(c), the results of return losses are shown for two-slot and four-slot MPA, respectively. For two slots into the patch, there is only one resonant frequency at 1.544 GHz which is 0.031 GHz less than the desired resonant frequency of 1.575 GHz (see Fig. 2(b)). For four-slot MPA, the return loss peak is obtained at a frequency of 1.536 GHz which is 0.039 GHz shorter than 1.575 GHz (see Fig. 2 (c)).

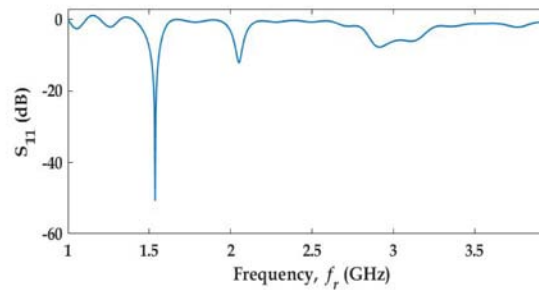
From Fig. 2 it is seen that the magnitude of return loss has been increased significantly for our proposed patch antenna. The magnitude of S_{11} is Found -21.94 dB for the conventional MPA (see Fig. 2(a)) whereas that of S_{11} is obtained -40.22 dB and -50.72 dB for two-slot and four-slot MPA, respectively (see Fig. 2 (b, c)). Thus our proposed antenna has only one dominant resonant frequency with a very large S_{11} magnitude.



(a)



(b)



(c)

Fig. 2: Simulated Return Loss Value of Simple MPA

(a) Conventional (without slot), (b) Proposed (with two-slot), (c) Proposed (with four-slot)

b) Far-Field Radiation Pattern

In Fig. 3, the obtained simulation results of the radiation patterns are shown. The main lobe magnitude (i.e., gain) of the conventional antenna is found to be 2.28 dB (see Fig. 3(a)). Introducing slots into the patch, the main lobe magnitude is obtained very close to the conventional one. For our proposed two-slot and four-slot MPAs, the main lobe magnitudes are found 1.97 dB and 2.12 dB, respectively. The main lobe direction has remained same at 0.0 deg for all MPAs.

From Fig. 3, it is seen that -3 dB beamwidths of conventional, two-slot, and four-slot MPAs are found at 92.0, 91.8, and 91.2 degrees, respectively. Thus -3 dB beamwidth for four-slot MPA is the smallest which means directivity has increased in comparison to the

conventional one. Also, the side lobe levels of conventional, two-slot, and four-slot MPAs are obtained -12.5, -12.5, and -12.6 dB, respectively. Therefore, our proposed MPA has the lowest value of side lobe level and its efficiency has increased.

The VSWR value decreases towards unity at or near desired resonant frequency for our proposed structure. The simulated values of VSWR are 1.17, 1.02 and 1.005 for conventional, double-slotted (two-slot) and tetra-slotted (four-slot) MPA, respectively. Finally, the bandwidth and the directivity of our proposed tetra-slotted antenna have been obtained 48.5 MHz and 7.13 dBi, respectively. The other directivities of the conventional and two-slotted MPA are quite similar to the proposed one.

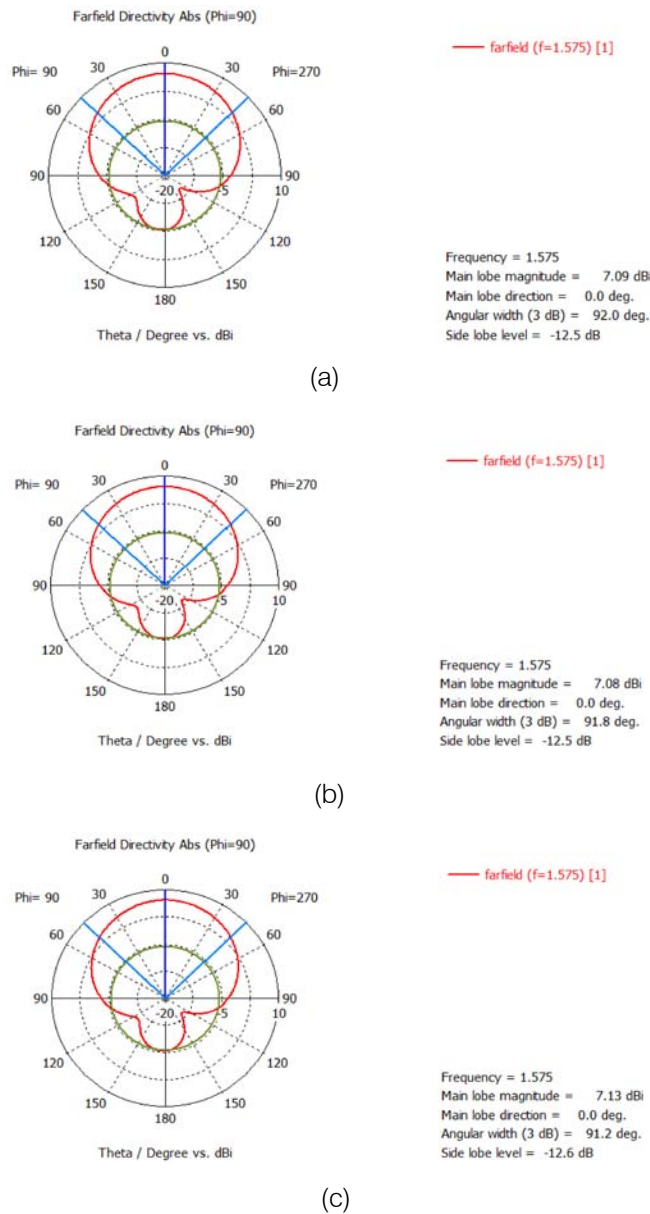


Fig. 3: Far-field Radiation Gain of Designed Antennas
(a) Without slot, (b) With Two Slots, (c) With Four Slots

All the results of simulation are shown in Table-2 for comparison. It is clear from Table-2 that the tetra (four) slotted MPA has better characteristics than other two antennas regarding resonant frequency, return loss and VSWR. But the main lobe magnitude, bandwidth, and directivity are somewhat comparable to the other two antennas. Thus our proposed four-slot microstrip patch antenna provides single resonant frequency in the range of 0 to 4 GHz range.

Table 2: Antenna Characteristics Obtained from Simulation

Parameters	Conventional MPA	MPA with two slots	MPA with four slots
Resonant Frequency, f_r (GHz)	1.59, 2.42, 2.90, 3.11	1.54	1.54
S_{11} (dB)	-21.94, -27.56, -14.17, -19.96	-40.22	-50.72
Bandwidth (MHz)	44.9, 52.6, 91, 119.1	48.8	48.5
VSWR	1.17, 1.09, 1.49, 1.22	1.02	1.005
Gain (dB)	2.28	1.97	2.12
Directivity (dBi)	7.09	7.08	7.13

IV. MEASURED RESULTS

Among the simulation results of all three antennas, better characteristics are found for tetra-slotted MPA which we have finally fabricated for experimental measurement. At first, the substrate has been cut into pieces having the dimensions of the antenna as given in Table-1. Then the patch antenna layout is printed on a tracing paper for photoresist masking. Lastly, chemical etching has been done to complete the fabrication process. The SMA (Sub Miniature version A) connectors have been attached to the antenna port through an aluminum mount at our Central Science Workshop. Both front and back view of the fabricated tetra-slotted antenna are shown in Fig. 4. Return loss value (S_{11}) and radiation pattern of the fabricated antenna have been measured using VNA (Rohde & Schwarz– ZVH8) and Wave and Antenna Training System (Man & Tel Co.).

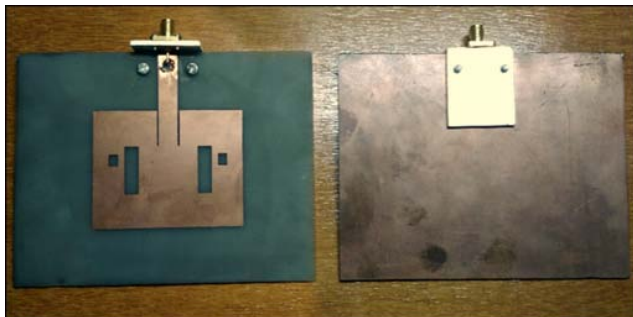


Fig. 4: Front Side (left) and Back Side (right) view of the proposed tetra slotted MPA.

Figure 5 shows the measured return loss characteristics of the proposed fabricated antenna. The return loss (S_{11}) value of the fabricated antenna is found

to be about -25 dB at 1.5 GHz. The deviation of return loss magnitude from simulated results may be due to the lossy FR-4 substrate and lack of precise fabrication of patch and slots with wet etching. At the resonant frequency, the bandwidth is found about 30 MHz. No significant return loss peaks at any other frequencies are found in the range of 1 GHz to 3 GHz.

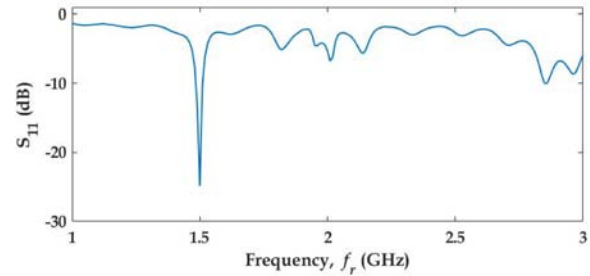


Fig. 5: Measured Return Loss (S_{11}) of the fabricated tetra slotted MPA.

The measured radiation pattern is shown in Fig. 6. The main lobe radiation pattern is quite hemispherical, and the back lobe pattern is very small as obtained in simulation. Small back lobe characteristics represent that our proposed MPA has good directivity. All the measurements are taken in a room without the anechoic chamber. From Fig. 6 it is seen that the experimental results agree to a great extent with the simulated radiation patterns.

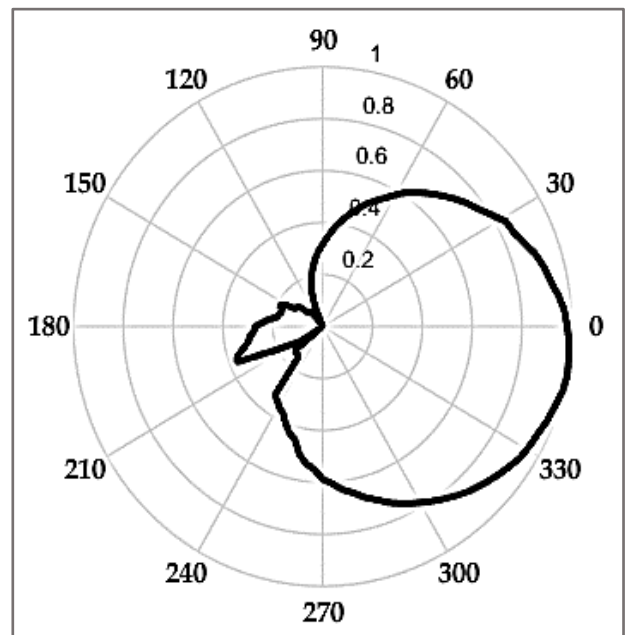


Fig. 6: Measured Radiation Pattern of the fabricated tetra slotted MPA.

V. CONCLUSION

For GPS application in the L-1 band, a tetra-slotted microstrip patch antenna is designed and fabricated at 1.575 GHz. The return loss characteristics are greatly enhanced by introducing four slots placed symmetrically on the patch in comparison to a conventional one without any slot. With two types of slots, our proposed antenna gives satisfactory results regarding single resonant frequency with improved directivity. From the simulation results, the return loss (S_{11}), VSWR, and directivity are found -50.72 dB, 1.005, and 7.13 dBi, respectively. The measured data of the tetra-slotted antenna are found very close to the simulated ones. The scope of precise fabrication and measurement in an anechoic chamber may have given improved data. Nevertheless, the antenna qualifies to work well in many applications related to GPS and other navigation systems.

ACKNOWLEDGMENT

The research work has been carried out at Microwave and Optical Fiber Communication Laboratory at the Department of Electrical and Electronic Engineering, the University of Dhaka, Bangladesh funded by Higher Education Quality Enhancement Project (HEQEP). Authors would like to thank Mr. M.A.R. Ohi, Mr. Sahil Hassan and Mr. Zahid Hasan for their assistance and also the technical persons of the Central Science Workshop, the University of Dhaka for their support.

REFERENCES RÉFÉRENCES REFERENCIAS

1. Sun, Y., Leung, K. and Lu, K. (2017). Broadbeam Cross-Dipole Antenna for GPS Applications. *IEEE Transactions on Antennas and Propagation*, 65(10), pp.5605-5610.
2. Rachmansyah, Antonius, Mutiara et al., "Designing and Manufacturing Microstrip Antenna for Wireless Communication at 2.4 GHz," *International Journal of Computer and Electrical Engineering*, Vol. 3, No. 5 (October 2011).
3. Za'aba, A., Ibrahim, S., Malek, N. and Ramly, A. (2017). Development of wearable patch antenna for medical application. 2017 IEEE Regional Symposium on Micro and Nanoelectronics (RSM).
4. K. Mondal et al., "Effect of feeding locations on bandwidth, gain and resonance frequency of the patch antenna", 2015 International Conference on Microwave and Photonics (ICMAP), 2015.
5. Prakash Kumar Mishra et al., "Multiband Microstrip Antenna for 4G Mobile Application", 2015 Fifth International Conference on Communication Systems and Network Technologies, IEEE, pp. 60-63, 2015.
6. Nandgaonkar, A., Deosarkar, S. and Shirbahadurkar, S. (2007). A modified half U-slot microstrip patch antennas with shorting wall. 2007 IEEE Sarnoff Symposium.
7. M.A.R. Ohi, M.S. Sadique, S. Hussain, A. Ahmed, "Design and Fabrication of Slot-Loaded Microstrip Patch Antenna at 2.45 GHz", *International Journal of Advanced Research in Electrical, Electronics and Instrumentation Engineering*, 2017.
8. Zahid Hasan, Ashiq Zaman, Dr. Anis Ahmed, "Design and Fabrication of a Circular Microstrip Patch Antenna for GPS Application", *The International Journal of Electronics & Communication Technology (IJECT)*, 2017.
9. Mario Reyes-Ayala, Edgar Alejandro Andrade-Gonzalez, Jose Raul, Miranda-Tello, "Rectangular Microstrip Antenna for GPS receiver", *Recent Advances on Systems, Signals, Control, Communications and Computers*.
10. K. N. Lal, A. K. Singh, "Modified design of microstrip patch antenna for WiMAX communication system", *Students' Technology Symposium (TechSym)*, 2014 IEEE, pp. 386-389, 2014.
11. B. T. Salokhe and S. N. Mali, "Analysis of Substrate Material Variation on Circular, Rectangular and Non-Linear Microstrip Patch Antenna," *International Journal of Current Engineering and Technology*, Vol.4, No.3 (June 2014).
12. Hemant Kumar Varshney et al., "A Survey on Different Feeding Techniques of Rectangular Microstrip Patch Antenna," *International Journal of Current Engineering and Technology*, Vol.4, No.3 (June 2014).
13. P. A. H. Vardhini and N. Koteswaramma, "Patch antenna design with FR-4 Epoxy substrate for multiband wireless communications using CST Microwave studio," in 2016 International Conference on Electrical, Electronics, and Optimization Techniques (ICEEOT), 2016.
14. Balanis. *Antenna Theory-Analysis And Design*. 3rd ed. John Wiley & Sons.
15. M. Ramesh and YIP KB, "Design Formula for Inset Fed Microstrip Patch Antenna", *Journal of Microwaves and Optoelectronics*, Vol. 3, No. 3, December 2003.
16. Palecek, J., Vestenicky, M., Vestenicky, P. and Spalek, J. (2012). Examination of SMA connector parameters. 2012 IEEE 16th International Conference on Intelligent Engineering Systems (INES).

This page is intentionally left blank



GLOBAL JOURNAL OF RESEARCHES IN ENGINEERING: F
ELECTRICAL AND ELECTRONICS ENGINEERING
Volume 18 Issue 1 Version 1.0 Year 2018
Type: Double Blind Peer Reviewed International Research Journal
Publisher: Global Journals
Online ISSN: 2249-4596 & Print ISSN: 0975-5861

Design and Manufacturing of an Array and Single Microstrip Patch Antenna to Transmit and Receive by using Same Patch Shape

By Ahmed Jameel Abdulqader & Yaser Ahmed Ali
University of Ninevah

Abstract- In the last years, the progress in communication systems requires the development of high gain and low-cost Microstrip array antennas with suitable feeding technique and a dielectric substrate for applications in 2.1 GHz. The array antenna and single antenna were constructed on a substrate FR4 with a relative permittivity of 4.3. The suggested single antenna is benefited of a compact size of 50×30 mm² at 2.1GHz frequency band and the suggested dimension array antenna is 160×52 mm². The antenna is Microstrip line feeder and is simulated on CST software. Performance parameter evaluated are increased by using reflection, the array design has directivity up to 8.955 dBi and Gain up to 8.506 dB with satisfactory radiation characteristics. The single design has directivity up to 2.352 dBi and Gain up to 2.206 dB with satisfactory radiation characteristics. Been fabricated the array and single Microstrip antenna using CNC Machine.

Keywords: *microstrip array antenna, single microstrip antenna, patch shape, 3g applications.*

GJRE-F Classification: FOR Code: 100501



Strictly as per the compliance and regulations of:



Design and Manufacturing of an Array an Single Microstrip Patch Antenna to Transmit and Receive by using Same Patch Shape

Ahmed Jameel Abdulqader^α & Yaser Ahmed Ali^σ

Abstract- In the last years, the progress in communication systems requires the development of high gain and low-cost Microstrip array antennas with suitable feeding technique and a dielectric substrate for applications in 2.1 GHz. The array antenna and single antenna were constructed on a substrate FR4 with a relative permittivity of 4.3. The suggested single antenna is benefited of a compact size of 50×30 mm² at 2.1GHz frequency band and the suggested dimension array antenna is 160×52 mm². The antenna is Microstrip line feeder and is simulated on CST software. Performance parameter evaluated are increased by using reflection, the array design has directivity up to 8.955 dBi and Gain up to 8.506 dB with satisfactory radiation characteristics. The single design has directivity up to 2.352 dBi and Gain up to 2.206 dB with satisfactory radiation characteristics. Been fabricated the array and single Microstrip antenna using CNC Machine. The practical results of radiation patterns and gain for two cases (array and single) are approximately similar to theoretical results. The computer simulation results show that the antenna having good impedance bandwidth ($S_{11} < -10$ dB) at the resonant frequency.

Keywords: microstrip array antenna, single microstrip antenna, patch shape, 3g applications.

I. INTRODUCTION

Modern wireless communication system requires simple structure, lightweight, low profile, and high gain antennas to assure high efficiency, mobility, and reliability characteristics. Microstrip antenna satisfies such requirements. This antenna provides all of the advantages of printed circuit technology. These features of Microstrip antennas create them public in many wireless communication applications such as radar, satellite communication, medical applications, etc. [1]. The restrictions of Microstrip antennas are narrow frequency band and disability to operate at high power levels of a coaxial line, waveguide or even strip line.

Therefore, the defy in Microstrip antenna design is to increase the bandwidth and gain [2]. Different array configurations of Microstrip antenna can give high gain, wide bandwidth and improved efficiency. The distribution of voltages through the elements of an array depends on feeding network. Suitable feeding network cumulate all of the induced voltages to feed into one point [3]. The proper impedance matching over the series and corporate feeding array configurations supplies high efficiency Microstrip antenna. Power distribution through antenna elements can be modified by corporate feed network. The corporate feed network can lead beam by introducing phase change [2].

In the array antennas, elements can be fed by a single line or by several lines in a feed network configuration. Based on their feeding methods, arrays are classified as Series feed network and T-shaped corporate feed network. Series-feed Microstrip array is molded by intersecting all the elements with high impedance transmission line and feeding the power at the first element. Because the feed arrangement is compact the line losses related to this type of array are lower than those of the corporate-feed type [2]. Series-fed arrays can be conveniently fabricated using photolithography for both the radiating elements and the feed network. However, this technique is limited to arrays with a fixed beam or those which are scanned by varying the frequency, but it can be applied to linear and planar arrays with single or dual polarization. Also, any changes in one of the elements or feed lines affect the performance of the others. Therefore in a design, it is important to be able to take in to account these and other effects, such as mutual coupling, and internal reflections. Those who have been designing and experiment arrays antennas mention that radiation from the feed line, using either series or corporate-feed network, is an earnest problem that limits the cross-polarization and sidelobe level of the arrays. Both cross polarization and sidelobe levels can be improved by isolating the feed network from the radiating face of the array. This can be accomplished using either probe feeds or aperture coupling. The main limitation in series-feed arrays is the big variation of the impedance and beam-pointing direction over a band of frequencies [2].

Author α: Assistant Lecturer in University of Ninevah College of Electronics Engineering Systems and Control Engineering.
e-mail: ah_8611@yahoo.com

Author σ: Baiji Oil Training Institute, Ministry of Oil.
e-mail: yaser_ah2000@yahoo.com

II. ARRAYS AND FEED NETWORKS

Performance of antenna arrays depends on our ability to feed the array elements with input currents having accurate phase relationships. This can be accomplished by using appropriately designed “feed networks” consisting of transmission line (TL) segments. We continue our study of antenna arrays with examples illustrating feed network design issues. The Microstrip antenna can be agitated either by a Microstrip line or coaxial probe. It can also be excited indirectly using electromagnetic coupling or aperture coupling and a coplanar waveguide feed, in which case there is no direct metallic contact between the feed line and the patch [4]. Feeding technique effective the input impedance and characteristics of an antenna and is an influential parameter. Elements of an array can be fed by a single line, known as a series-feed network, or by multiple lines, known as a corporate-feed network, shown in Fig 1.

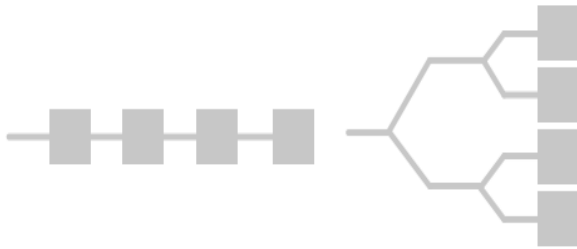


Fig. 1: Series Feed and Corporate Feed Networks.

III. CORPORATE FEED NETWORK

This Network gives more control of the feed of each element (amplitude and phase) and they are perfect for multi-beam arrays or formed-beam arrays. The amplitude can be changed with an amplifier or an attenuator when the phase can be controlled using a phase shifter. This network is used to supply power division of $2n$ (i.e. $n = 2, 4, 6$, etc.). This idea can be checked by using either tapered lines as shown in Fig 2 or by using $(\lambda/4)$ quarter wavelength transformers as shown in Fig 3 [2].

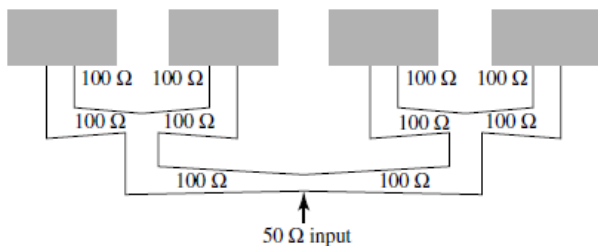


Fig. 2: Corporate-Feed Networks with Tapered Lines.

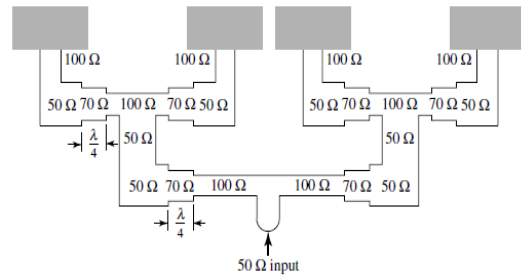


Fig. 3: Corporate-Feed Networks with $\lambda/4$ Transformers.

This power split can be achieved by using three port power dividers of equal division (3dB) with the use of a T-junction power divider. An ideal power divider is lossless, reciprocal and matched at all ports. A T-junction power divider is reciprocal and can be considered lossless if the transmission line loss is not taken into account [5]. Helmholtz reciprocity theorem (generalized by Carson) states that “If an emf (electromagnetic force) is applied to the terminals of an antenna A and the current measured at the terminals of another antenna B, then an equal current (in both amplitude and phase) will be obtained at the terminals of antenna A if the same emf is applied to the terminals of antenna B [6]”. A T-junction can be modeled as a junction of three transmission lines as shown in Fig 4.

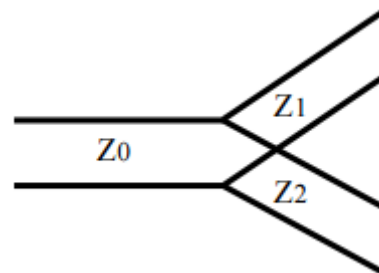


Fig. 4: Lossless T-Junction Models.

The divider, illustrated in Fig 4, is matched to the input characteristic impedance „ Z_0 ” by the following formula:

$$\frac{1}{Z_1} + \frac{1}{Z_2} = \frac{1}{Z_0}$$

For an input impedance of $Z_0 = 50 \Omega$, Z_1 and $Z_2 = 100 \Omega$. Quarter-wave transformers are introduced into a corporate-feed network to connect two transmission lines with different impedances together without causing an impedance mismatch. Fig 5 shows a quarter-wave transformer between the load impedance Z_L and input impedance Z_C' .

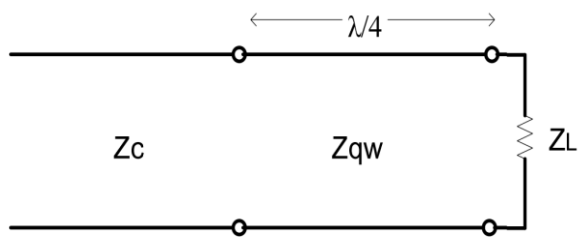


Fig. 5: $\lambda/4$ Matching Transformer.

The following formula is applicable when the transformer is a quarter-wavelength or an odd multiple of a quarter-wavelength for a perfect impedance match:

$$Z_{qw} = \sqrt{Z_c Z_L}$$

A quarter-wave transformer with the input impedance of $Z_C = 50\Omega$ and load impedance of $Z_L = 100\Omega$ is equal to $Z_0 = 70.71\Omega$. These formulas explain the values used in Fig 3.

IV. BENDS IN TRANSMISSION LINES

There is no best way to bend a Microstrip or stripline transmission line. The first problem is that the discontinuity changes the line characteristic impedance; without compensation, the bend adds shunt capacitance. But in reality, the small capacitance that is usually a result doesn't change the circuit's performance

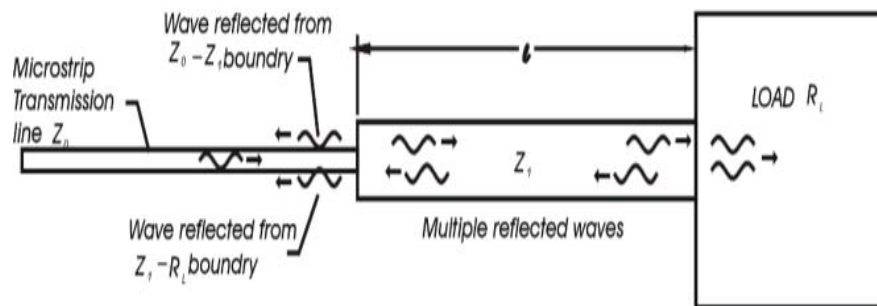


Fig. 7: Quarter wave Impedance Transformer.

In a quarter-wave transformer, a load resistance R_L needs to be matched to the characteristic feed line impedance Z_0 through a short length of transmission line of unknown length l and impedance. The input impedance Z_1 looking into the matching section of line is given by:

$$Z_{in} = Z_1 \frac{R_L + jZ_1 \tan \beta l}{Z_1 + jR_L \tan \beta l}$$

very much. The other problem associated with bends it can cause far more damage to the intended performance of a highly tuned circuit: the effective length of the transmission line becomes shorter than the centerline length. Show Fig 6.

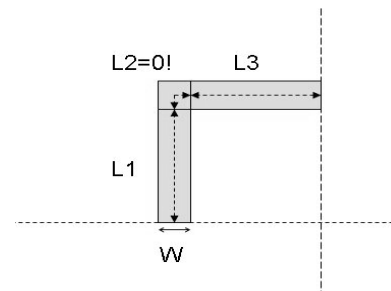


Fig. 6: Model of Corner Bend.

V. QUARTER-WAVE TRANSFORM

In the case of mismatch in impedance between two points on a transmission line can be compensated with a $(\lambda/4)$ quarter-wave transformer [7]. The quarter-wave transformer $(\lambda/4)$ is a very profitable matching technique that also explains the properties of standing waves on a mismatched line. First, an impedance-based illustration of how a quarter-wave transformer works will be qualified; then a more intuitive illustration that is similar to ruinous interference in thin films will be discussed. A quarter wave transformers $(\lambda/4)$ in Microstrip are shown in Fig 7.

In the case of an ideal transition with no reflections at the interface between Microstrip $Z_{in} = Z_0$ and load, and this gives us characteristic impedance Z_1 as:

$$Z_1 = \sqrt{Z_0 R_L}$$

which is the geometric mean of the load and source impedances. From this conFig, there will be no standing

waves on the feedline although there will be standing waves on the quarter wave transformers ($\lambda/2$) matching section. In fact, any odd multiple $(2n + 1)$ of $l = \lambda/4$ will also work.

When the line length is precisely $\lambda/4$ the reflected wave from the load destructively interferes with the wave reflected from Z_0, Z_1 the interface and they cancel each other out. It should be noted that this method can only match a real load. If the load has an appreciable imaginary component, it must be matched differently. It can be transformed into a purely real load, at a single frequency, by adding an appropriate length of feedline. Fig 8 shows the complete feed network with the patches. There are many transmission lines, V grooves, power splitters, and quarter wave transformers.

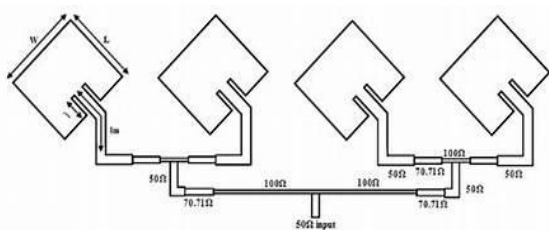


Fig. 8: Feed Network for the Array.

VI. DESIGN PROCEDURE

A Microstrip antennas is designed to resonate at 2.1 GHz frequency with dielectric constant $\epsilon_r = 4.3$, substrate thickness $h=1.6$ mm, $L=50$ mm, $W=35$ mm on a ground plane. All dimensions of the antenna are in mm. Fig 9, A,B shows the design of microstrip antenna (single and array antenna) .Table 1 shows the value of the parameter for microstrip array antenna.

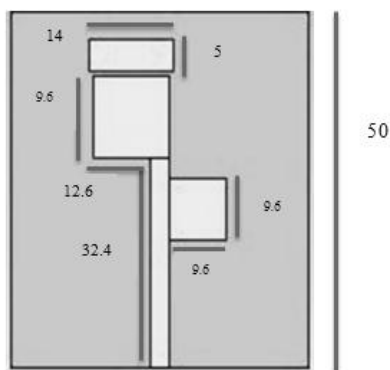


Fig. 9: (A) Suggested Single Microstrip Antenna.

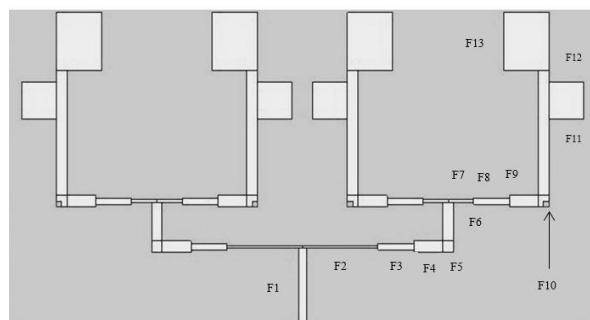


Fig. 9: (B) Suggested Array Microstrip Antenna.

Table 1: Various dimensions of patch, ground plane and corporate feed line network

1.Patch dimensions:

Length of the patch	160 mm
Width of the patch	52 mm

2.Ground plane dimensions:

Length of the ground plane	160 mm
Width of the ground plane	30 mm

3. Corporate feed line dimensions

F1 feed dimensions (WxL)	(2.22*19.8
F2 feed dimensions (WxL)	(0.67*21) mm
F3 feed dimensions (WxL)	(1.6*10) mm
F4 feed dimensions (WxL)	(3*8) mm
F5 feed dimensions (WxL)	(3*3) mm
F6 feed dimensions (WxL)	(3*10) mm
F7 feed dimensions (WxL)	(0.67*7) mm
F8 feed dimensions (WxL)	(1.6*10) mm
F9 feed dimensions (WxL)	(3*8) mm
F10 feed dimensions (WxL)	(0.67*0.67) mm
F11 feed dimensions (WxL)	(3*42) mm
F12 feed dimensions (WxL)	(9.6*9.6) mm
F13 feed dimensions (WxL)	(9.6*9.6) mm

VII. SIMULATION RESULTS FOR SINGLE AND ARRAY ANTENNA

Fig 10 (A, B), shows the return loss of the single element antenna and Array antenna. From the diagram it has been observed that the value of return loss is -24.44 dB at 2.1 GHz with bandwidth equal to 339MHz for a single and return loss is -18.65 dB at 2.1 GHz with bandwidth equal to 181MHz for an array. This parameter is determined that how well devices are matched. A match is good if return loss is high in negative value.

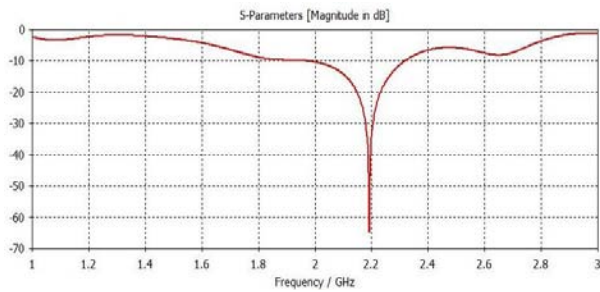


Fig. 10: (A) Return Loss for a Single Antenna.

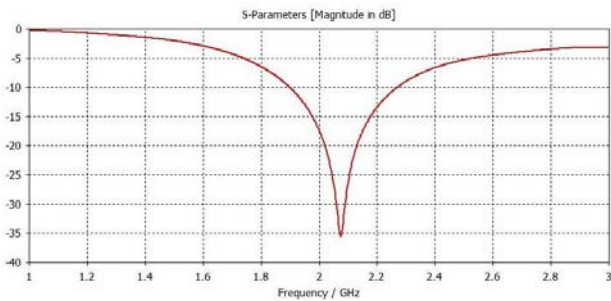


Fig. 10: (B) Return Loss for an Array Antenna.

Fig 11 (A), (B), shows the input impedance of the suggested single and array antenna. The real impedance nearest from 50Ω and the imaginary from 0Ω and also the real impedance of the array nearest from 50Ω and the imaginary from 0Ω and this means that the antenna has a good matching.

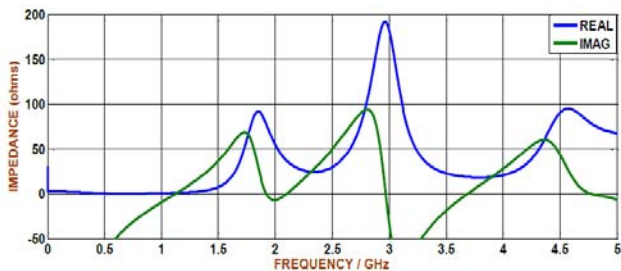


Fig. 11: (A) Input Impedance of Single Antenna.

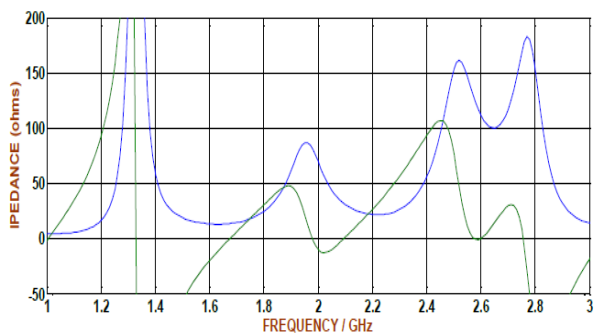


Fig. 11: (B) Input Impedance of Array Antenna.

Fig 12 (A), (B), shows the gain versus frequency for the single and array antenna. The gain of the antenna is the quantity which describes the performance of the antenna or the capability to concentrate energy through a direction to give a better picture of the radiation performance. In this suggested design we obtained gain are 2.2 dB and 8.5dB respectively.

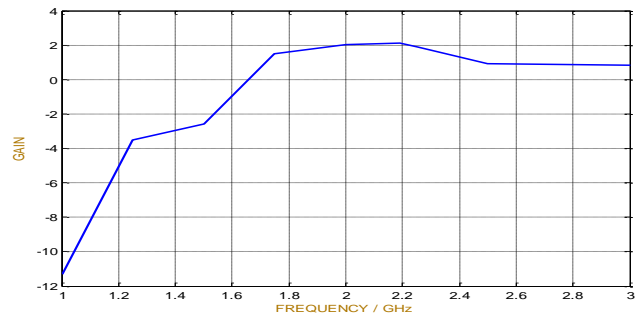


Fig. 12: (A) Gain of a Single Antenna.

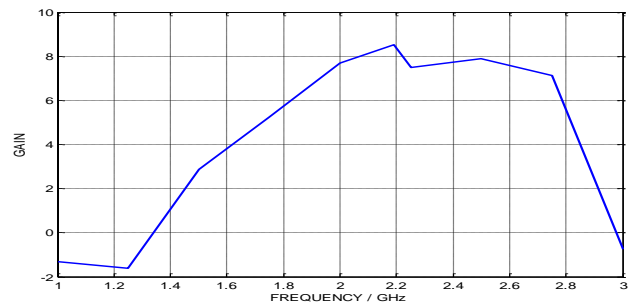


Fig. 12: (B) Gain of an Array Antenna.

In this design we obtained the directivity for the single and array antenna. The directivity of a single and the array are 2.235 dBi and 8.955 dB respectively. Show Fig 13 (A), (B).

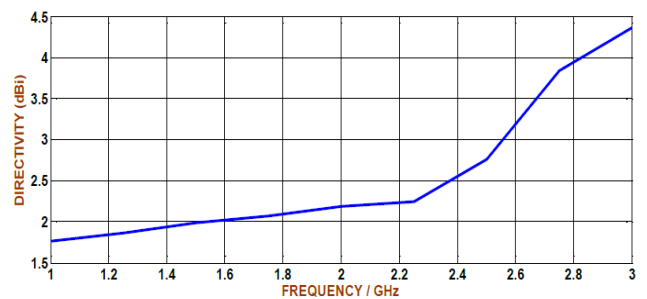


Fig. 13: (A) Directivity of Single Antenna.

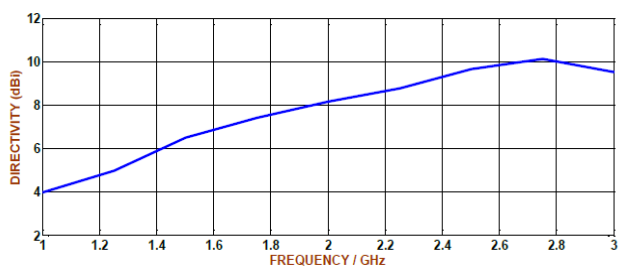


Fig. 13: (B) Directivity of Array Antenna.

Fig 14 (A), (B), shows the efficiency of the single antenna and array antennas. From fig. 12 the efficiency of single antenna is 94% at 2.1 GHz and the efficiency of array antenna is 82%.

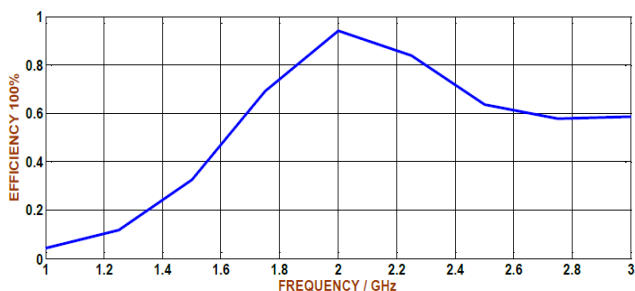


Fig. 14: (A) Efficiency of Single Antenna.

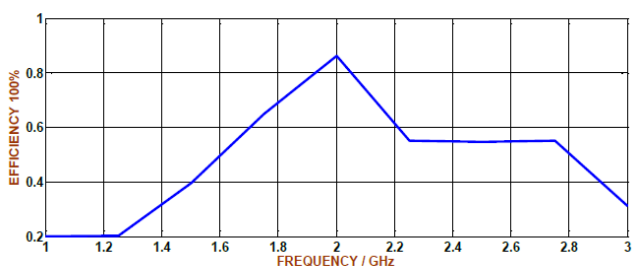


Fig. 14: (B) Efficiency of Array Antenna.

The 2D far - field radiation patterns at E – plane (x-y plane) and H - plane (x- z plane) for the center frequency of single antenna and array antenna are plotted in Fig 15 (A), (B). The simulated results show that the radiation patterns at single and array antennas are similar to that of a conventional simple monopole antenna radiation patterns. Established on these radiation patterns, the proposed antenna demonstrate omnidirectional radiation characteristics in the E-plane, and broadside radiation characteristics in the H-plane at the considered frequencies.

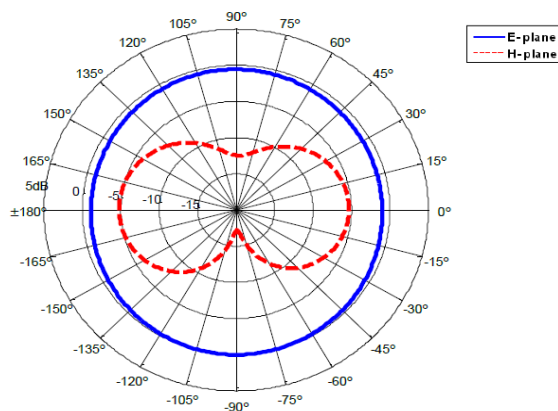


Fig. 15: (A) Radiation Pattern of Single Antenna.

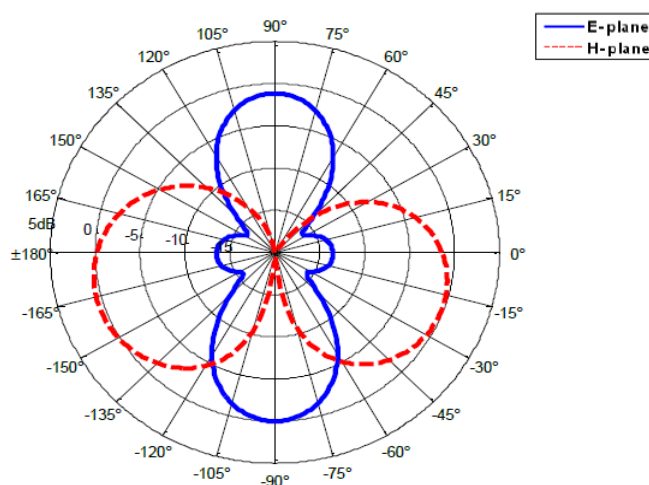


Fig. 15: (B) Radiation Pattern of Array Antenna.

VIII. MANUFACTURING OF ARRAY AND SINGLE MICROSTRIP ANTENNA

In this section I will manufacture the array and single antenna, and then I obtained the practical results of the antennas in the laboratory after the manufacturing and compare with simulation results. In the Fig 16 you can see the final prototype of antennas after manufacturing by using CNC machine. Been connect Transmitting (Array Antenna) and Receiving (Single Antenna) as shown Fig 17.



Fig. 16: Manufacturing of Antennas.

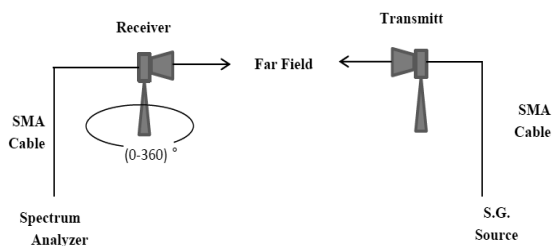


Fig. 17: Connection methods inside of lab.

IX. RADIATION PATTERN MEASUREMENTS

Radiation patterns measured in side anechoic chamber. Practically, Radiation patterns measured on two planes (E- Plane & H- Plane). The practical results of radiation patterns for two cases (array and single) are approximately similar to theoretical results. Fig 18 shows the comparison between the practical and theoretical results for the single patch antenna.

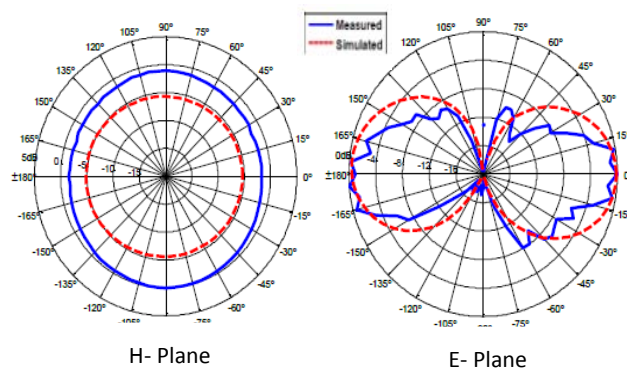


Fig. 18: Compare between the practical and theoretical Radiation patterns results for single.

Fig 19 shows the practical and theoretical radiation patterns for Array Antenna

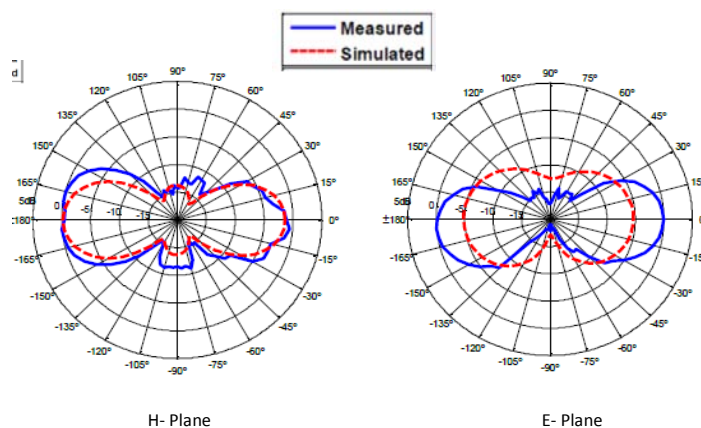


Fig. 19: Compare Between the Practical and Theoretical Results for Array.

X. GAIN MEASUREMENTS

To gain measurements, we use the Friis formula.

$$P_r = P_t G_t G_r FSL$$

By writing the Friis formula as (dB), we obtained:

$$P_r = P_t + G_t + G_r - FSL$$

$$FSL = 20 \log\left(\frac{4\pi D}{\lambda}\right)$$

Where FSL is Free Space Loss. P_r and P_t are received and transmitted power respectively. G_r and G_t

are received and transmitted Gain respectively. D , the distance between transmitter and receiver, λ is Wavelength. From the measuring the transmitted and received power

Table 2: Comparison Between Simulated and Measuring Gain

Antenna	Simulated gain (dB)	Measuring gain (dB)
Single Microstrip Antenna	2.206	2.04
Array Microstrip Antenna	8.506	8.313

XI. CONCLUSION

In this research, single and four elements Microstrip patch antenna array by corporate (parallel)-feed network at 2.1 GHz application are presented. This suggested array antenna is investigated and successfully simulated in this research; the simulated return loss, radiation pattern and bandwidth showed well performance for the single antenna at 2.1GHz. They investigate higher directivity, gain and better bandwidth with practical technology and theoretical analysis. The results of the array antenna are compared with those of single antenna of novel patch Microstrip antenna. It is found that there is an important change in the radiation features of array antenna. It can be concluded from the top results that, designing a proper feed network and impedance matching are very important parameters in Microstrip patch antenna design (single and array). Selection a proper position for ending the feed line affects the overall performance of the antenna. The simulation results show return loss of -64.45 dB for the array antenna and -36.44 dB for the single antenna.

From the results, it is seen that the suggested array and single antenna achieve good value of directivity, gain performance and the antenna has good bandwidth, this makes the suggested antenna design suitable for use in the 2.1GHz applications as a transmitting and a receiving.

REFERENCES RÉFÉRENCES REFERENCIAS

1. M. T. I. Huque, and et al., (2011)"Design and Simulation of a Low-cost and High Gain Microstrip Patch Antenna Arrays for the X-band Applications," *International Conference on Network Communication and Computer - ICNCC2011*, New Delhi,India.
2. C. A. Balanis, (2005)"Antenna Theory Analysis and Design," 3rdEdition, *John Wiley & Sons*.
3. M. M. Alam, R. Ahmmed, and M. Toufikul, (2012)" Gain Improvement of Micro Strip Antenna Using Dual Patch Array Micro Strip Antenna ," *Journal of Emerging Trends in Computing and Information Sciences*, Vol. 3, pp. 1642-1648.
4. G. Kumar and K. P. Ray, (2003)"Broadband Microstrip Antenna," *Artech House*.
5. M. A. Yepes, (2010)"Multilayer Antenna Array for Environmental Sensing Application," *Georgia*,.J. D. Kraus, "Antennas," *McGraw Hill*.
6. H. J. Riblet, (1957)"General Synthesis of Quarter-Wave Impedance Transformer," *IRE Transactions on Microwave Theory and techniques*, Vol. 5, pp. 36-43.
7. S. Pattanaik(2012)," A Study on The Engineering Techniques Adopted for Microstrip Antenna for Achieving Some Specific Performance for Commercial/Personal Communication", *European Journal of Applied Engineering and Scientific Research*, Vol. 1 , pp. 50-56.
8. D. Singh and A. Kumar and others, (2013)" Design and Analysis of Linear Array of Two S-Shaped Microstrip Patch Antenna", *International Journal of Advanced Research in Electrical, Electronics and Instrumentation Engineering*, Vol. 2, Issue 9.



GLOBAL JOURNAL OF RESEARCHES IN ENGINEERING: F
ELECTRICAL AND ELECTRONICS ENGINEERING
Volume 18 Issue 1 Version 1.0 Year 2018
Type: Double Blind Peer Reviewed International Research Journal
Publisher: Global Journals
Online ISSN: 2249-4596 & Print ISSN: 0975-5861

Transient Stability Enhancement of DFIG based Wind Generator by Switching Frequency Control Strategy with Parallel Resonance Fault Current Limiter

By M. R. Islam & M. R. I. Sheikh

Rajshahi University of Engineering & Technology

Abstract- Doubly fed induction generator (DFIG) based wind turbine generation system is generally sensitive to the grid faults as its stator windings are directly connected to the grid. As the wind power penetration to the grid increases day by day, a complete shutdown of a large wind farm is not supported and continuity of power supply during grid faults according to the grid codes is very important. So, it is essential to improve the transient stability of DFIG based wind generation system. This paper investigates the impact of increasing the switching frequency of power converters of DFIG during fault conditions, and this switching frequency control (SFC) strategy is conjugated with parallel resonance fault current limiter (PRFCL) to enhance the fault ride through (FRT) of DFIG.

Keywords: doubly-fed induction generator (DFIG), fault ride through (FRT), bridge type fault current limiter (BFCL), parallel resonance fault current limiter (PRFCL), switching frequency control (SFC) strategy.

GJRE-F Classification: FOR Code: 290901



TRANSIENTSTABILITYENHANCEMENTOFDFIGBASEDWINDGENERATORBYSWITCHINGFREQUENCYCONTROLSTRATEGYWITHPARALLELRESONANCEFAULTCURRENTLIMITER

Strictly as per the compliance and regulations of:



RESEARCH | DIVERSITY | ETHICS

© 2018. M. R. Islam & M. R. I. Sheikh. This is a research/review paper, distributed under the terms of the Creative Commons Attribution-Noncommercial 3.0 Unported License <http://creativecommons.org/licenses/by-nc/3.0/>, permitting all non commercial use, distribution, and reproduction in any medium, provided the original work is properly cited.

Transient Stability Enhancement of DFIG based Wind Generator by Switching Frequency Control Strategy with Parallel Resonance Fault Current Limiter

M. R. Islam^α & M. R. I. Sheikh^ο

Abstract- Doubly fed induction generator (DFIG) based wind turbine generation system is generally sensitive to the grid faults as its stator windings are directly connected to the grid. As the wind power penetration to the grid increases day by day, a complete shutdown of a large wind farm is not supported and continuity of power supply during grid faults according to the grid codes is very important. So, it is essential to improve the transient stability of DFIG based wind generation system. This paper investigates the impact of increasing the switching frequency of power converters of DFIG during fault conditions, and this switching frequency control (SFC) strategy is conjugated with parallel resonance fault current limiter (PRFCL) to enhance the fault ride through (FRT) of DFIG. It is found that the proposed SFC strategy with PRFCL (SFC-PRFCL) is a very effective mean to augment the FRT capability. To check the effectiveness of that SFC-PRFCL, its performance is compared with the bridge type fault current limiter (BFCL)[3] and PRFCL [30]. Simulations were carried out using the PSCAD/EMTDC software. Both symmetrical and asymmetrical faults are considered here to check the transient responses.

Keywords: doubly-fed induction generator (DFIG), fault ride through (FRT), bridge type fault current limiter (BFCL), parallel resonance fault current limiter (PRFCL), switching frequency control (SFC) strategy.

I. INTRODUCTION

Public opposition is growing towards the use of fossil fuels as the conventional electricity generation ingredients because fossil fuels are responsible for emitting huge CO₂ and contributing global warming problems. Also because of the limited stock of fossil fuels, renewable energies can be the alternative. Among those renewable energies, wind energy is very fast growing, and it is expected that by 2020, almost 10% of global electricity generation will be provided by the wind energy [1].

Recently fixed speed wind turbine generation system lost its popularity mainly because it suffers various problems, particularly during the transient

conditions. So, at present variable speed wind turbine generation system is more popular choice [2]. Due to variable speed operation, superior energy capture ability from wind, excellent power quality, higher efficiency, reduced losses, less mechanical stress on turbine, fractionally rated converter, separate control ability of active and reactive power make doubly fed induction generator (DFIG) one of the most popular choices in wind energy market [3, 4].

Although DFIG has many unique advantages, it suffers from grid disturbances as its stator windings are directly connected to the grid, and rotor windings are connected to the grid via back to back power electronic converters. The shutdown of that DFIG based wind farm during a fault is the easiest solution but not the wise one as more and more wind power is integrated into the grid. Therefore various grid codes [5] have been defined to avoid the complete shutdown of a large wind farm. DFIG may experiences high current in both stator and rotor windings, DC-link overvoltage, torque oscillation, acute mechanical stress to the rotor shaft and gearbox during the fault condition. So, enhance the fault ride through (FRT), or low voltage ride through (LVRT) capability of DFIG is very important.

To enhance the FRT capability of the DFIG based wind generation system, many solutions have been proposed, which can be categorized into two groups.

- Using new converter modeling and control techniques. It increases the complexity of the system.
- Using auxiliary devices, also known as hardware solutions. It increases the overall cost of the system.

In [6-12] describe some FRT solutions by using the first group. The second group uses auxiliary devices, where in [13-16] a crowbar was used to improve the FRT capability of DFIG, while in [17, 18] a DC-chopper was used. Use of series dynamic braking resistor (SDBR) and dynamic voltage restorer (DVR) were described in [19-21] and [22, 23] respectively. Static synchronous compensator (STATCOM) [24], switch type

Author α σ: Department of Electrical & Electronic Engineering, Rajshahi University of Engineering & Technology, Rajshahi-6204, Bangladesh.
e-mails: rashu_ruet@yahoo.com, ris_eee@ruet.ac.bd

fault current limiter (STFCL) [25], resistive type superconducting fault current limiter (SFCL) connected in a series with the DFIG rotor winding [26], superconducting magnetic energy storage (SMES) [27], nine-switch converter (NSC) instead of six-switch converter [28] are also proposed as a solution to improve the FRT capability of DFIG.

In previous work, it has proved that bridge type fault current limiter (BFCL) [3] is an excellent solution to enhance FRT capability of DFIG based variable speed wind generation system. As a new auxiliary device named parallel resonance fault current limiter (PRFCL) has a promising application in power systems [29]. Application of PRFCL to augment the FRT capability of DFIG based wind farm is reported in [30], and it has found from that paper that the PRFCL has better FRT augmentation capability than the BFCL. Now in this paper, the effect of increasing the switching frequency of power converters of DFIG during fault conditions is observed, and this switching frequency control (SFC) strategy is conjugated with the PRFCL (SFC-PRFCL) to augment the FRT capability of DFIG. Both symmetrical and asymmetrical faults are considered at the most vulnerable point of the system. In order to check the effectiveness of that SFC-PRFCL, its performance is compared with both the BFCL and the PRFCL. Simulation results show that SFC-PRFCL outperforms

both the BFCL and the PRFCL. Simulations were carried out in PSCAD/EMTDC environment.

II. MODEL SYSTEM

The effectiveness of the proposed SFC-PRFCL is demonstrated through a test wind energy conversion system. Here in Fig. 1, a DFIG (10 MVA) is connected to the point of common coupling (PCC). The output of the wind turbine is supplied to the utility grid through a 0.69/11-kV step-up transformer and double circuit transmission lines. The rotor of that DFIG is fed through a 0.34/0.69-kV step-down transformer and back-to-back converters named rotor side converter (RSC) and grid side converter (GSC) that use insulated gate bipolar transistors (IGBTs). A capacitor is connected to the DC side acts as the DC voltage source. The SFC-PRFCL is connected in series with one of the transmission lines to protect it. At the most vulnerable point of the system, both symmetrical and asymmetrical faults were considered.

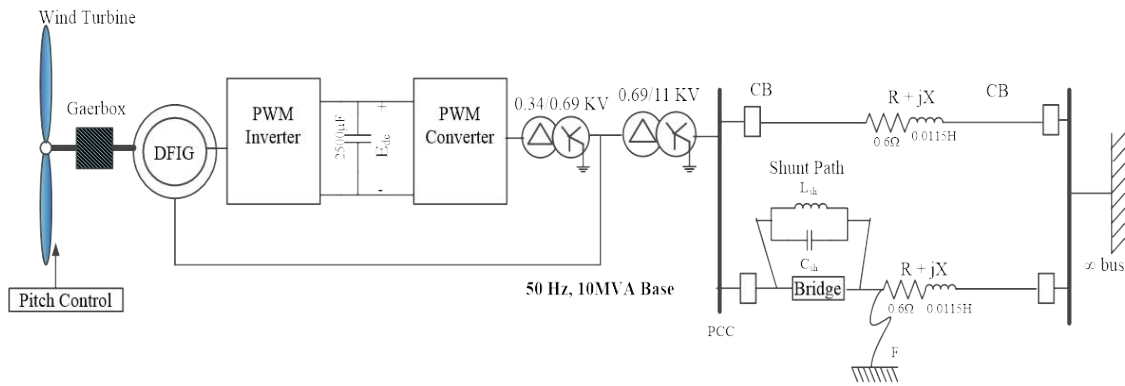


Fig. 1: Schematic diagram of the study system.

III. WIND TURBINE AND DFIG MODELING

Modeling of the wind turbine, the DFIG, and the converter controllers are as follows.

a) Wind Turbine Modeling

The turbine rotor, a shaft, and a gearbox unit are the primary components in the modeling of a wind turbine. Also, various physical and geometrical aspects have to take in consideration for proper modeling of a wind turbine. Normally a simplified method of modeling the wind turbine is used. The commonly used mathematical relations for the aerodynamic torque and

mechanical power extracted from the wind can be given by [19]:

$$T_M = \frac{1}{2} \pi \rho C_t(\lambda) R^3 V_w^2 [NM] \quad (1)$$

$$P_{wt} = \frac{1}{2} \pi \rho C_p(\lambda, \beta) R^2 V_w^3 [W] \quad (2)$$

where ρ is the air density, R is the radius of the turbine, V_w is the wind speed, and $C_p(\lambda, \beta)$ is the power coefficient given by

$$C_p(\lambda, \beta) = \frac{1}{2}(\Gamma - 0.02\beta^2 - 5.6)e^{-0.17\Gamma} \quad (3)$$

The relationship between C_t and C_p can be expressed as

$$C_t(\lambda) = \frac{C_p(\lambda)}{\lambda} \quad (4)$$

$$\lambda = \frac{\omega_{wt}R}{V_w} \quad (5)$$

$$\Gamma = \frac{R(3600)}{\lambda(1609)} \quad (6)$$

Here, ω_{wt} is the rotational speed of the wind turbine, λ is the tip speed ratio, and β is the blade pitch angle.

b) DFIG Modeling

Modeling of DFIG has described in many works. Here the Park's transformation model is chosen to model the DFIG. Two mass drive train model used in this study. Drive train model has a great impact on transient stability. The generator parameters and excitation parameters are given in Table I [19, 31].

Table 1: Generator and excitation parameters

Characteristic	Value
Rated power	10 [MVA]
Rated voltage	0.69[kV]
Rated frequency	50[Hz]
Stator resistance	0.01[pu]
Wound rotor resistance	0.01[pu]
Magnetizing inductance	3.5[pu]
Stator leakage inductance	0.15[pu]
Wound rotor leakage inductance	0.15[pu]
Generator inertia constant	0.3 [pu]
Turbine inertia constant	3.0 [pu]
Shaft stiffness between two masses	90 [pu]
DC-link voltage	0.7 [kV]
DC-link capacitor	25,000 [μ F]
Device for the power converter	IGBT

c) RSC Controller

Fig. 2 shows the RSC controller which is actually a two level, six pulse, IGBT based power converter in this study. It regulates the terminal voltage to 1.0 pu. The active power and reactive power are

controlled by d-axis current and q-axis current respectively. The Park's transformation is used to convert abc-to-dq0 and vice versa. Phase lock loop (PLL) provides the angle θ_{PLL} and θ_r is the effective angle for that transformation. After getting V_{dr} and V_{qr} , those are through the dq0-to-abc transformation to produce three phase reference signal, then sent to pulse width modulation (PWM) signal generator block, so that it can generate pulses for the IGBT switches of the RSC.

DC reactor L_{dc} . A very small value resistor R_{dc} is considered in series with L_{dc} to include the latent resistance of the DC reactor.

The shunt or resonance part is constructed of a capacitor C_{sh} and an inductor L_{sh} . To form an LC resonance circuit at line power frequency, they are arranged in parallel to each other as shown in Fig. 4.

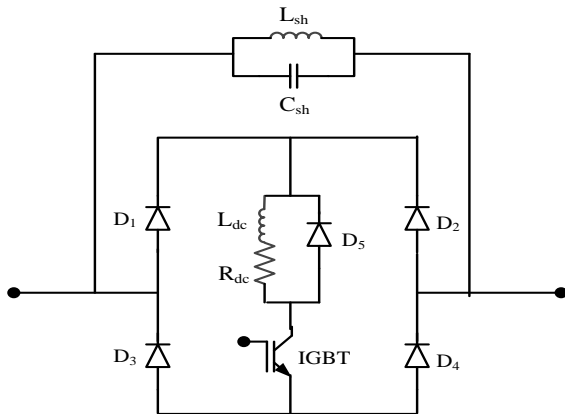


Fig. 4: Per phase PRFCL configuration.

b) PRFCL Operation and Control

In normal operating condition, the IGBT switch in Fig. 4 is in ON state. In the positive half cycle, the $D_1 - L_{dc} - R_{dc} - D_4$ path and in the negative half cycle, the $D_2 - L_{dc} - R_{dc} - D_3$ path carries the line current. So, the current through the DC reactor L_{dc} is in the same direction, and this is the DC current i_{dc} for L_{dc} . This L_{dc}

offers no impedance for this DC current. There are some voltage drop in the bridge part during normal operating condition due to the latent resistance R_{dc} of the DC reactor, ON-state resistance of IGBT switch and diode forward voltage drop. But the aggregated voltage drop of those is ignorable compared to the large line voltage drop. So, this bridge part has no impact on normal operating condition. As the shunt path is in the parallel resonance condition, its impedance seems very high. Therefore in normal condition, the full line current is flown through the bridge part except some negligible leakage current.

Now, when a fault occurs, the line current wants to rise very quickly, but the DC reactor L_{dc} does not permit this. So, safe operation for IGBT switch is ensured as L_{dc} limits the high di/dt value during fault. To take the turn OFF decision for IGBT switch during a fault and bypass the line current to the high impedance resonating shunt path, DC current i_{dc} through the DC reactor is compared with a threshold value i_{th} . Here, i_{th} is taken 1.3 times the nominal value of i_{dc} for optimum operation. When i_{dc} exceeds i_{th} , IGBT switch gets a low gate signal V_{gate} and turned OFF. Per phase PRFCL controller is shown in Fig.5. Some other parameters like the line current, the terminal voltage, the active power or the reactive power can be used for IGBT control, but the DC current i_{dc} through the DC reactor L_{dc} is used in this study. This is because i_{dc} is very sensitive to line current and has a faster rate of rise than line current and other parameters.

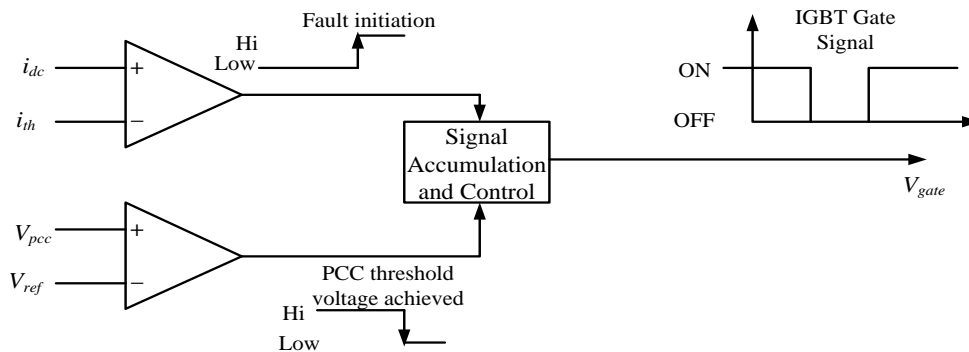


Fig. 5: Per phase controller for PRFCL.

After turning OFF of the IGBT, i_{dc} becomes zero. So, to resume the normal operation and turn ON the IGBT switch, another parameter has to choose. For that purpose, the voltage at PCC, V_{PCC} is chosen in this study. After the circuit breakers opening of the faulty section and isolating that faulty part, bus voltage starts to rise, and the system starts to recover. The V_{PCC} is compared with a reference value V_{ref} which is set 90% of the nominal value of V_{PCC} . After starting the rise of bus

voltage, when V_{PCC} exceeds V_{ref} , the IGBT switch will get a high signal and normal operation resume as shown in Fig. 5.

c) PRFCL Design Consideration

To design the PRFCL, the ultimate task is to determine the values of shunt capacitor C_{sh} and shunt inductor L_{sh} . At power frequency, so many combinations of C_{sh} and L_{sh} would give the resonance condition. Standard values of C_{sh} are picked from [32], and L_{sh} is

calculating considering the resonance at power frequency. At power frequency, many pairs of C_{sh} and L_{sh} are trialed, and among those, $C_{sh} = 125 \mu F$ and $L_{sh} = 80 mH$ gave the best result during the fault. The values of L_{dc} and R_{dc} are picked $1 mH$ and $0.3m\Omega$ respectively, which give a time constant of 3.33 s. This is good enough for smoothing the DC reactor current.

d) SFC Configuration

To investigate the impact of increasing the switching frequency of the carrier wave during the fault condition, the proposed pulse generation system for both RSC and GSC is shown in Fig. 6. In both RSC and GSC, the triangular signal is used as the carrier wave of PWM operation. In Fig. 6, f_{c_normal} is the switching

frequency in normal operating condition, and f_{c_fault} is the increased switching frequency during the fault. How long the increased switching frequency f_{c_fault} will remain active is decided by the IGBT gate signal V_{gate} . As long as V_{gate} in Fig. 5 remains a low state that means the IGBT switch in Fig. 4 is in OFF state, which indicates the fault situation, f_{c_fault} is activated. Otherwise, in normal operating condition and after resuming the normal condition after the fault, f_{c_normal} is activated. A frequency of 1650 Hz is chosen as f_{c_normal} . And the increased switching frequency f_{c_fault} is chosen eight times of f_{c_normal} in this study, which is implementable. This SFC strategy with PRFCL forms the SFC-PRFCL.

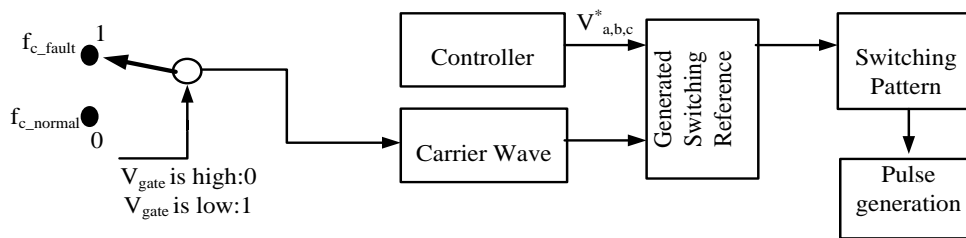


Fig. 6: Pulse generation system for both RSC and GSC (SFC strategy).

V. BFCL

To observe the effectiveness of the proposed SFC-PRFCL, its performance is compared with that the BFCL. Just like the PRFCL, the BFCL has two distinct parts namely the bridge part and the shunt path as shown in Fig. 7. Bridge part is exactly the same as PRFCL and the shunt path composed of a resistor R_{sh} in series with an inductor L_{sh} . The detail of BFCL topology is discussed in [3]. The same operation and control strategy is used for BFCL as PRFCL. The same controller is used for BFCL as shown in Fig. 5. The values of R_{sh} and L_{sh} are taken as the same procedure discussed in [3].

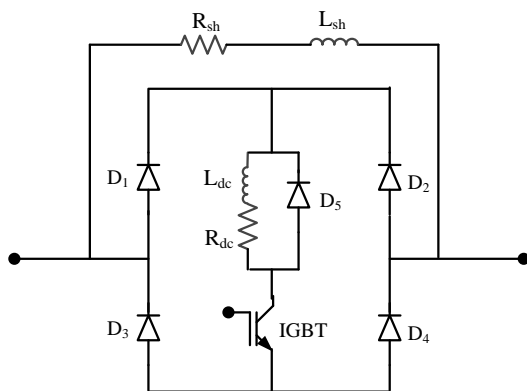


Fig. 7: Per phase BFCL configuration.

VI. SIMULATION RESULTS AND DISCUSSION

Detail simulation results are described in the following subsections.

a) Simulation Considerations

Simulations were carried out by using PSCAD/EMTDC software. Here for transient analysis, a fixed wind speed of 15 m/s is considered. Duration of fault is too short to make any impact on wind speed, so fixed speed is considered. Analysis is carried out, and results are shown for most severe three line to ground (3LG) and most common line to ground (1LG) faults. Those faults were applied at the most vulnerable point of the system near the PCC denoted by point F in Fig. 1. Those faults were applied at 0.1 s and withdrawn at 0.6 s. Circuit breakers on the faulted line open and reclose at 0.2 s and 1.1 s respectively. Results are shown for a time duration of 0 s to 3 s, and per unit (pu) measurements are used. All those figures have a zoomed portion for better visualization.

b) FRT Improvement by SFC-PRFCL for 3LG fault

Fault responses for 3LG fault are shown in Figs. 8-11. Fig. 8 shows the terminal voltage profile for DFIG. With no controller, terminal voltage goes nearly zero just after the fault occurrence and continues the same way till the breakers opening. After the breaker opening, terminal voltage rises beyond 1.2 times the nominal value and takes much time to come back the pre-fault

value. The BFCL has good voltage response as compared to no controller case, but PRFCL gives a better voltage profile than the BFCL. But among those all, SFC-PRFCL has the best voltage profile with least amount of voltage fluctuation.

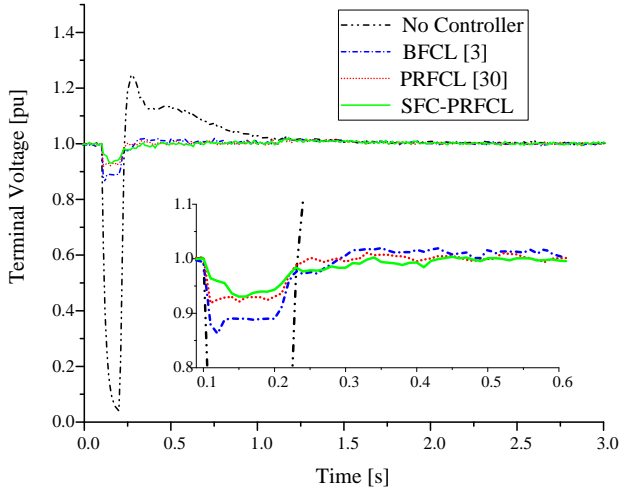


Fig. 8: Terminal voltage response for 3LG fault.

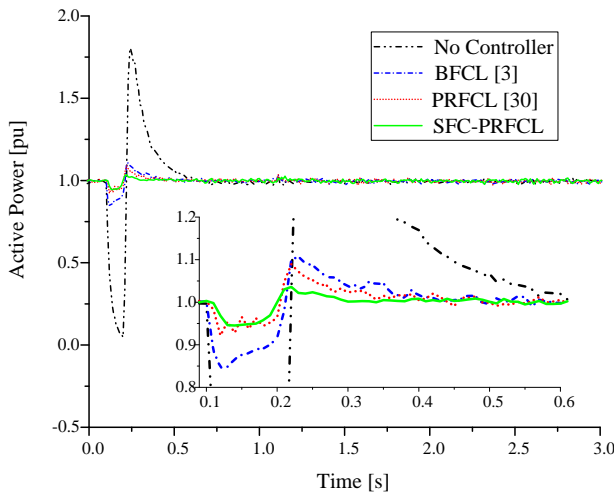


Fig. 9: Active power response for 3LG fault.

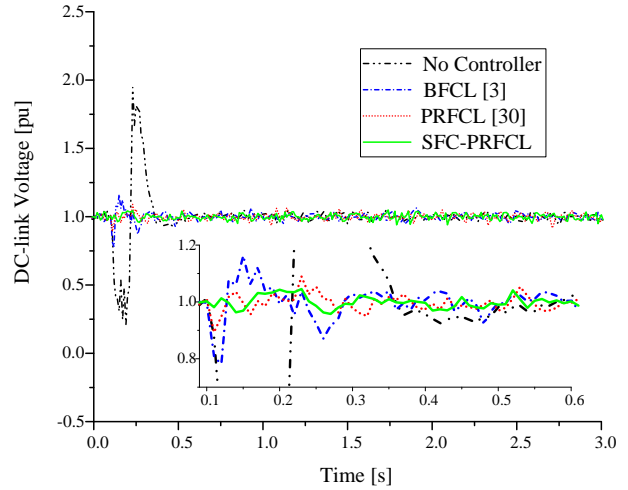


Fig. 10: DC-link voltage response for 3LG fault.

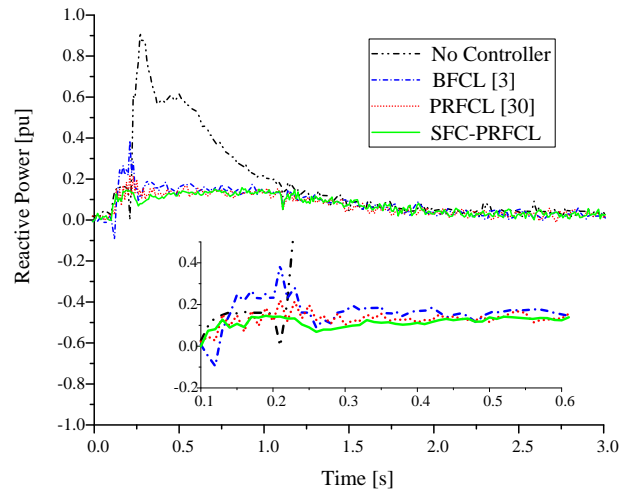


Fig. 11: Reactive power response for 3LG fault.

It is clear from the Fig. 9 that the SFC-PRFCL keeps the active power profile smooth during a 3LG fault. Output power goes very close to zero after the fault event with no controller case. Also, the breakers opening causes a large imbalance of output power. The BFCL and the PRFCL both have better active power profile than no controller case, but SFC-PRFCL gives the best response.

The DFIG DC-link voltage profile is shown in Fig. 10 for 3LG fault. With no controller case, DC-link voltage profile is not good during the 3LG fault. It is seen that the DC-link voltage profile can be controlled within permissible limit by BFCL, PRFCL, and SFC-PRFCL. Among those, SFC-PRFCL gives the best DC-link voltage profile with least deviation of DC-link voltage from the nominal value.

Fig. 11 provides the reactive power profile of DFIG. It is illustrated from this figure that, BFCL and PRFCL can contribute to keep better reactive power profile, but SFC-PRFCL has superior performance than both of them.

c) *FRT Improvement by SFC-PRFCL for 1LG fault*

Fault responses for 1LG fault are shown in Figs. 12-15. Fig. 12 and Fig. 13 represent the terminal voltage profile and output active power profile respectively. It is clear from those figures that, BFCL and PRFCL have better terminal voltage and active power profiles than no controller case, but their performances are inferior to the SFC-PRFCL.

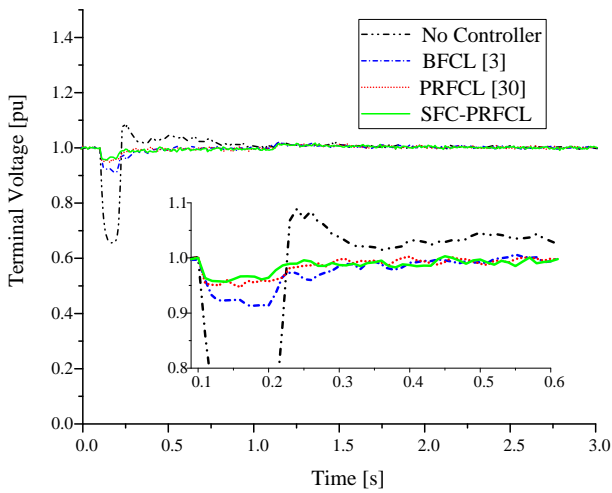


Fig. 12: Terminal voltage response for 1LG fault.

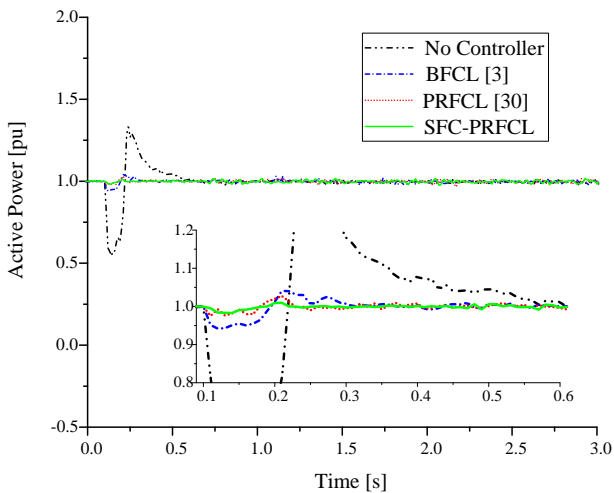


Fig. 13: Active power response for 1LG fault.

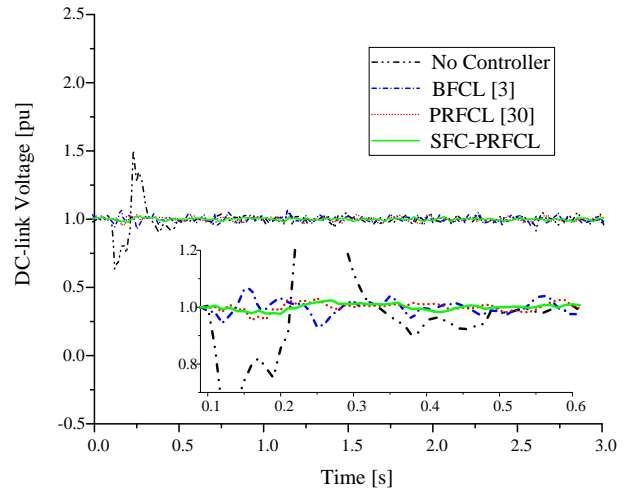


Fig. 14: DC-link voltage response for 1LG fault.

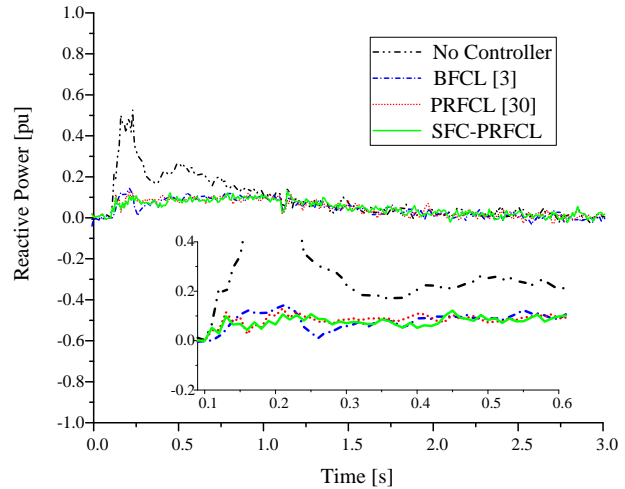


Fig. 15: Reactive power response for 1LG fault.

The DFIG DC-link voltage profile and reactive power profile are shown in Fig. 14 and Fig. 15 respectively for 1LG fault. It is apparent that the more stable operation is obtained when SFC-PRFCL is used. Figs. 8-15 indicate that the system is less affected by 1LG fault than the 3LG fault.

VII. CONCLUSION

The application of the SFC-PRFCL to enhance the FRT capability of DFIG is proposed in this paper. The effectiveness of the SFC-PRFCL is compared with that of the BFCL [3] and the PRFCL [30]. Following points are mentionable from the simulation results and discussions.

- The SFC-PRFCL is a very effective means to enhance the FRT capability of DFIG-based wind

turbine generation system for both symmetrical and asymmetrical faults.

- The proposed SFC-PRFCL ensures more stable operation of the DFIG-based wind turbine generation system.
- Performances of BFCL and PRFCL are outperformed by the SFC-PRFCL in every aspect.

In our future work, the usefulness of SFC-PRFCL on a high capacity DFIG-based wind farm connected to a multi-machine power system will be considered.

REFERENCES RÉFÉRENCES REFERENCIAS

1. P. Musgrove, *Wind Power*. New York: Cambridge Univ. Press, 2010, pp. 221–222.
2. S. M. Mueen, R. Takahashi, T. Murata and J. Tamura, "A Variable Speed Wind Turbine Control Strategy to Meet Wind Farm Grid Code Requirements," *IEEE Trans. Power Syst.*, vol. 25, pp. 331-340, Feb. 2010.
3. G. Rashid and M. Ali, "Transient stability enhancement of doubly fed induction machine-based wind generator by bridge-type fault current limiter," *IEEE Trans. Energy Convers.*, vol. 30, pp. 939- 947, Sept. 2015.
4. Sajjad Tohidi, Mohammadi-ivatloo Behnam, "A comprehensive review of low voltage ride through of doubly fed induction wind generators", *Renewable and Sustainable Energy Reviews*, Volume 57, Pages 412-419, May 2016.
5. M. Tsili and S. Papathanassiou, "A review of grid code technical requirements for wind farms," *IET Renew. Power Gener.*, vol. 3, no. 3, pp. 308- 332, Sept. 2009.
6. Bo Yang, Lin Jiang, Lei Wang, Wei Yao, Q.H. Wu, "Nonlinear maximum power point tracking control and modal analysis of DFIG based wind turbine", *International Journal of Electrical Power & Energy Systems*, Volume 74, Pages 429-436, January 2016.
7. G. Kenne, J. d. D. Nguimfack Ndongmo, R. Fochie Kuate and H. B. Fotsin, "An Online Simplified Nonlinear Controller for Transient Stabilization Enhancement of DFIG in Multi-Machine Power Systems," in *IEEE Transactions on Automatic Control*, vol. 60, no. 9, pp. 2464-2469, Sept. 2015.
8. T. D. Vrionis, X. I. Koutiva and N. A. Vovos, "A Genetic Algorithm-Based Low Voltage Ride-Through Control Strategy for Grid Connected Doubly Fed Induction Wind Generators," in *IEEE Transactions on Power Systems*, vol. 29, no. 3, pp. 1325-1334, May 2014.
9. Q. Huang, X. Zou, D. Zhu and Y. Kang, "Scaled Current Tracking Control for Doubly Fed Induction Generator to Ride-Through Serious Grid Faults," in *IEEE Transactions on Power Electronics*, vol. 31, no. 3, pp. 2150-2165, March 2016.
10. Bhinal Mehta, Praghnes Bhatt, Vivek Pandya, "Small signal stability enhancement of DFIG based wind power system using optimized controllers parameters", *International Journal of Electrical Power & Energy Systems*, Volume 70, Pages 70-82, September 2015.
11. Y. Liu, Q. H. Wu and X. X. Zhou, "Co-Ordinated Multiloop Switching Control of DFIG for Resilience Enhancement of Wind Power Penetrated Power Systems," in *IEEE Transactions on Sustainable Energy*, vol. 7, no. 3, pp. 1089-1099, July 2016.
12. J. Chen, W. Zhang, B. Chen and Y. Ma, "Improved Vector Control of Brushless Doubly Fed Induction Generator under Unbalanced Grid Conditions for Offshore Wind Power Generation," in *IEEE Transactions on Energy Conversion*, vol. 31, no. 1, pp. 293-302, March 2016.
13. S. Swain and P. K. Ray, "Short circuit fault analysis in a grid connected DFIG based wind energy system with active crowbar protection circuit for ridethrough capability and power quality improvement", *Int. J. Elect. Power Energy Syst.*, vol. 84, page 64-65, Jan. 2017.
14. G. Pannell, D. J. Atkinson and B. Zahawi, "Minimum-Threshold Crowbar for a Fault-Ride-Through Grid-Code-Compliant DFIG Wind Turbine," in *IEEE Transactions on Energy Conversion*, vol. 25, no. 3, pp. 750-759, Sept. 2010.
15. J. Vidal, G. Abad, J. Arza and S. Aurtenechea, "Single-Phase DC Crowbar Topologies for Low Voltage Ride Through Fulfillment of High-Power Doubly Fed Induction Generator-Based Wind Turbines," in *IEEE Transactions on Energy Conversion*, vol. 28, no. 3, pp. 768-781, Sept. 2013.
16. S. Swain and P. K. Ray, "Fault ridethrough and power quality improvement of Doubly-Fed Induction Generator based wind turbine system during grid fault with Novel Active Crowbar Protection design," *IEEE Region 10 Conference (TENCON)*, Singapore, 2016, pp. 2628-2633.
17. G. Pannell, B. Zahawi, D. J. Atkinson and P. Missailidis, "Evaluation of the Performance of a DC-Link Brake Chopper as a DFIG Low-Voltage Fault-Ride-Through Device," in *IEEE Transactions on Energy Conversion*, vol. 28, no. 3, pp. 535-542, Sept. 2013.
18. A. Jalilian, S. B. Naderi, M. Negnevitsky, M. T. Hagh and K. M. Muttaqi, "Controllable DC-link fault current limiter augmentation with DC chopper to improve fault ride-through of DFIG," *IET Renew. Power Gener.* vol. 11, pp. 313-324, Feb. 2017.

19. K. E. Okedu, S. M. Muyeen, R. Takahashi and J. Tamura, "Wind Farms Fault Ride Through Using DFIG With New Protection Scheme," in *IEEE Transactions on Sustainable Energy*, vol. 3, no. 2, pp. 242-254, April 2012.
20. J. Yang, J. E. Fletcher and J. O'Reilly, "A Series-Dynamic-Resistor-Based Converter Protection Scheme for Doubly-Fed Induction Generator During Various Fault Conditions," in *IEEE Transactions on Energy Conversion*, vol. 25, no. 2, pp. 422-432, June 2010.
21. A. Causebrook, D. J. Atkinson, and A. G. Jack, "Fault ride-through of large wind farms using series dynamic braking resistors," *IEEE Trans. Power Syst.*, vol. 22, no. 3, pp. 966-975, Aug. 2007.
22. B. Wessels, F. Gebhardt and F. W. Fuchs, "Fault Ride-Through of a DFIG Wind Turbine Using a Dynamic Voltage Restorer During Symmetrical and Asymmetrical Grid Faults," in *IEEE Transactions on Power Electronics*, vol. 26, no. 3, pp. 807-815, March 2011.
23. C. O. Ibrahim, T. H. Nguyen, D. C. Lee and S. C. Kim, "A Fault Ride-Through Technique of DFIG Wind Turbine Systems Using Dynamic Voltage Restorers," in *IEEE Transactions on Energy Conversion*, vol. 26, no. 3, pp. 871-882, Sept. 2011.
24. D.V.N. Ananth, G.V. Nagesh Kumar, "Fault ride-through enhancement using an enhanced field oriented control technique for converters of grid connected DFIG and STATCOM for different types of faults", *ISA Transactions*, Volume 62, Pages 2-18, May 2016.
25. W. Guo, L. Xiao, S. Dai, Y. Li, X. Xu, W. Zhou and L. Li, "LVRT capability enhancement of DFIG with switch type fault current limiter " *IEEE Trans. Ind. Electron.*, vol. 62, pp. 332-342, Jan. 2015.
26. Z. C. Zou, X. Y. Xiao, Y. F. Liu, Y. Zhang and Y. H. Wang, "Integrated Protection of DFIG-Based Wind Turbine With a Resistive-Type SFCL Under Symmetrical and Asymmetrical Faults," in *IEEE Transactions on Applied Superconductivity*, vol. 26, no. 7, pp. 1-5, Oct. 2016.
27. A. M. S. Yunus, M. A. S. Masoum and A. Abu-Siada, "Application of SMES to Enhance the Dynamic Performance of DFIG During Voltage Sag and Swell," in *IEEE Transactions on Applied Superconductivity*, vol. 22, no. 4, Aug. 2012.
28. G. Wen, Y. Chen, Z. Zhong and Y. Kang, "Dynamic Voltage and Current Assignment Strategies of Nine-Switch-Converter-Based DFIG Wind Power System for Low-Voltage Ride-Through (LVRT) Under Symmetrical Grid Voltage Dip," in *IEEE Transactions on Industry Applications*, vol. 52, no. 4, pp. 3422-3434, July-Aug. 2016.
29. S. B. Naderi, M. Jafari and M. Tarafdar Hagh, "Parallel-Resonance-Type Fault Current Limiter," in *IEEE Transactions on Industrial Electronics*, vol. 60, no. 7, pp. 2538-2546, July 2013.
30. G. Rashid and M. H. Ali, "Application of parallel resonance fault current limiter for fault ride through capability augmentation of DFIG based wind farm," in *Proc. IEEE/PES Transmission and Distribution (T&D) Conference and Exposition*, Dallas, TX, May 2016, pp. 1-5.
31. M. R. Islam, M. R. I. Sheikh and Z. Tasneem, "A frequency converter control strategy of DFIG based wind turbine to meet grid code requirements," in *Proc. 2nd IEEE International Conference on Electrical, Computer & Telecommunication Engineering (ICECTE)*, Rajshahi, Dec. 2016, pp. 1-4.
32. General Atomics Electronics Systems, "High voltage capacitors and power supplies." [Online]. Available: <http://www.ga.com/capacitors>. (Date accessed: 15 Aug. 2017).



GLOBAL JOURNAL OF RESEARCHES IN ENGINEERING: F
ELECTRICAL AND ELECTRONICS ENGINEERING

Volume 18 Issue 1 Version 1.0 Year 2018

Type: Double Blind Peer Reviewed International Research Journal

Publisher: Global Journals

Online ISSN: 2249-4596 & Print ISSN: 0975-5861

Green Improving by Autonomous PV Mini-Grid Model in Central Myanmar

By Aung Ze Ya

Yangon Technological University

Abstract- This research work verifies how can be able to gain Sustainability Benefits by improving Green Energy harvesting. The Goal is in line with the Goal No.7 of the world's 2030 Agenda: SDGs (Sustainable Development Goals) as well as Myanma 2030 Agenda: NEP (National Electrification Planning towards Universal Access). The location of a focused village, Nat Kan Lel (Nagale) is near the beneath and National Park of Mount Popa in Kyaukpadaung Township, Mandalay Region. It has high demands due to 800 households with 4000 populations. This research explores the site experience, the problem statement and the evaluation of current demands for CO₂ Emissions. That village enriched high solar potential and blessed for a Novel Imagination of this work: change to Autonomous Photovoltaic Mini-Grid from existing 3 Diesel Mini-Grids. The thousands of models are simulated by a very powerful tool, HOMER Pro (version 3.11.4). New Diesel Mini-Grid (100% Non-Renewable Energy) is modeled and compared with the proposed PV Mini-Grid (100% RE) model. The simulative results spotlighted the feasible 100 % RE model in Off-Grid area of central Myanmar.

Keywords: *autonomous photovoltaic mini-grid, central myanmar, HOMER pro, village nat kan lel, optimum.*

GJRE-F Classification: FOR Code: 090699



Strictly as per the compliance and regulations of:



Green Improving by Autonomous PV Mini-Grid Model in Central Myanmar

Aung Ze Ya

Abstract- This research work verifies how can be able to gain Sustainability Benefits by improving Green Energy harvesting. The Goal is in line with the Goal No.7 of the world's 2030 Agenda: SDGs (Sustainable Development Goals) as well as Myanmar 2030 Agenda: NEP (National Electrification Planning towards Universal Access). The location of a focused village, Nat Kan Lel (Nagale) is near the beneath and National Park of Mount Popa in Kyaukpadaung Township, Mandalay Region. It has high demands due to 800 households with 4000 populations. This research explores the site experience, the problem statement and the evaluation of current demands for CO₂ Emissions. That village enriched high solar potential and blessed for a Novel Imagination of this work: change to Autonomous Photovoltaic Mini-Grid from existing 3 Diesel Mini-Grids. The thousands of models are simulated by a very powerful tool, HOMER Pro (version 3.11.4). New Diesel Mini-Grid (100% Non-Renewable Energy) is modeled and compared with the proposed PV Mini-Grid (100% RE) model. The simulative results spotlighted the feasible 100 % RE model in Off-Grid area of central Myanmar.

Keywords: *autonomous photovoltaic mini-grid, central myanmar, HOMER pro, village nat kan lel, optimum.*

I. INTRODUCTION

Nowadays, the world is suffering impacts, Global Warming and Climate Change, results of previous Green House Gas (GHG) emissions from the usages of the fossil fuels. Renewables inherent possesses Sustainability due to the reliance upon infinitely available resources that are naturally recharging with Zero fuel cost, Clean, Green, Eco-friendly and no or fewer emissions. To create the better world for our next generations, Renewables promotion is the predominant backbone of all strategies towards Sustainable Future of Mother Earth [1].

UN's 2030 Agenda formulates a set of 17 Sustainable Development Goals (SDGs). SDG 7 urges to ensure access to affordable, reliable, sustainable, and modern energy for all. It is not only the Goal that explicitly addresses the energy sector and mentions Renewable Energy (RE) as a mean to achieve it but also crucial to gain the other SDGs. Renewables offer equally solutions to the problems of Local and Global Environmental Sustainability [9].

Author: PhD, Post Doc, Honorary Professor and Honorary Doctor of Science, Professor of Department of Electrical Power Engineering, and Director of Department of Maintenance Engineering, Yangon Technological University (YTU), Myanmar.

e-mails: dr.aungzeya010@gmail.com, profazytumm10@gmail.com

a) Background: Off-Grid Electricity Access

About 95 % of 1.2 billion people without Grid Access live in sub-Saharan Africa, South and East Asia, with the remainder spread almost equally across the Middle East, Central Asia, and Latin America. Nearly 60% of additional generation needed to achieve universal electricity access by 2030 will come from Off-Grid options. Standalone Mini-Grids powered by Renewables provide electricity to 90 million people [4] and meet a hierarchy of needs, from lighting to productive uses, thereby enabling people to climb the energy ladder. These are cost-effective and can be installed in the modular fashion, linked to Grid-extension plans [9].

Myanmar is situated in the northwestern-most country on the mainland of South East Asia as the strategic location. The geographical coordinate is between latitude 9° 58' N and 28° 29' N; and longitude 92° 10' E and 101° 10' E, the total area of 676,563 km², near to the Equator and along the belt of the sun's radiation, and availability of sun shine hour is average 6 to 7 hours in dry season. Myanmar has tremendous natural resources and potentials of Renewables. The country's Energy Policy encourages the development of RE. In 2014, Myanmar National Electrification Planning (NEP) targeted to electrify 7.2 million households and achieve universal access to electricity by 2030. In the long term, it expected that more than 95% of the population connected by the extension of National Grid System as a least-cost solution. In the medium term, Mini-Grids and Solar Home Systems (SHS) will play the role in providing electricity to the hundreds of thousands of households in the areas that National Grid will take many years to reach [8].

The key player of the implementation of the Off-Grid sector of the NEP is the Department of Rural Development (DRD) under the Ministry of Agriculture, Livestock, and Irrigation (MOALI). DRD is boosting Off-Grid Rural Electrification, and as a result, out of 63899 villages in total, 22911, nearly 36 % are electrified by the end of FY 2016-2017. That amount is 10 % increased than FY 2015-2016 [5-7]. From [7], villages powered by each type observed that 7507 by SHS (Solar Home System), 94 by PV Mini-Grid, 2769 by Diesel, and 1296 by Mini/Micro Hydro and 154 by Biomass/Biogas.

b) *State-of-the-Art*

Fig. 1 illustrates the State-of-the-Art. It is the combination of complicated works consists of different pieces and several steps. The site visit is the vital work to observe the real situation and the problems. Based on the site visit experience, the appropriate solutions and load profiles predicted. Besides, the resources studied. Energy, the technology, design, and the main components are selected. The parameters and costs validated. As the final and crucial work, the feasible models simulated in HOMER (Hybrid Optimization of Multiple Energy Resources) Pro (version 3.11.4) environment and then, the Optimum/Sustainable Model selected.

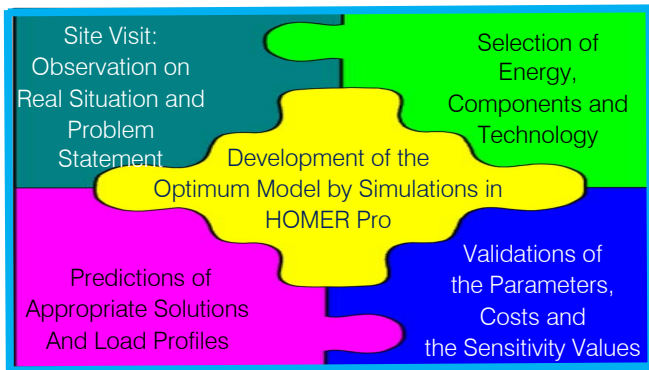
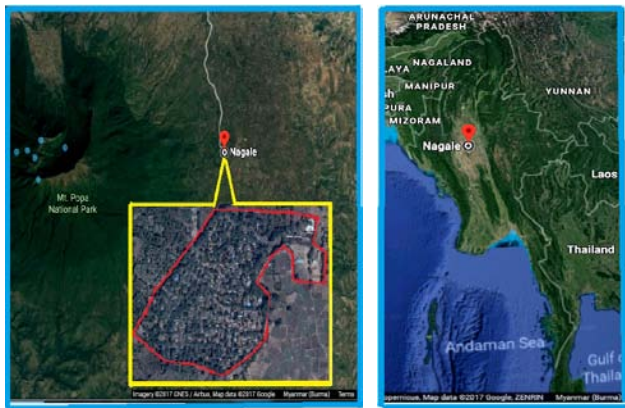


Fig. 1: State-of-the-Art

II. SITE VISIT: GROUND HIGHLIGHTS

a) *Location*



(a) Village Map

(b) State Map

Fig. 2: Satellite-Map of Nat Kan Lel (Nagale) [13]

A village Nat Kan Lel (Nagale) situated at geographical coordinate: Lat 20.922N and Lon 95.299E, near the National Park of famous Mount Popa in Kyaukpadaung Township, Mandalay Region, and Central Myanmar as shown in Fig. 2. It located at 10 km from National Grid System, 2 km from the road [11], and nearly 13 km from pozzolan mill.

b) *Interviews and Data Collection*

The village Nat Kan Lei is in the list of electrified villages. It observed that some existing electrification scenarios in rural areas are ineffective and inefficient systems [2]. Hence, the case study and data collection were performed at it in October 2017. There are 800 households with about 4000 population. Different places, Pagodas, Monasteries, water tube-wells, Diesel Mini-Grids, Rural Health Clinic (RHC) and high school observed. About 100 villagers from different roles were interviewed as obviously reflected in Figs. 3 to 6.



Fig. 3: Interview with the Village Authorities



Fig. 4: Interview with the Owners of Water Tube-Well



Fig. 5: Interview at RHC



Fig. 6: Interview with the Owner of DG3

c) Diesel Mini-Grids

That village is currently powered by three self-reliant Diesel Mini-Grids: DG1 (10 kW), DG2 (15 kW), and DG3 (15 kW) to 3 clusters; each has about 100 households. 3 Pagodas, 3 Monasteries and street lightings are also supplied by DG3. The single-phase, Synchronous type, 4-pole, 1500 rpm, 50 Hz low-cost Generators are operated with belt-drives from the Diesel engines. The capacities are engine 22 HP (horsepower) with 10 kW Generator and engine 25 HP with 15 kW Generators. Their service years are: DG1 is ten years; DG2 and DG3 are five years. It found that another Diesel system (22 HP Diesel engine with 10 kW Generator) for water pumping at the DG2 site as identified in Fig. 7.

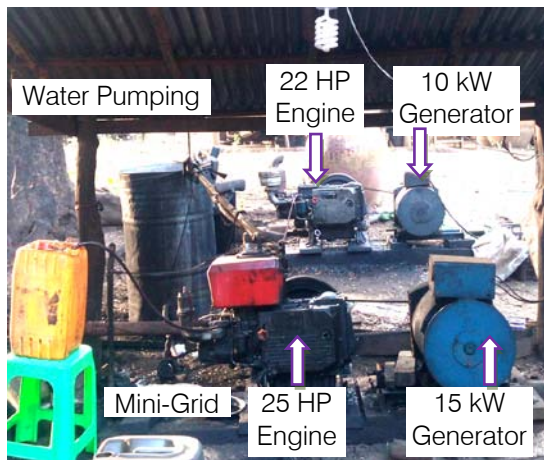


Fig. 7: View of the Machines at DG1 Site

These are usually operating for only 3 hours per day, from 18 hr to 21 hr in the cold season (November, December, January, and February) and from 19 hr to 22 hr in the other months.

As the other Off-Grid villages, monthly tariff is 2000 MMK (nearly 1.5 \$) for 2ft FL (20 W Fluorescent Lamp) or 26 W CFL (Compact Fluorescent Lamp) and

5000-6000 MMK (3.8-4.5 \$) for the combined use of 2ftFL, mobile phone charging and TV (Television). Sometimes, the extra operating hour requested from the villagers and then, the charge is 2000 MMK per hour for each generator. Additionally, there are other Diesel Generators (each 10 kW) at Pagodas, and Monasteries. Only the fuel cost is needed to pay; then, these operated for the donation events.

d) SHS

At Village Nat Kan Lel, SHS with conventionally ground-mounted and rooftop structures found. Fig. 8 (a) mentions the rooftop PV modules (each 300 W) at one home and Fig. 8 (b) shows the ground-mounted PV (960 W) modules at the clinic. Fig. 9 highlights the villagers and their mounted PV (300 W) module.



(a) Rooftop PV

(b) Ground-Mounted PV

Fig. 8: PV System Deployments at Village Nat Kan Lel



Fig. 9: The Villagers and their PV Module (300W)

250 households have SHS and deployed PV modules are the polycrystalline type, and the ratings are from 100 W to 300 W and are made in China and Thailand. The maximum installed capacities of PV modules are up to 600 W at the households and 960 W (for vaccine refrigerator) at RHC. All the batteries are 12 V and average ratings are 60 Ah to 200 Ah. Two per households mostly used. These are made in Myanmar, China, and Thailand. The inverters are 300 VA, 500 VA, 100 VA and 1500 VA. These are made in Myanmar and India.

Fig. 10 significantly reflected that the villagers do not install or use the charge controller that maintains

the battery within the operation limits and its lifetime. Also, it contributes the substantial cost factor, and there may be undesirable hazards as a consequence of the overcharging of the battery in the tropical areas. Thus, it is needed to aware the villagers to use it.



Fig. 10: The Villager and Components of his SHS

III. PROBLEMS AND DEMANDS

a) Generation Systems

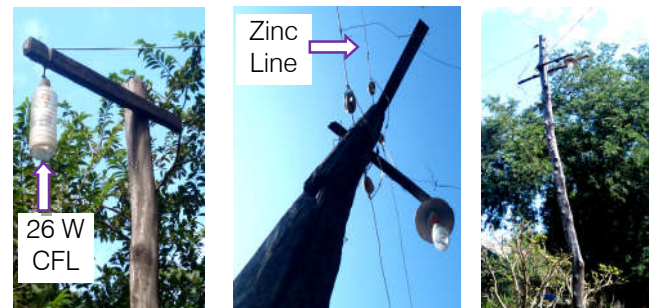
Due to the interviews' results, 100 % of the local villagers desire Electrical power supply for the whole day. They believe that it will be developed if they access 24-hour supply. The operating time of DGs is a few hours per day, and also SHS cannot perform 24 hour supply. Besides, they do not obtain the sufficient power. Furthermore, there are design and quality issues. It observed that the DG systems required to repair and

maintenance. Its replacement costs of spare parts for two months are about 25 \$ to 35 \$ for each machine.

Also, the overhauling per year is about 80 \$ to 100 \$ for each machine. Hence, the combined of all machines for long years may be quite large. Also, the total Diesel fuel cost is for 20 years. Then, the sum of the maintenance cost and fuel cost for all Electrical and Mechanical machines may be tremendously large. Another problem is the possibility of fire hazards from the Diesel storage tank. Moreover, there is significant noise and emissions from the DGs.

b) Distribution System and Loads

Currently, the villagers are commonly using the lightings as 2 ft FL, 26 W CFL (Compact Fluorescent Lamp), rechargeable DVD player, 21" TV and mobile phone charger. Fig. 11 mentions the current situation of the distribution lines from Diesel Mini-Grids. There are about 100 streetlights are using 26 W CFL. Total numbers of CFL in that village is nearly 600. CFL is Energy saving. But, it has hidden Environmental Impacts dealt with mercury content in the tube [14, 15]. Due to the study in [16], it is evident that there are multiple negative impacts of CFL as shown in Fig. 12.



(a) Streetlight (b) Distribution Pole (c) Bent Pole

Fig. 11: Distribution System of Existing Mini-Grid

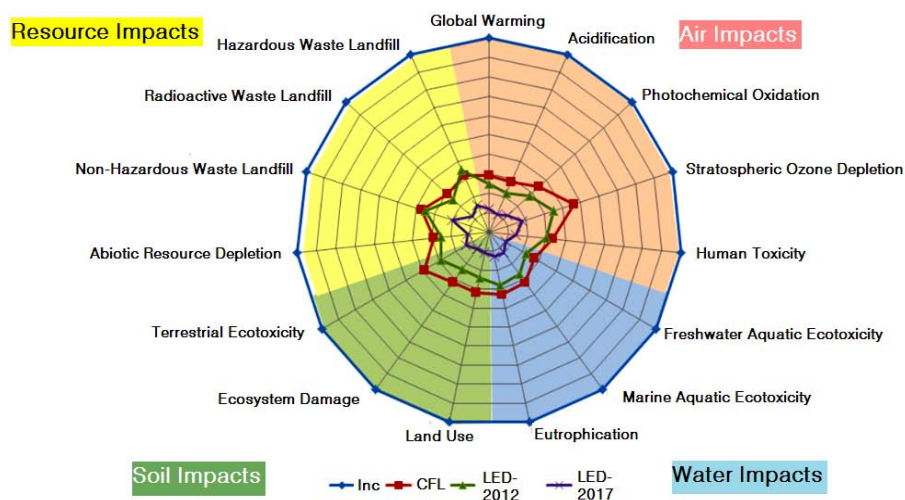


Fig. 12: Different Impacts from the Lighting Loads[16]

Due to the study in [16], it is evident that there are multiple negative impacts of CFL as shown in Fig. 12. Also, there are harmonics problems, high reactive power demands, and power factor problem by using FL and CFL. Due to evaluation in [17], the aggregated sum of the injected harmonics by FLs and CFLs in residential houses and commercial buildings contributes to the increased current distortion within distribution systems.

From Fig. 12, LEDs are more environmentally friendly, cost-effective and Energy efficient than CFL and incandescent lights [16]. From Fig. 11(b), the conductor is Zinc. The conductivity of Zinc is lower than others [18]. Thus, it should be changed to conducting lines, also other design issues.

There are other problems concerned with the Distribution board of one of Mini-Grid as shown in Fig. 13. Such kind of board can be dangerous for electrical hazards. Therefore, these should change. Also, the installations at some houses needed to renovate



Fig. 13: Distribution Board of Mini-Grid

c) Wood Energy for Cooking



Fig. 14: Conventional Firewood Cooking at Village

The rice and curry are daily main food as well as traditional donation food in Myanmar, especially at the

village. Consequently, the villagers always apply the firewood for cooking. Also, they use it for making Myanmar traditional snacks and the tea. Fig. 14 reveals how the villagers are cooking at the focused village. Consequently, the negative impacts are:

i. *Deforestation towards Climate Change*

Based on the collected data, average fuelwood consumption per household is 7 to 8 tons per year. Besides, there is other fuelwood consumption for the donation events. Then, the total fuelwood consumption for the whole village is nearly 6000 tons per year. That amount will cause the significant impacts of deforestation, and as a consequence, Climate Change will contribute.

ii. *GHG Emissions towards Global Warming*

CO₂ Emissions from the burning wood is 109.6 kg CO₂ per GJ [19]. Other chemicals are produced, including nitrogen dioxide; 200 g of CO₂ equivalent per kg of wood burnt, the gas is 300 times more potent as a greenhouse gas than CO₂ and lasts 120 years in the atmosphere. Methane produced (70 g of CO₂ equivalent per kg of wood) – 21 times more potent than CO₂. Carbon monoxide is also in large amounts. Overall, although figures vary depending on a multitude of factors, there is no doubt that wood burning is contributing to Global Warming [20]. Due to [27], the Emissions from fuelwood consumption at that village calculated as nearly 8981128 kg CO₂/year.

iii. *Health Problems from the Wood Burning*

The health implications of wood burning derive from the emissions which contain carbon monoxide, nitrogen dioxide, and particulates, as well as other noxious gases [20]. More than four million people die each year from illnesses attributable to indoor air pollution from cooking with traditional biomass and inefficient cook-stoves. For the one billion people who depend on health facilities in remote and rural areas that presently lack electricity [9, 21].

iv. *Cost for Fuelwood*

According to the interviews' results, the monthly fuelwood per household is 5 \$. Then, the total cost for the whole village is 48000 \$ per year. That amount calculated for the fuelwood usage in the households. It is sure that there is more cost of the fuelwood combination with the fuelwood cost for donation ceremonies.

v. *High Possibility of Fire Hazard*

Due to site study, there is easy to be fire hazard from the combinational effects of conventional firewood cooking and the constructional materials of the rural house. It located in the Central Dry Zone Area that is also easy to be the fire hazard due to its weather condition. Moreover, there is Diesel fuel storage for

Diesel Mini-Grids. The combinational effects of these three causes may lead to being the high possibility of fire hazard towards damages.

d) *Vital Needs of the Water*

The water predominantly need for the life of human being. It is essential for daily uses: drinking, cooking, cleaning, showering, washing the clothes and others, food, waste disposal, and the recreation. The soil of the village Nat Kan Lel is blessed for agricultural businesses: especially for the fruits such as dragon fruit, tamarind, mango, banana, and the seeds (sunflower and the nuts). The villagers achieve the income of 2200 to 2950 \$ from planting of the mango for one acre. They also gained the income of 5162 \$ from planting of the one acre dragon fruit. Thus, the water is also vitally needed for the crops production livestock at that village.

The interviews results identify that average water need for each villager is about 25 gallons per day. Then, the water needs (including the agriculture) for the whole village is around 120000 gallons (454249 liters) per day.

It observed that there are seven water tube-wells (including one well at RHC) in that village to fulfill the water needs. Among these tube-wells, the one tube-well is supported by the Government in June 2010. That tube-well was deepest (600 ft depth, 4 inches diameter, 2200 gallon per hour) and its water has pH (power of Hydrogen) 7.5. Humans have a higher tolerance for pH levels, and drinkable levels range from 4-11 [22]. Hence, the villagers obtained the drinking water from it. There is 5000 gal water storage tank at that tube-well. The others are 300 depths with 3 inches diameters. The tube-well of RHC has 5000 gal water storage tank, and the others have their tanks around 4000 gal storage. The village has other rain water storage facilities at the monasteries and households as reflected in Figs. 15 and 16.

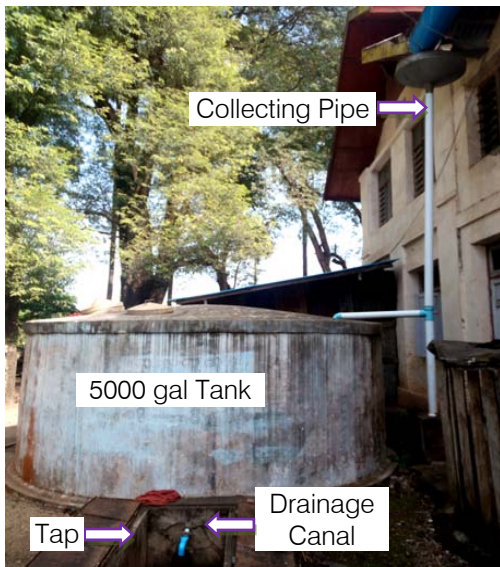


Fig.15: Rain Water Storage at the Monastery



Fig. 16: Rain Water Storage at the Household

e) *Energy Needs for Small Enterprise*

During the ground visit, it saw that there are two categories of the industrial loads dealt with the small enterprises. The former is needed for daily use as revealed in Figs. 17 and 18. The latter are required for seasonal use. Two oil mills usually operate during the harvest periods. The villagers want to develop small enterprise like carpentry workshop and others when they achieve sufficient Electrical Energy. Currently, the annual Diesel fuel consumption is about 500 gal (1893 liters) per year. Then, from [28], the emissions evaluated as 4995 kg CO₂ per year at that village.

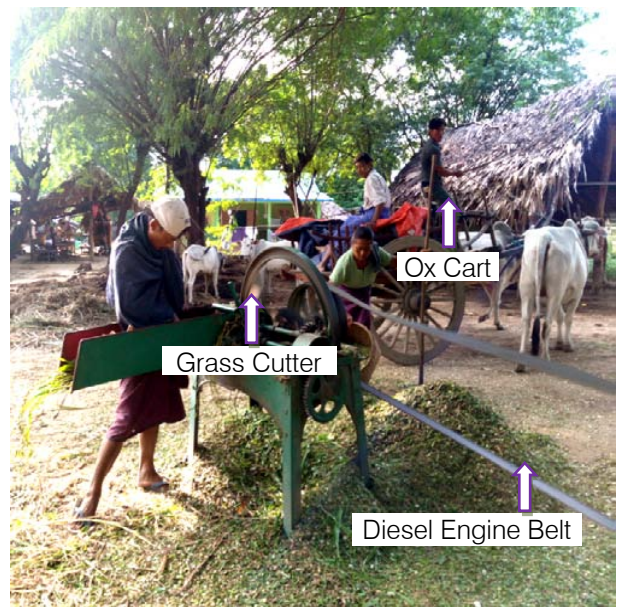


Fig. 17: Villager is Grass Cutting for Cow-Feed



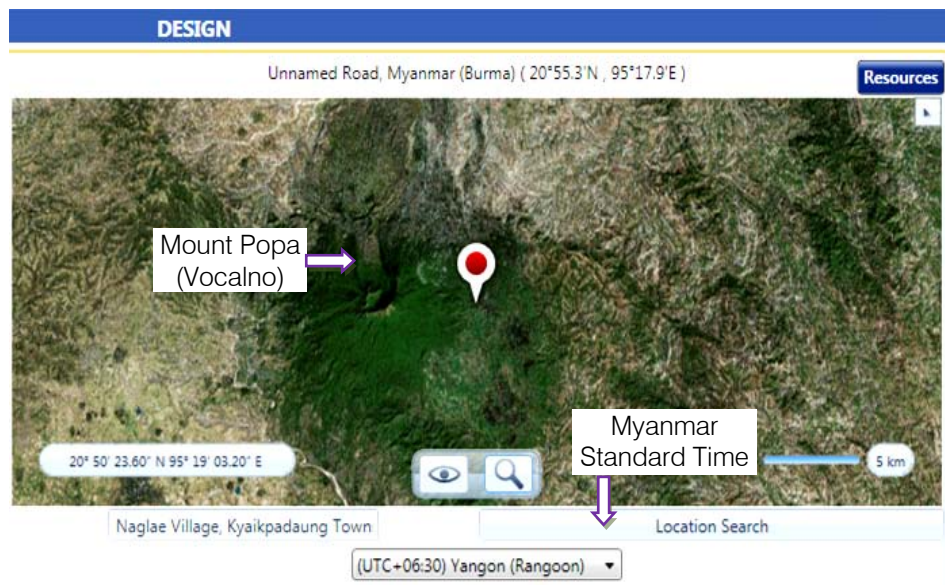
Fig. 18: Drilling Machine at Rural Workshop

IV. AUTONOMOUS PV MINI-GRID MODEL IN HOMER PRO

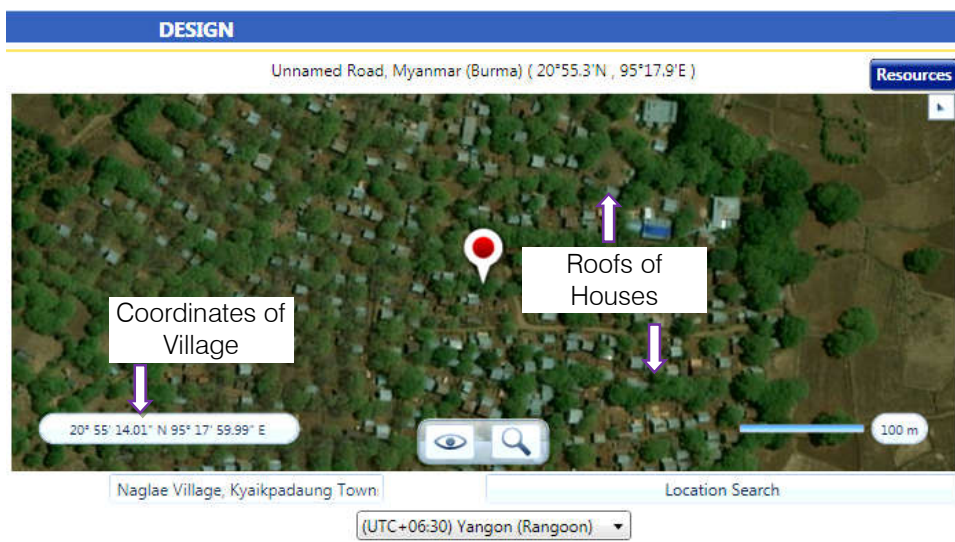
Based on the site visit data, Autonomous or Standalone PV Mini-Grid modeled in HOMER Pro. Firstly, it is important to locate the project. Then, the parameters are inputted step by step as the follows.

a) Location in the Map-Box of HOMER Pro

The village searched in the map-box of HOMER Pro with its geographical coordinate and Myanmar Standard Time: six hours and thirty minutes ahead of GMT (Greenwich Mean Time) as shown in Fig. 19.



(a) Aerial Region View of Village Nat Kan Lel (Naglae) near Mount Popa



(b) Aerial Zoom of Village Nat Kan Lel (Naglae)

Fig. 19: Location of a Village Nat Kan Lel in the Map-box of HOMER Pro

b) Economics, Constraints and Sensitivity Values

The Economics parameters inserted with the sensitivity values for the analysis. Discount rates and the inflation rates took from [12, 23]. The Currency set as US Dollar (\$) in the Economics menu box in HOMER Pro. The parameters of the Constraints: Annual capacity shortage and Project lifetime are also validated. For Operating Reserve as a percentage of loads, Load in current time step set as 10%.

c) Input of the Resources

GHI (Global Horizon Irradiation) is the key parameter for designing of PV power generation system. The highest GHI identified in the central lowland area of Myanmar where average daily totals reach yearly total of 1900 kWh/m² (average daily total up to 5.2 kWh/m²) or higher [24]. In this work, GHI is downloaded from NREL (National Renewable Energy Lab) database in HOMER Pro. It is evident that the downloaded GHI data as mentioned in Fig. 21 are relevant with the map data of Fig. 20 [25]. It is also appropriate with [26]; Central Dry Zone Area of Myanmar (Magway, Mandalay, and Sagaing regions) is highly suitable with average radiation of more than 5 kWh per m² per day and limited variation in radiation during the rainy season. Hence, the proposed project located in Mandalay region is very feasible to implement PV Mini-grid system. The required temperature data also downloaded from NREL in HOMER Pro.

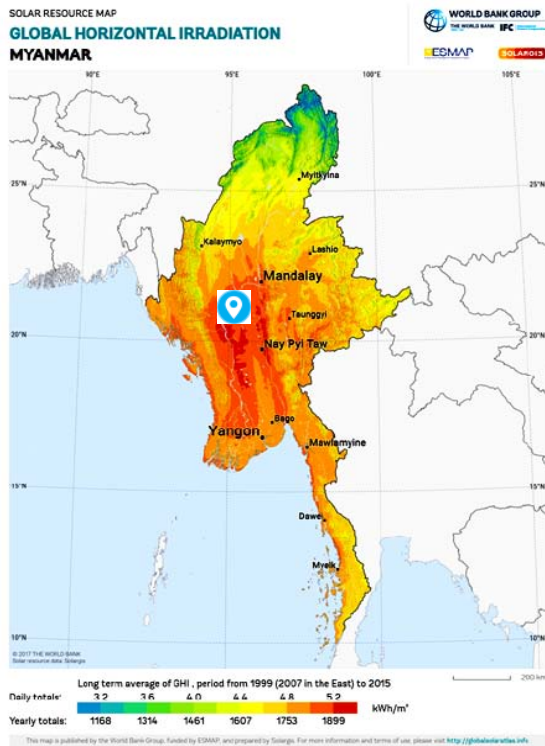


Fig. 20: GHI of Myanmar [25]

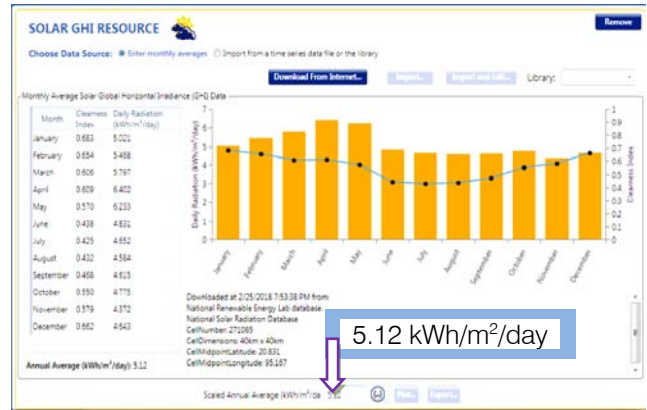


Fig. 21: GHI of Village Nat Kan Lel

Average wind speed required for modern wind turbines is at least 6 m/sec; most of Myanmar considered unattractive as average wind speeds are below 4 m/sec, except for coastline and mountain ranges such as Shan and Chin states [26]. The focused village not located in these states. Again, the wind speed is also downloaded in HOMER Pro, just to know its wind potential how many (with Anemometer height 50 m) at that location. Then, it found that Scaled Annual Average is 3.08 m/sec. That value is relevant to the above point. Hence, the wind system is not feasible. During site study, there is no hydropower site around the focused village. For more confirmed, it investigated from [11]. The resulting figure obtained as highlighted in Fig. 22. Then, there is only one left, PV Mini-grid to create zero emissions power generation.

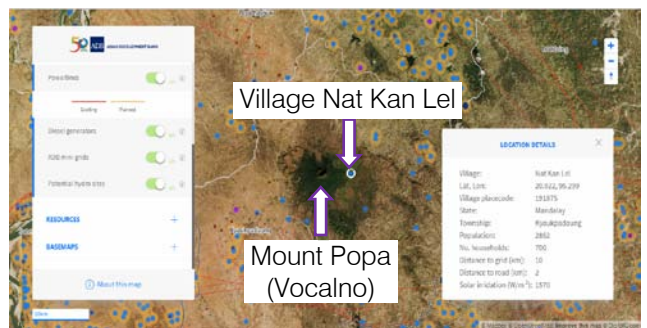


Fig. 22: Investigating the Potential of Hydropower [11]

d) Demand Scenarios

According to the data collection from a site visit, the demand scenarios inputted. These predicted for 3 Pagodas, 3 Monasteries, 800 households (HH), RHC and High School. Based on load consumptions, HH is distinguished as 500 low power consumption HH, 200 medium power consumption HH and 100 high power consumption HH. Combined with lighting and TV loads are inputted as primary electric load 1 with 293.6 kWh per day and 92.5 kW peak as described in Fig. 23.

These considered with LEDs due to the negative impacts of CFL that mentioned in sub-session III-A.

(Alternating Current) Power by the converter to supply the AC Demands.

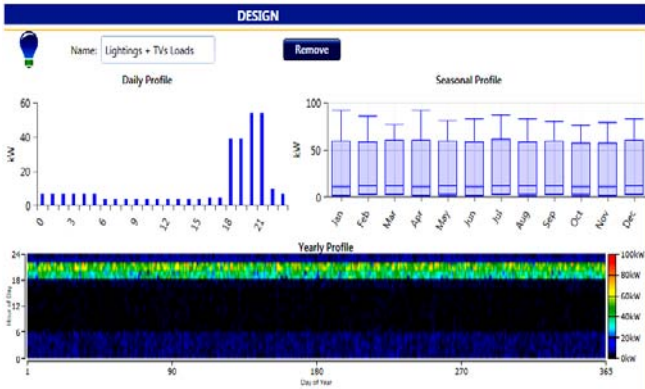


Fig. 23: Inputs of Lightings and TV Loads

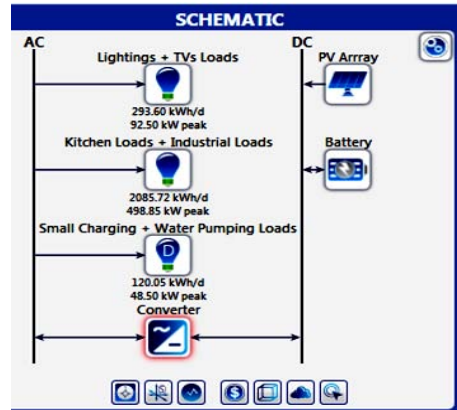


Fig. 25: Proposed PV Mini-Grid Model (100%RE)

As reported in sub-session III-C, the firewood cooking causes the significant drawbacks including Environmental impacts; Global Warming and Climate Change. To solve these issues, electric appliances (rice cooker, Cooking Pot, and Kettle) are involved in the demand scenarios. The industrial loads combined in primary load 2 of HOMER Pro. Then, kitchen and industrial loads inputted; 2085.72 kWh per day with 498.85 kW peak as reflected in Figs. 24 and 25.

f) Components of Autonomous PV Mini-Grid

The parameters of the main components of Autonomous PV Mini-grid modeled in HOMER Pro. The costs of PV for 1 kW are: Capital cost 950 \$; Replacement cost 0 \$; Operation and maintenance cost 10 S/year. The advanced input is the ground reflectance 20% and the array (panel) slope is 20.92°. Temperature inputs with Sensitivity values are set with PV Array temperature coefficient (%/°C) -0.43, -0.45 and -0.47 linked with PV Array operating cell temperatures 43; 45 and 47 as mentioned in Fig. 26. The battery inputs for 1 kWh are: Capital cost 200 \$; Replacement cost 160 \$; Operation and maintenance cost 20 S/year; lifetime ten years. The converter inputs are: for 1 kW are: Capital cost 340 \$; Replacement cost 280 \$; Operation and maintenance cost 5 S/year and lifetime fifteen years.

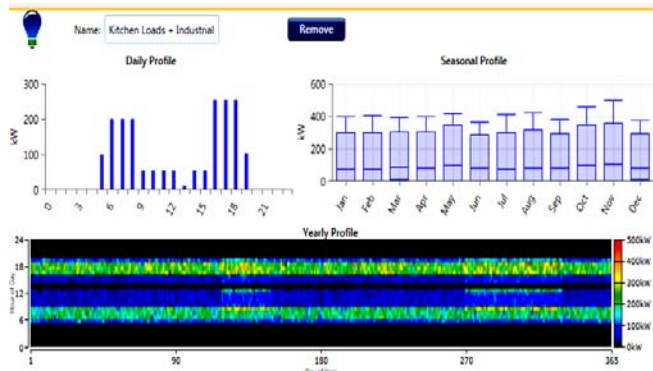


Fig. 24: Inputs of Kitchen and Industrial Loads

e) PV Mini-Grid Model in HOMER Pro

As mentioned in IV-C, only PV is reliable at the focused location. Thus, PV arrays are involved. At night time, PV cannot generate. Hence, the storage battery bank considered for the backup power system as proposed in Fig. 23. Then, the DC (Direct Current) power in the battery bank is transformed to AC

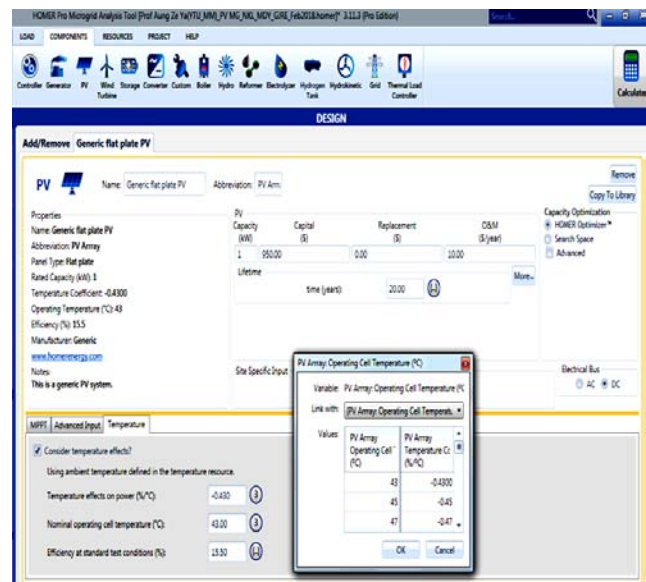


Fig. 26: Inputs of PV System in HOMER Pro

g) Diesel Mini-Grid Model in HOMER Pro

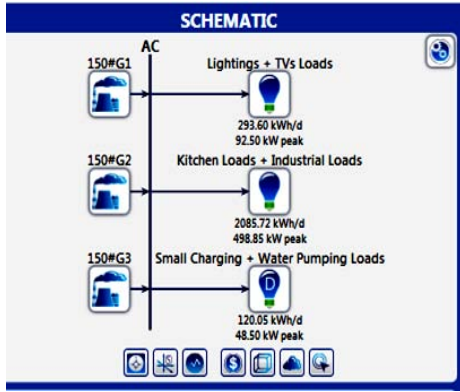


Fig. 27: Diesel Mini-Grid Model (100% NRE)

Fig. 27 shows the model of Diesel Mini-Grid with three 150 kVA Diesel Generators for same demands of the focused village to investigate the impacts of Diesel

System. It is also for comparison of 100% RE System and 100% NRE (Non-Renewable Energy) System. The inputs are Diesel price 0.62 to 0.72 \$/L (for Sensitivity Analysis), Capital cost 52500 \$; Replacement cost 52500 \$; Operation and maintenance cost 2 \$ per hour for Diesel Generators.

V. RESULTS AND DISCUSSIONS

a) Comparison of Two Models

In HOMER Pro, the thousands of PV and Diesel Mini-Grid models simulated with the mix-analysis of Techno-Economic feasibilities.

Then, the optimum designs are achieved with the Tabular results of different portions (architecture, cost, system, and each component) as mentioned in Figs. 28 and 29. The upper table is Sensitivity results, and the lower one is Optimization results. The optimum model is at the first row of these tables.

Sensitivity Cases

Sensitivity			Architecture				Cost			System			
NominalDiscountRate (%)	ExpectedInflationRate (%)	Capacity Shortage (%)	PV Array (kW)	Battery	Converter (kW)	Dispatch	COE (\$)	NPC (\$)	Operating cost (\$/yr)	Initial capital (\$)	Ren Frac (%)	Total Fuel (L/yr)	Cap
7.12	4.47	15.0	1,032	2,436	292	LF	\$0.289	\$3.63M	\$132,826	\$1.57M	100	0	980
8.63	4.47	15.0	1,032	2,436	292	LF	\$0.307	\$3.38M	\$132,895	\$1.57M	100	0	980
7.12	7.50	15.0	1,394	1,908	400	LF	\$0.261	\$4.32M	\$119,335	\$1.84M	100	0	1.3
8.63	7.50	15.0	1,032	2,436	292	LF	\$0.272	\$3.95M	\$132,488	\$1.57M	100	0	980
7.12	4.47	20.0	819	2,340	429	LF	\$0.286	\$3.36M	\$126,607	\$1.39M	100	0	778
8.63	4.47	20.0	819	2,340	429	LF	\$0.302	\$3.12M	\$126,640	\$1.39M	100	0	778

Optimization Results

Architecture				Cost				System		PV Array		Battery		
PV Array (kW)	Battery	Converter (kW)	Dispatch	COE (\$)	NPC (\$)	Operating cost (\$/yr)	Initial capital (\$)	Ren Frac (%)	Total Fuel (L/yr)	Capital Cost (\$)	Production (kWh/yr)	Autonomy (hr)	Annual Throughput (kWh/yr)	Nomin
1,032	2,436	292	LF	\$0.289	\$3.63M	\$132,826	\$1.57M	100	0	980,732	1,536,344	14.0	434,801	2,438
1,068	2,376	295	LF	\$0.289	\$3.63M	\$131,555	\$1.59M	100	0	1,014,702	1,589,559	13.7	430,032	2,378
1,029	2,472	288	LF	\$0.290	\$3.65M	\$133,658	\$1.57M	100	0	977,174	1,530,771	14.3	437,417	2,474
1,021	2,472	299	LF	\$0.290	\$3.65M	\$134,047	\$1.57M	100	0	970,166	1,519,791	14.3	438,650	2,474
999	2,520	297	LF	\$0.290	\$3.65M	\$135,007	\$1.55M	100	0	948,929	1,486,523	14.5	441,891	2,522
1,047	2,472	287	LF	\$0.291	\$3.67M	\$133,882	\$1.59M	100	0	994,832	1,558,432	14.3	437,688	2,474

Fig. 28: Simulative Results of PV Mini-Grid Model (100%RE)

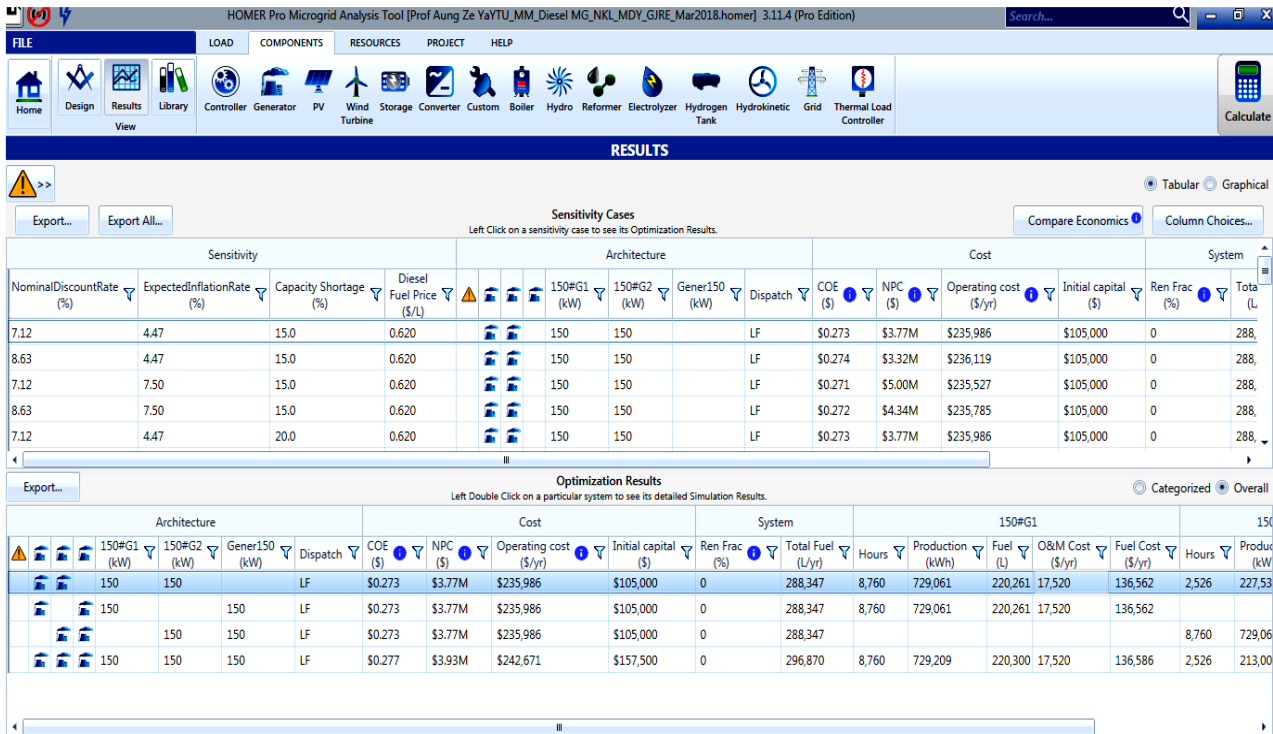


Fig. 29: Simulative Results of Diesel Mini-Grid Model (100% NRE)

Table 1: Comparison of PV Mini-Grid (100% RE) and Diesel Mini-Grid (100% NRE)

Model	Design	Annual Production (kWh/yr)	COE (\$)	Net Present Cost (\$)	Operating Cost (\$/ yr)	Initial Capital (\$)	Diesel Fuel			
							Each (L/yr)	Total (L/y)	Each Cost (\$/yr)	Total Cost (\$/yr)
PVMG (100 % RE)	PV (1032 kW)	1536344	0.289	3.63 M	132826	1.57 M	-	-	-	-
	Battery (2436 kWh)	434801 (Through-put)								
	Converter (292 kW)	808240								
DMG (100% NRE)	DG1 (150 kW)	729061	0.273 (at 0.62 \$/L)	3.77 M (at 0.62 \$/L)	235986 (at 0.62 \$/L)	105000	220261	288348	136562 (at 0.62 \$/L)	178776 (at 0.62 \$/L)
			0.307 (at 0.72 \$/L)	4.85 M (at 0.72 \$/L)	264619 (at 0.72 \$/L)	105000		158588 (at 0.72 \$/L)	207610 (at 0.72 \$/L)	
	DG2 (150 kW)	227535				68087		42214 (at 0.62 \$/L) 49022 (at 0.72 \$/L)		

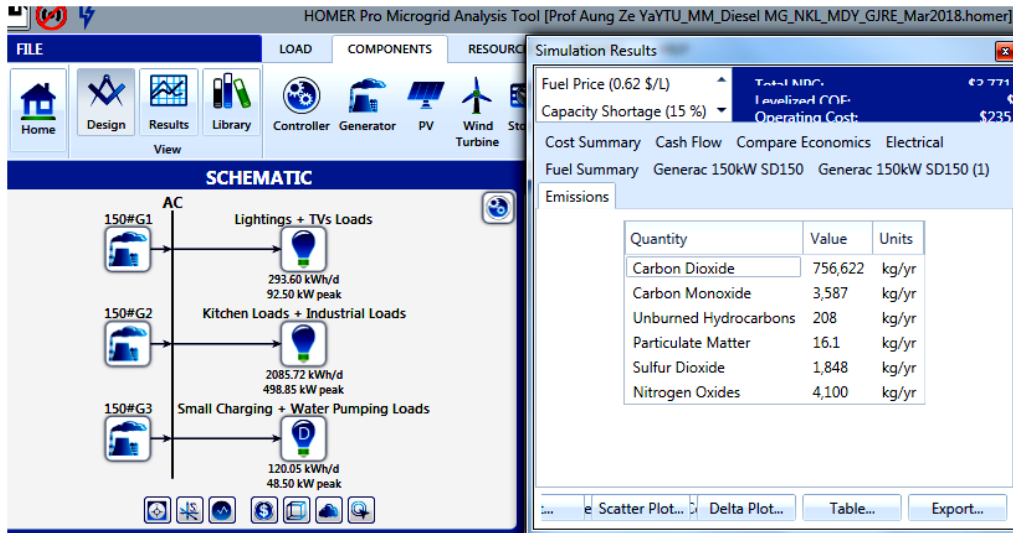


Fig. 30: Simulative Results of Emissions from Diesel Mini-Grid

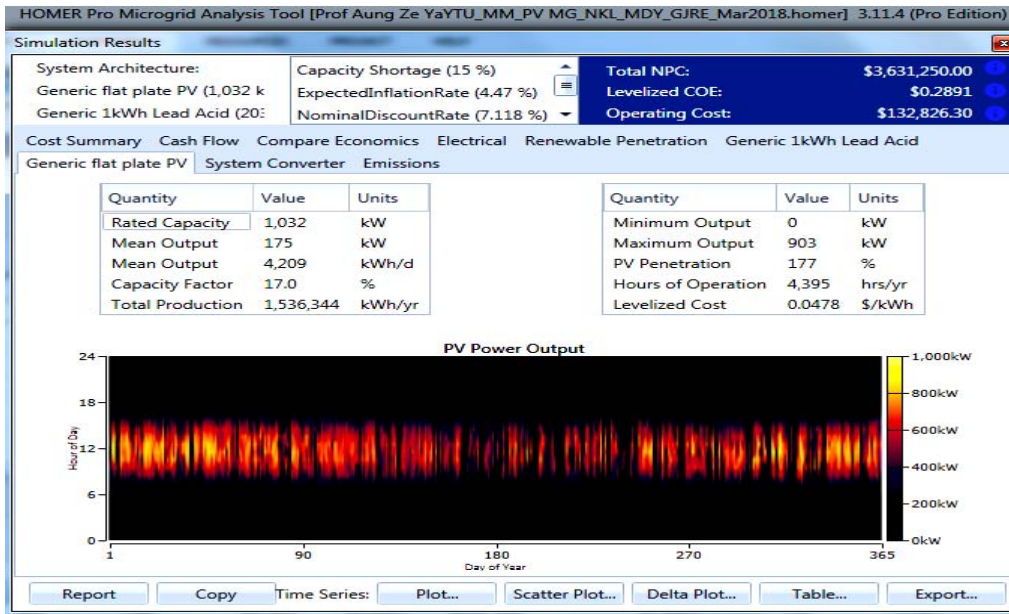


Fig. 31: Simulative Results of PV System

The comparison of the simulative results of PV Mini-Grid (100% RE) and Diesel Mini-Grid (100% NRE) mentioned in Table 1. Cost of Energy (COE) of PV Mini-Grid is slightly (0.016 \$) higher than Diesel Mini-Grid at Diesel fuel price 0.62 \$/L. However, COE of Diesel Mini-Grid at Diesel fuel price 0.72 \$/L is 0.018 \$ higher than the PV Mini-Grid. Again, the Initial capital cost of PV Mini-Grid is higher than Diesel Mini-Grid. Meanwhile, the operating cost of Diesel Mini-Grid is higher than PV Mini-Grid.

The main advantages of 100% RE model are there is no fuel consumption, no fuel cost, no worries about the increasing of fuel price and no emission. For 100% NRE model there is needed to consume the large

fuel and fuel cost according to the fuel price as expressed in the right side of Table 1. Moreover, the Diesel Mini-Grid significantly contributes GHG emissions as reflected in the Fig. 30. Hence, it is evident that 100% RE model is the appropriate option from both economical and ecological point of views for long years.

b) Results of PV Mini-Grid (100% RE) Model

HOMER Pro evaluated the performance of PV Mini-Grid model with different kinds of results: Tabular and Graphical forms as expressed in Figs. 31 to 37.

i. PV Results

Simulative results of PV reflected in Fig. 31 are PV rated capacity 1032 kW, maximum output 903 kW,

capacity factor 17%, production 1536344 kWh/yr, mean output 4209 kWh/day, and hours of operation 4395 hr/yr.

ii. *Battery Results*

Fig. 32 identified the simulative results of the Battery storage system. It has 2436 batteries with 203 strings in parallel and the bus voltage is 144 V. Its annual energy data is: input 484765 kWh/yr, output 388898 kWh/yr, losses 97081 kWh/yr, and throughput 434801. Its lifetime throughput is 194800 kWh, and the expected life is 4.48 years.

iii. *Converter Results*

Fig. 33 highlighted the Converter results as: capacity 292 kW, mean output 92.33 kW, minimum output 0 kW, maximum output 292 kW, capacity factor

31.5%, hours of operation 8594 hr/yr, energy output 808240 kWh/yr, energy input 850779 kWh/yr, and losses 42539 kWh/yr. All primary and deferrable loads considered as AC in the load profiles of village Nat Kan Lel. Therefore, in the waveform description of Fig. 33, there is no rectifier output.

iv. *Electrical Results*

Fig. 34 mentioned the Electrical results. These are: AC primary load 764563 kWh/yr (94.8%), deferrable load 43677 kWh/yr (5.4%), total consumption 808240 kWh/yr, excess electricity 589698 kWh/yr, unmet electric load 103891kWh/yr, capacity shortage 137542 kWh/yr, and maximum renewable penetration 10211.

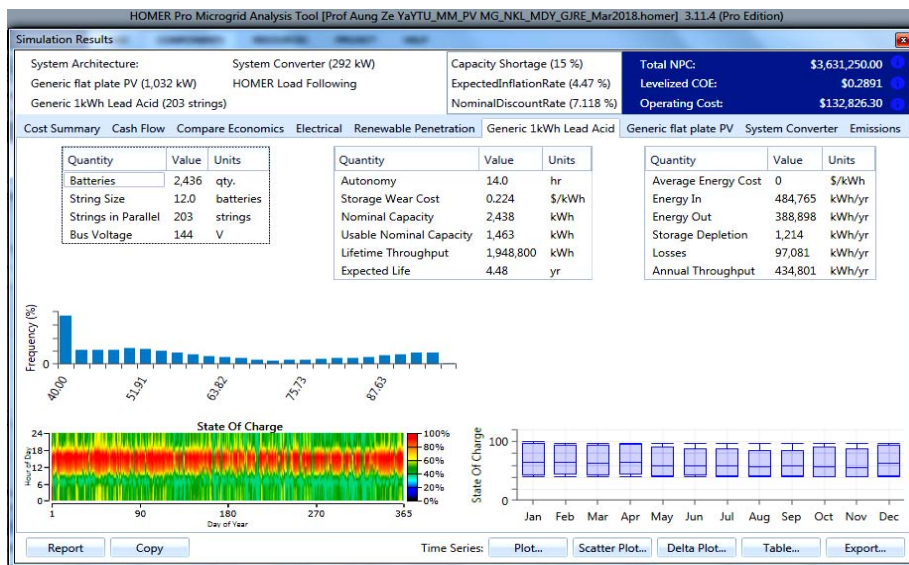


Fig. 32: Simulative Results of Battery Storage System

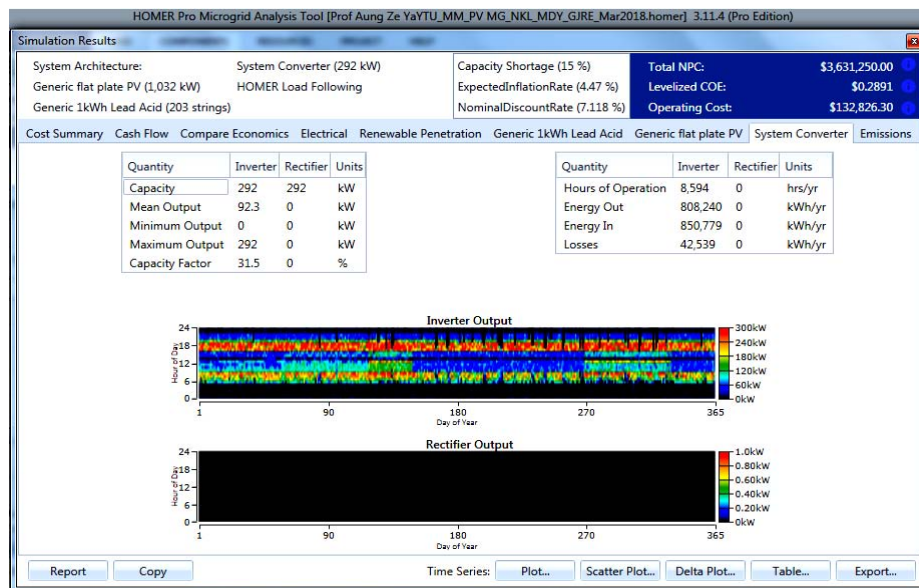


Fig. 33: Simulative Results of Converter

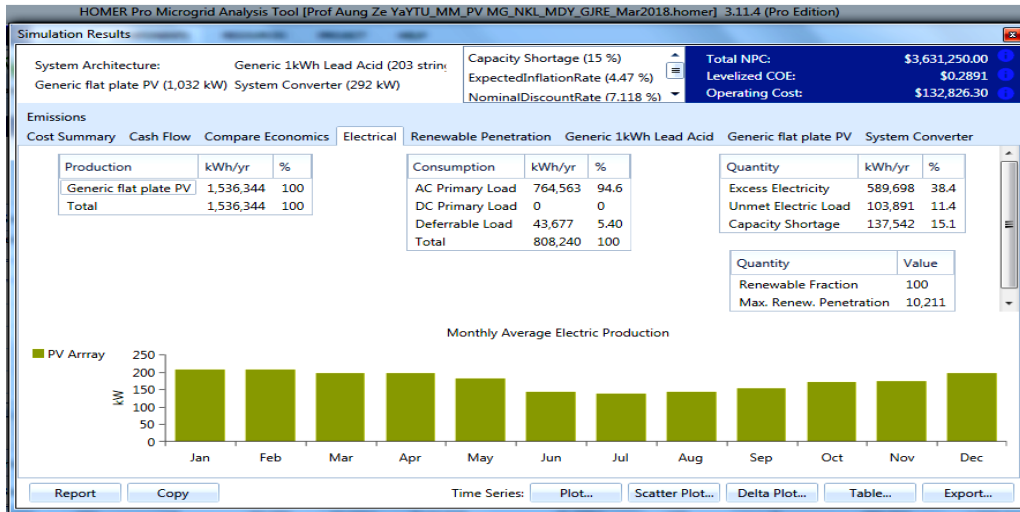


Fig. 34: Electrical Results of 100% RE Model

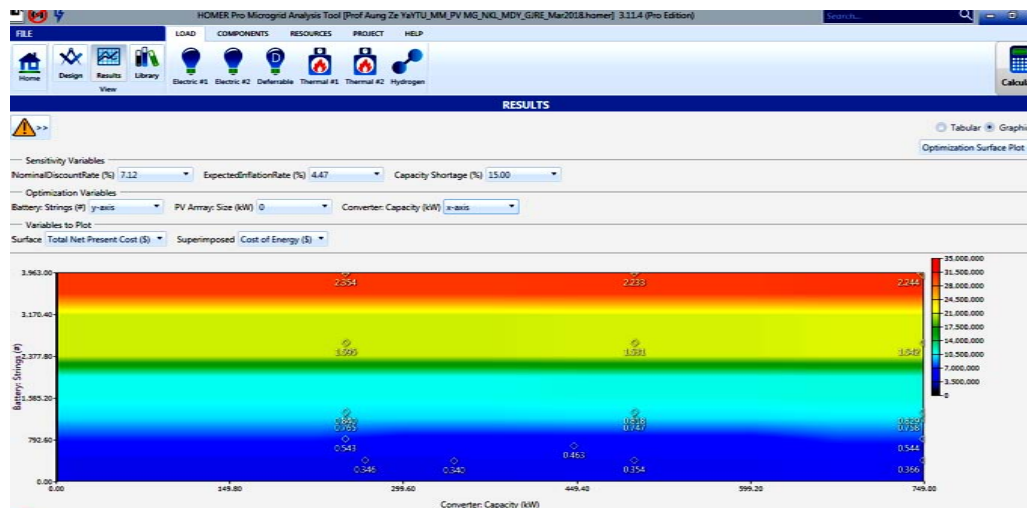


Fig. 35: Optimization Surface Plot of Battery Strings vs. Converter Capacity (kW) with Variables: Total NPC and COE

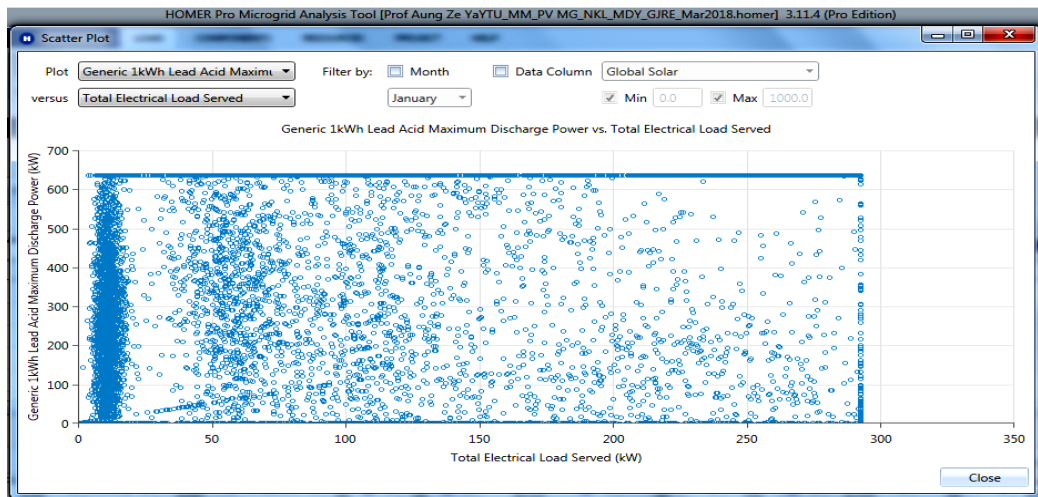


Fig. 36: The Battery Discharge vs. Total Electrical Load Served of Proposed PV Mini-Grid (100% RE)

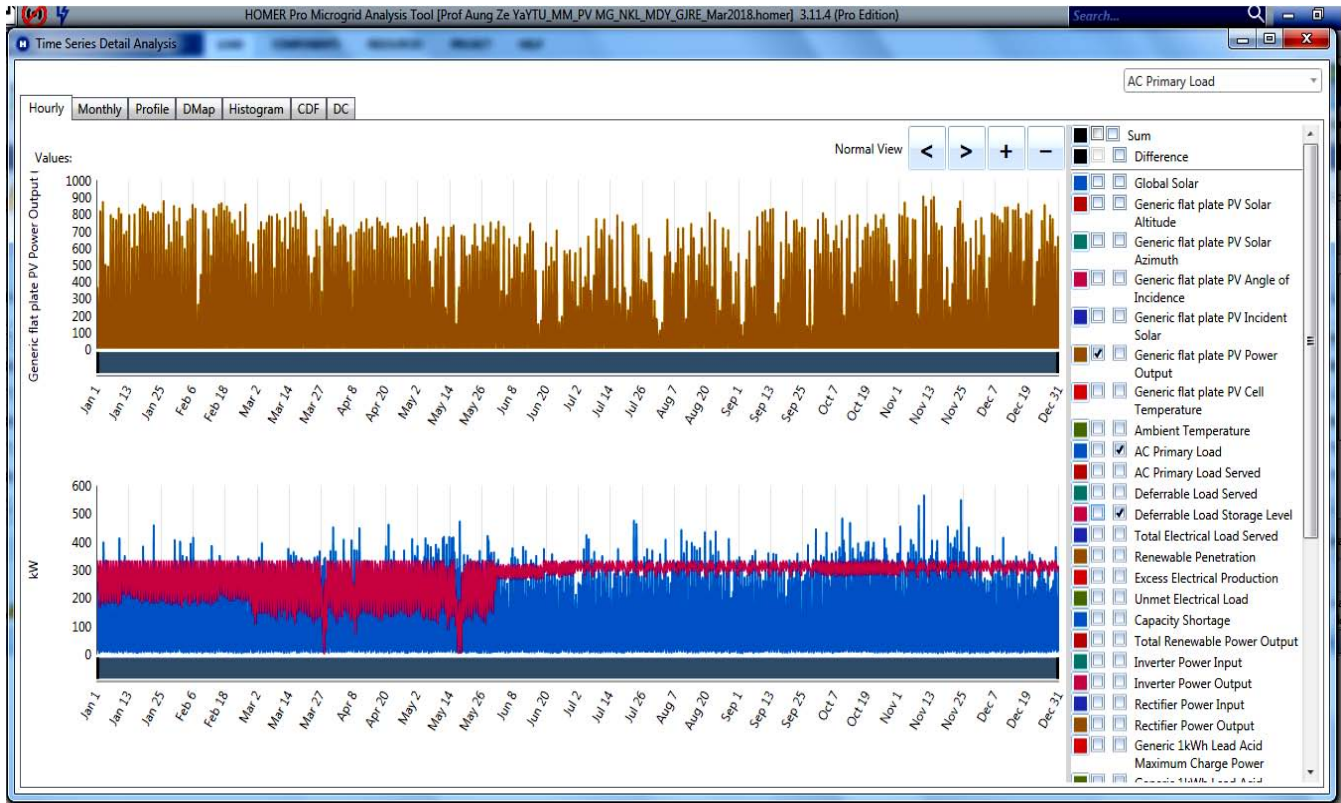


Fig. 37: Time Series Analysis of PV Power Output (Upper), Primary Load and Deferrable Load Storage Level (Lower)

VI. CONCLUSIONS

Rural Electrification is the one of the country's prioritized work because Rural Development is directly proportional to Rural Electrification. The Village Nat Kan Lel (Nagale) located near the National Park of Mount Popa, one of the legends of Myanmar. Hence, it is more important to conserve the forests as well as the Eco-system near it. Thus, the Novel Aim of this research is the development of 100% RE System.

The focused place is a big village blessed with high potential of Solar PV Energy as well as high soil quality of Agricultural business. At the present time, the inhabitants cannot access sufficient Electricity for 24 hours/day. In sub-session III, The existing problems defined, and the adverse impacts evaluated. At the current situation, there is CO₂ Emissions 4995 kg/yr from the Diesel fuel consumption 1893 L/yr. The fuelwood consumption is 6000 tons/yr and its cost is about 48000 \$/yr. If the Diesel generation system install to fulfill all of the electrical demands, the fuel consumption will be 288348 L/yr, the fuel cost be 178776 \$/yr for the fuel price 0.62 S/L and 207610 S/yr for 0.72 S/L. Also, there will be the significant amount of GHG Emissions: CO₂ 756622 kg/yr, Carbon Monoxide 3587 kg/yr, Unburned Hydrocarbons 208 kg/yr, Particulate Matter 16.1 kg/yr,

Sulfur Dioxide 1848 kg/yr and Nitrogen Oxides 4100 kg/yr. These issues can be solved by the implementation of the proposed PV Mini-Grid model. It composed of PV 1032 kW, Battery 2436 kWh, and Converter 292 kW. The annual productions are: PV 1536344 kWh/yr, Battery throughput 434801 kWh/yr, and Converter 808240 kWh/yr. COE is 0.289\$.

This research work reflected how can improve Green Growth by PV Mini-Grid system. The simulative results are within the acceptable limits. The predicted Optimum model can fulfill the Electrical Energy needs of the whole village with 24-hour supply, uplift the quality of life of the villagers, and contribute to the SDGs. This research work can guide the strategic planning of the PV Mini-Grid system with linking the ground study as well as the application of the impressive tool, HOMER Pro.

ACKNOWLEDGEMENTS

First of all, the author expresses the deepest acknowledges to his father, U Sein Hla (Ret. Executive Electrical Engineer, Seven National Literatures Awarded Author, and the member of Central Executive Committee of Myanmar Writers Association), and also his mother, Daw Htway Lay for their infinite encouragements.

The author is much obliged to U Nyi Hla Nge (Ret. Deputy Minister of Ministry of Science and Technology, Chairman of Steering Committee for Centre of Excellence Technological Universities, and Vice Chairman of National Education Policy Commission) for his great leadership. The author deeply thanks to Dr. Myint Thein, Rector of Yangon Technological University (YTU) for his instruction. Also, the author is grateful to Dr. Khin Than Yu, Pro-Rector of Yangon Technological University for her guidance. Special thanks are due to Dr. Peter Lilienthal (CEO and Founder of HOMER Energy, USA) for sharing his invaluable experience. The author offers the heartfelt appreciations to JICA EEHE (Japan International Cooperation Agency, Enhancement of Engineering Higher Education) Project at YTU in Myanmar for covering the author charge.

REFERENCES RÉFÉRENCES REFERENCIAS

1. Z. Ya, "French Green Growth Paradigm in-Line with Eu Targets Towards Sustainable Development Goals", *European Journal of Sustainable Development*, Vol.5, No.2, Pp143-169, Rome: European Center of Sustainable Development, 2016.
2. A. Z. Ya, "Scoping Renovation-Options and Strategic Issues for Micro-Grid Deployment of Renewable Energy Scenarios in Myanmar's Rural Areas", Reinit, 2014.
3. Z. Ya, "Feasibility Study on a Stand-Alone Photovoltaic Hybrid Mini-Grid Power Generation System to Promote the Rural Electrification Rate in Mandalay Region of Myanmar", *Transactions on Gigaku*, Vol.2, No.2, So1009/1-7, Nagaoka University of Technology, 2014.
4. Bloomberg New Energy Finance (BNEF) Et All., "off-Grid Solar Market Trends Report", 2016.
5. Department of Rural Development (DRD), Rural Electricity Access: Molfrd and Wb off-Grid Electrification in Myanmar National Electrification Project, Nay Pyi Taw, 2015.
6. Department of Rural Development (DRD), 2016. 70% Rural Electrification Villages with the Household Data: Myanmar Census by the End of Fy 2015-2016, Nay Pyi Taw, 2016.
7. Department of Rural Development (DRD), List of Electrified Villages by the End of Fy 2016-2017, National Electrification Project", Nay Pyi Taw, 2018.
8. Wb, "National Electrification Project of Myanmar", Washington D.C, Usa, 2015.
9. IRENA, "RE thinking Energy2017: Accelerating the global energy transformation", Abu Dhabi, 2017.
10. <http://www.homerenergy.com/>
11. <http://adb-myanmar.integration.org/>
12. <https://www.adb.org/countries/myanmar/>
13. <https://www.google.com.mm/maps/>
14. <https://www.litetronics.com/true-environmental-impact-of-mercury-in-cfls/>
15. <https://www.wondermakers.com/Portals/0/docs/Hiden%20Enviornmental%20Hazards%20of%20CFLs.pdf?ver=2014-03-25-093208-543>
16. <https://energy.gov/eere/articles/study-environmental-benefits-leds-greater-cfls>
17. Muhyaddin J. H. Rawa et all., "Experimental Measurements and Computer Simulations of FL and CFL Lamps for Harmonic Studies", UK Sim-AMSS 16th International Conference on Computer Modelling and Simulation, UK, 2014.
18. <http://www.tibtech.com/conductivity.php>
19. https://www.volker-quaschnig.de/datserv/CO2-spez/index_e.php
20. <https://www.transitionculture.org/2008/05/19/is-burning-wood-really-a-long-term-energy-descent-strategy/>
21. Who and The World Bank, "Access to Modern Energy Services for Health Facilities in Resource-Constrained Settings". Geneva, Switzerland: Who, 2014.
22. <http://www.fondriest.com/environmental-measurements/parameters/water-quality/ph/>
23. <http://www.cbm.gov.mm/>
24. The World Bank; ESMAP, "Solar Resource and Photovoltaic Potential of Myanmar", Washington DC, USA, The World Bank, 2017.
25. <https://solargis.com/products/maps-and-gis-data/download/myanmar>
26. ADB, "Developing Renewable Energy Mini-Grids in Myanmar". ADB: Mandaluyong City, Metro Manila, Philippines, 2017.
27. <http://www.kaltimber.com/blog/2017/6/19/how-much-co2-is-stored-in-1-kg-of-wood>
28. <https://carbonpositivelife.com/co2-per-litre-diesel/>

GLOBAL JOURNALS GUIDELINES HANDBOOK 2018

WWW.GLOBALJOURNALS.ORG

FELLOWS

FELLOW OF ASSOCIATION OF RESEARCH SOCIETY IN ENGINEERING (FARSE)

Global Journals Incorporate (USA) is accredited by Open Association of Research Society (OARS), U.S.A and in turn, awards “FARSE ” title to individuals. The 'FARSE' title is accorded to a selected professional after the approval of the Editor-in-Chief /Editorial Board Members/Dean.



- The “FARSE” is a dignified title which is accorded to a person’s name viz. Dr. John E. Hall, Ph.D., FARSE or William Walldroff, M.S., FARSE.

FARSE accrediting is an honor. It authenticates your research activities. After recognition as FARSE, you can add 'FARSE' title with your name as you use this recognition as additional suffix to your status. This will definitely enhance and add more value and repute to your name. You may use it on your professional Counseling Materials such as CV, Resume, and Visiting Card etc.

The following benefits can be availed by you only for next three years from the date of certification:



FARSE designated members are entitled to avail a 40% discount while publishing their research papers (of a single author) with Global Journals Incorporation (USA), if the same is accepted by Editorial Board/Peer Reviewers. If you are a main author or co-author in case of multiple authors, you will be entitled to avail discount of 10%.

Once FARSE title is accorded, the Fellow is authorized to organize a symposium/seminar/conference on behalf of Global Journal Incorporation (USA).The Fellow can also participate in conference/seminar/symposium organized by another institution as representative of Global Journal. In both the cases, it is mandatory for him to discuss with us and obtain our consent.



You may join as member of the Editorial Board of Global Journals Incorporation (USA) after successful completion of three years as Fellow and as Peer Reviewer. In addition, it is also desirable that you should organize seminar/symposium/conference at least once.

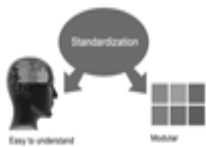
We shall provide you intimation regarding launching of e-version of journal of your stream time to time.This may be utilized in your library for the enrichment of knowledge of your students as well as it can also be helpful for the concerned faculty members.





The FARSE can go through standards of OARS. You can also play vital role if you have any suggestions so that proper amendment can take place to improve the same for the benefit of entire research community.

As FARSE, you will be given a renowned, secure and free professional email address with 100 GB of space e.g. johnhall@globaljournals.org. This will include Webmail, Spam Assassin, Email Forwarders, Auto-Responders, Email Delivery Route tracing, etc.



The FARSE will be eligible for a free application of standardization of their researches. Standardization of research will be subject to acceptability within stipulated norms as the next step after publishing in a journal. We shall depute a team of specialized research professionals who will render their services for elevating your researches to next higher level, which is worldwide open standardization.

The FARSE member can apply for grading and certification of standards of their educational and Institutional Degrees to Open Association of Research, Society U.S.A. Once you are designated as FARSE, you may send us a scanned copy of all of your credentials. OARS will verify, grade and certify them. This will be based on your academic records, quality of research papers published by you, and some more criteria. After certification of all your credentials by OARS, they will be published on your Fellow Profile link on website <https://associationofresearch.org> which will be helpful to upgrade the dignity.



The FARSE members can avail the benefits of free research podcasting in Global Research Radio with their research documents. After publishing the work, (including published elsewhere worldwide with proper authorization) you can upload your research paper with your recorded voice or you can utilize chargeable services of our professional RJs to record your paper in their voice on request.

The FARSE member also entitled to get the benefits of free research podcasting of their research documents through video clips. We can also streamline your conference videos and display your slides/ online slides and online research video clips at reasonable charges, on request.





The FARSE is eligible to earn from sales proceeds of his/her researches/reference/review Books or literature, while publishing with Global Journals. The FARSE can decide whether he/she would like to publish his/her research in a closed manner. In this case, whenever readers purchase that individual research paper for reading, maximum 60% of its profit earned as royalty by Global Journals, will be credited to his/her bank account. The entire entitled amount will be credited to his/her bank account exceeding limit of minimum fixed balance. There is no minimum time limit for collection. The FARSE member can decide its price and we can help in making the right decision.

The FARSE member is eligible to join as a paid peer reviewer at Global Journals Incorporation (USA) and can get remuneration of 15% of author fees, taken from the author of a respective paper. After reviewing 5 or more papers you can request to transfer the amount to your bank account.



MEMBER OF ASSOCIATION OF RESEARCH SOCIETY IN ENGINEERING (MARSE)

The 'MARSE' title is accorded to a selected professional after the approval of the Editor-in-Chief / Editorial Board Members/Dean.

The "MARSE" is a dignified ornament which is accorded to a person's name viz. Dr. John E. Hall, Ph.D., MARSE or William Walldroff, M.S., MARSE.



MARSE accrediting is an honor. It authenticates your research activities. After becoming MARSE, you can add 'MARSE' title with your name as you use this recognition as additional suffix to your status. This will definitely enhance and add more value and repute to your name. You may use it on your professional Counseling Materials such as CV, Resume, Visiting Card and Name Plate etc.

The following benefits can be availed by you only for next three years from the date of certification.



MARSE designated members are entitled to avail a 25% discount while publishing their research papers (of a single author) in Global Journals Inc., if the same is accepted by our Editorial Board and Peer Reviewers. If you are a main author or co-author of a group of authors, you will get discount of 10%.

As MARSE, you will be given a renowned, secure and free professional email address with 30 GB of space e.g. johnhall@globaljournals.org. This will include Webmail, Spam Assassin, Email Forwarders, Auto-Responders, Email Delivery Route tracing, etc.





We shall provide you intimation regarding launching of e-version of journal of your stream time to time. This may be utilized in your library for the enrichment of knowledge of your students as well as it can also be helpful for the concerned faculty members.

The MARSE member can apply for approval, grading and certification of standards of their educational and Institutional Degrees to Open Association of Research, Society U.S.A.



Once you are designated as MARSE, you may send us a scanned copy of all of your credentials. OARS will verify, grade and certify them. This will be based on your academic records, quality of research papers published by you, and some more criteria.

It is mandatory to read all terms and conditions carefully.



AUXILIARY MEMBERSHIPS

Institutional Fellow of Open Association of Research Society (USA)-OARS (USA)

Global Journals Incorporation (USA) is accredited by Open Association of Research Society, U.S.A (OARS) and in turn, affiliates research institutions as “Institutional Fellow of Open Association of Research Society” (IFOARS).



The “FARSC” is a dignified title which is accorded to a person’s name viz. Dr. John E. Hall, Ph.D., FARSC or William Walldroff, M.S., FARSC.

The IFOARS institution is entitled to form a Board comprised of one Chairperson and three to five board members preferably from different streams. The Board will be recognized as “Institutional Board of Open Association of Research Society”-(IBOARS).

The Institute will be entitled to following benefits:



The IBOARS can initially review research papers of their institute and recommend them to publish with respective journal of Global Journals. It can also review the papers of other institutions after obtaining our consent. The second review will be done by peer reviewer of Global Journals Incorporation (USA) The Board is at liberty to appoint a peer reviewer with the approval of chairperson after consulting us.

The author fees of such paper may be waived off up to 40%.

The Global Journals Incorporation (USA) at its discretion can also refer double blind peer reviewed paper at their end to the board for the verification and to get recommendation for final stage of acceptance of publication.



The IBOARS can organize symposium/seminar/conference in their country on behalf of Global Journals Incorporation (USA)-OARS (USA). The terms and conditions can be discussed separately.

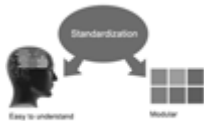
The Board can also play vital role by exploring and giving valuable suggestions regarding the Standards of “Open Association of Research Society, U.S.A (OARS)” so that proper amendment can take place for the benefit of entire research community. We shall provide details of particular standard only on receipt of request from the Board.



The board members can also join us as Individual Fellow with 40% discount on total fees applicable to Individual Fellow. They will be entitled to avail all the benefits as declared. Please visit Individual Fellow-sub menu of GlobalJournals.org to have more relevant details.



We shall provide you intimation regarding launching of e-version of journal of your stream time to time. This may be utilized in your library for the enrichment of knowledge of your students as well as it can also be helpful for the concerned faculty members.



After nomination of your institution as “Institutional Fellow” and constantly functioning successfully for one year, we can consider giving recognition to your institute to function as Regional/Zonal office on our behalf. The board can also take up the additional allied activities for betterment after our consultation.

The following entitlements are applicable to individual Fellows:

Open Association of Research Society, U.S.A (OARS) By-laws states that an individual Fellow may use the designations as applicable, or the corresponding initials. The Credentials of individual Fellow and Associate designations signify that the individual has gained knowledge of the fundamental concepts. One is magnanimous and proficient in an expertise course covering the professional code of conduct, and follows recognized standards of practice.



Open Association of Research Society (US)/ Global Journals Incorporation (USA), as described in Corporate Statements, are educational, research publishing and professional membership organizations. Achieving our individual Fellow or Associate status is based mainly on meeting stated educational research requirements.

Disbursement of 40% Royalty earned through Global Journals : Researcher = 50%, Peer Reviewer = 37.50%, Institution = 12.50% E.g. Out of 40%, the 20% benefit should be passed on to researcher, 15 % benefit towards remuneration should be given to a reviewer and remaining 5% is to be retained by the institution.



We shall provide print version of 12 issues of any three journals [as per your requirement] out of our 38 journals worth \$ 2376 USD.

Other:

The individual Fellow and Associate designations accredited by Open Association of Research Society (US) credentials signify guarantees following achievements:

- The professional accredited with Fellow honor, is entitled to various benefits viz. name, fame, honor, regular flow of income, secured bright future, social status etc.



- In addition to above, if one is single author, then entitled to 40% discount on publishing research paper and can get 10% discount if one is co-author or main author among group of authors.
- The Fellow can organize symposium/seminar/conference on behalf of Global Journals Incorporation (USA) and he/she can also attend the same organized by other institutes on behalf of Global Journals.
- The Fellow can become member of Editorial Board Member after completing 3yrs.
- The Fellow can earn 60% of sales proceeds from the sale of reference/review books/literature/publishing of research paper.
- Fellow can also join as paid peer reviewer and earn 15% remuneration of author charges and can also get an opportunity to join as member of the Editorial Board of Global Journals Incorporation (USA)
- • This individual has learned the basic methods of applying those concepts and techniques to common challenging situations. This individual has further demonstrated an in-depth understanding of the application of suitable techniques to a particular area of research practice.

Note :

//

- In future, if the board feels the necessity to change any board member, the same can be done with the consent of the chairperson along with anyone board member without our approval.
- In case, the chairperson needs to be replaced then consent of 2/3rd board members are required and they are also required to jointly pass the resolution copy of which should be sent to us. In such case, it will be compulsory to obtain our approval before replacement.
- In case of “Difference of Opinion [if any]” among the Board members, our decision will be final and binding to everyone.

//



PREFERRED AUTHOR GUIDELINES

We accept the manuscript submissions in any standard (generic) format.

We typeset manuscripts using advanced typesetting tools like Adobe In Design, CorelDraw, TeXnicCenter, and TeXStudio. We usually recommend authors submit their research using any standard format they are comfortable with, and let Global Journals do the rest.

Alternatively, you can download our basic template from <https://globaljournals.org/Template.zip>

Authors should submit their complete paper/article, including text illustrations, graphics, conclusions, artwork, and tables. Authors who are not able to submit manuscript using the form above can email the manuscript department at submit@globaljournals.org or get in touch with chiefeditor@globaljournals.org if they wish to send the abstract before submission.

BEFORE AND DURING SUBMISSION

Authors must ensure the information provided during the submission of a paper is authentic. Please go through the following checklist before submitting:

1. Authors must go through the complete author guideline and understand and *agree to Global Journals' ethics and code of conduct*, along with author responsibilities.
2. Authors must accept the privacy policy, terms, and conditions of Global Journals.
3. Ensure corresponding author's email address and postal address are accurate and reachable.
4. Manuscript to be submitted must include keywords, an abstract, a paper title, co-author(s) names and details (email address, name, phone number, and institution), figures and illustrations in vector format including appropriate captions, tables, including titles and footnotes, a conclusion, results, acknowledgments and references.
5. Authors should submit paper in a ZIP archive if any supplementary files are required along with the paper.
6. Proper permissions must be acquired for the use of any copyrighted material.
7. Manuscript submitted *must not have been submitted or published elsewhere* and all authors must be aware of the submission.

Declaration of Conflicts of Interest

It is required for authors to declare all financial, institutional, and personal relationships with other individuals and organizations that could influence (bias) their research.

POLICY ON PLAGIARISM

Plagiarism is not acceptable in Global Journals submissions at all.

Plagiarized content will not be considered for publication. We reserve the right to inform authors' institutions about plagiarism detected either before or after publication. If plagiarism is identified, we will follow COPE guidelines:

Authors are solely responsible for all the plagiarism that is found. The author must not fabricate, falsify or plagiarize existing research data. The following, if copied, will be considered plagiarism:

- Words (language)
- Ideas
- Findings
- Writings
- Diagrams
- Graphs
- Illustrations
- Lectures



- Printed material
- Graphic representations
- Computer programs
- Electronic material
- Any other original work

AUTHORSHIP POLICIES

Global Journals follows the definition of authorship set up by the Open Association of Research Society, USA. According to its guidelines, authorship criteria must be based on:

1. Substantial contributions to the conception and acquisition of data, analysis, and interpretation of findings.
2. Drafting the paper and revising it critically regarding important academic content.
3. Final approval of the version of the paper to be published.

Changes in Authorship

The corresponding author should mention the name and complete details of all co-authors during submission and in manuscript. We support addition, rearrangement, manipulation, and deletions in authors list till the early view publication of the journal. We expect that corresponding author will notify all co-authors of submission. We follow COPE guidelines for changes in authorship.

Copyright

During submission of the manuscript, the author is confirming an exclusive license agreement with Global Journals which gives Global Journals the authority to reproduce, reuse, and republish authors' research. We also believe in flexible copyright terms where copyright may remain with authors/employers/institutions as well. Contact your editor after acceptance to choose your copyright policy. You may follow this form for copyright transfers.

Appealing Decisions

Unless specified in the notification, the Editorial Board's decision on publication of the paper is final and cannot be appealed before making the major change in the manuscript.

Acknowledgments

Contributors to the research other than authors credited should be mentioned in Acknowledgments. The source of funding for the research can be included. Suppliers of resources may be mentioned along with their addresses.

Declaration of funding sources

Global Journals is in partnership with various universities, laboratories, and other institutions worldwide in the research domain. Authors are requested to disclose their source of funding during every stage of their research, such as making analysis, performing laboratory operations, computing data, and using institutional resources, from writing an article to its submission. This will also help authors to get reimbursements by requesting an open access publication letter from Global Journals and submitting to the respective funding source.

PREPARING YOUR MANUSCRIPT

Authors can submit papers and articles in an acceptable file format: MS Word (doc, docx), LaTeX (.tex, .zip or .rar including all of your files), Adobe PDF (.pdf), rich text format (.rtf), simple text document (.txt), Open Document Text (.odt), and Apple Pages (.pages). Our professional layout editors will format the entire paper according to our official guidelines. This is one of the highlights of publishing with Global Journals—authors should not be concerned about the formatting of their paper. Global Journals accepts articles and manuscripts in every major language, be it Spanish, Chinese, Japanese, Portuguese, Russian, French, German, Dutch, Italian, Greek, or any other national language, but the title, subtitle, and abstract should be in English. This will facilitate indexing and the pre-peer review process.

The following is the official style and template developed for publication of a research paper. Authors are not required to follow this style during the submission of the paper. It is just for reference purposes.



Manuscript Style Instruction (Optional)

- Microsoft Word Document Setting Instructions.
- Font type of all text should be Swis721 Lt BT.
- Page size: 8.27" x 11", left margin: 0.65, right margin: 0.65, bottom margin: 0.75.
- Paper title should be in one column of font size 24.
- Author name in font size of 11 in one column.
- Abstract: font size 9 with the word "Abstract" in bold italics.
- Main text: font size 10 with two justified columns.
- Two columns with equal column width of 3.38 and spacing of 0.2.
- First character must be three lines drop-capped.
- The paragraph before spacing of 1 pt and after of 0 pt.
- Line spacing of 1 pt.
- Large images must be in one column.
- The names of first main headings (Heading 1) must be in Roman font, capital letters, and font size of 10.
- The names of second main headings (Heading 2) must not include numbers and must be in italics with a font size of 10.

Structure and Format of Manuscript

The recommended size of an original research paper is under 15,000 words and review papers under 7,000 words. Research articles should be less than 10,000 words. Research papers are usually longer than review papers. Review papers are reports of significant research (typically less than 7,000 words, including tables, figures, and references)

A research paper must include:

- a) A title which should be relevant to the theme of the paper.
- b) A summary, known as an abstract (less than 150 words), containing the major results and conclusions.
- c) Up to 10 keywords that precisely identify the paper's subject, purpose, and focus.
- d) An introduction, giving fundamental background objectives.
- e) Resources and techniques with sufficient complete experimental details (wherever possible by reference) to permit repetition, sources of information must be given, and numerical methods must be specified by reference.
- f) Results which should be presented concisely by well-designed tables and figures.
- g) Suitable statistical data should also be given.
- h) All data must have been gathered with attention to numerical detail in the planning stage.

Design has been recognized to be essential to experiments for a considerable time, and the editor has decided that any paper that appears not to have adequate numerical treatments of the data will be returned unrefereed.

- i) Discussion should cover implications and consequences and not just recapitulate the results; conclusions should also be summarized.
- j) There should be brief acknowledgments.
- k) There ought to be references in the conventional format. Global Journals recommends APA format.

Authors should carefully consider the preparation of papers to ensure that they communicate effectively. Papers are much more likely to be accepted if they are carefully designed and laid out, contain few or no errors, are summarizing, and follow instructions. They will also be published with much fewer delays than those that require much technical and editorial correction.

The Editorial Board reserves the right to make literary corrections and suggestions to improve brevity.

FORMAT STRUCTURE

It is necessary that authors take care in submitting a manuscript that is written in simple language and adheres to published guidelines.

All manuscripts submitted to Global Journals should include:

Title

The title page must carry an informative title that reflects the content, a running title (less than 45 characters together with spaces), names of the authors and co-authors, and the place(s) where the work was carried out.

Author details

The full postal address of any related author(s) must be specified.

Abstract

The abstract is the foundation of the research paper. It should be clear and concise and must contain the objective of the paper and inferences drawn. It is advised to not include big mathematical equations or complicated jargon.

Many researchers searching for information online will use search engines such as Google, Yahoo or others. By optimizing your paper for search engines, you will amplify the chance of someone finding it. In turn, this will make it more likely to be viewed and cited in further works. Global Journals has compiled these guidelines to facilitate you to maximize the web-friendliness of the most public part of your paper.

Keywords

A major lynchpin of research work for the writing of research papers is the keyword search, which one will employ to find both library and internet resources. Up to eleven keywords or very brief phrases have to be given to help data retrieval, mining, and indexing.

One must be persistent and creative in using keywords. An effective keyword search requires a strategy: planning of a list of possible keywords and phrases to try.

Choice of the main keywords is the first tool of writing a research paper. Research paper writing is an art. Keyword search should be as strategic as possible.

One should start brainstorming lists of potential keywords before even beginning searching. Think about the most important concepts related to research work. Ask, "What words would a source have to include to be truly valuable in a research paper?" Then consider synonyms for the important words.

It may take the discovery of only one important paper to steer in the right keyword direction because, in most databases, the keywords under which a research paper is abstracted are listed with the paper.

Numerical Methods

Numerical methods used should be transparent and, where appropriate, supported by references.

Abbreviations

Authors must list all the abbreviations used in the paper at the end of the paper or in a separate table before using them.

Formulas and equations

Authors are advised to submit any mathematical equation using either MathJax, KaTeX, or LaTeX, or in a very high-quality image.

Tables, Figures, and Figure Legends

Tables: Tables should be cautiously designed, uncrowned, and include only essential data. Each must have an Arabic number, e.g., Table 4, a self-explanatory caption, and be on a separate sheet. Authors must submit tables in an editable format and not as images. References to these tables (if any) must be mentioned accurately.



Figures

Figures are supposed to be submitted as separate files. Always include a citation in the text for each figure using Arabic numbers, e.g., Fig. 4. Artwork must be submitted online in vector electronic form or by emailing it.

PREPARATION OF ELETRONIC FIGURES FOR PUBLICATION

Although low-quality images are sufficient for review purposes, print publication requires high-quality images to prevent the final product being blurred or fuzzy. Submit (possibly by e-mail) EPS (line art) or TIFF (halftone/ photographs) files only. MS PowerPoint and Word Graphics are unsuitable for printed pictures. Avoid using pixel-oriented software. Scans (TIFF only) should have a resolution of at least 350 dpi (halftone) or 700 to 1100 dpi (line drawings). Please give the data for figures in black and white or submit a Color Work Agreement form. EPS files must be saved with fonts embedded (and with a TIFF preview, if possible).

For scanned images, the scanning resolution at final image size ought to be as follows to ensure good reproduction: line art: >650 dpi; halftones (including gel photographs): >350 dpi; figures containing both halftone and line images: >650 dpi.

Color charges: Authors are advised to pay the full cost for the reproduction of their color artwork. Hence, please note that if there is color artwork in your manuscript when it is accepted for publication, we would require you to complete and return a Color Work Agreement form before your paper can be published. Also, you can email your editor to remove the color fee after acceptance of the paper.

TIPS FOR WRITING A GOOD QUALITY ENGINEERING RESEARCH PAPER

Techniques for writing a good quality engineering research paper:

1. Choosing the topic: In most cases, the topic is selected by the interests of the author, but it can also be suggested by the guides. You can have several topics, and then judge which you are most comfortable with. This may be done by asking several questions of yourself, like "Will I be able to carry out a search in this area? Will I find all necessary resources to accomplish the search? Will I be able to find all information in this field area?" If the answer to this type of question is "yes," then you ought to choose that topic. In most cases, you may have to conduct surveys and visit several places. Also, you might have to do a lot of work to find all the rises and falls of the various data on that subject. Sometimes, detailed information plays a vital role, instead of short information. Evaluators are human: The first thing to remember is that evaluators are also human beings. They are not only meant for rejecting a paper. They are here to evaluate your paper. So present your best aspect.

2. Think like evaluators: If you are in confusion or getting demotivated because your paper may not be accepted by the evaluators, then think, and try to evaluate your paper like an evaluator. Try to understand what an evaluator wants in your research paper, and you will automatically have your answer. Make blueprints of paper: The outline is the plan or framework that will help you to arrange your thoughts. It will make your paper logical. But remember that all points of your outline must be related to the topic you have chosen.

3. Ask your guides: If you are having any difficulty with your research, then do not hesitate to share your difficulty with your guide (if you have one). They will surely help you out and resolve your doubts. If you can't clarify what exactly you require for your work, then ask your supervisor to help you with an alternative. He or she might also provide you with a list of essential readings.

4. Use of computer is recommended: As you are doing research in the field of research engineering then this point is quite obvious. Use right software: Always use good quality software packages. If you are not capable of judging good software, then you can lose the quality of your paper unknowingly. There are various programs available to help you which you can get through the internet.

5. Use the internet for help: An excellent start for your paper is using Google. It is a wondrous search engine, where you can have your doubts resolved. You may also read some answers for the frequent question of how to write your research paper or find a model research paper. You can download books from the internet. If you have all the required books, place importance on reading, selecting, and analyzing the specified information. Then sketch out your research paper. Use big pictures: You may use encyclopedias like Wikipedia to get pictures with the best resolution. At Global Journals, you should strictly follow [here](#).



6. Bookmarks are useful: When you read any book or magazine, you generally use bookmarks, right? It is a good habit which helps to not lose your continuity. You should always use bookmarks while searching on the internet also, which will make your search easier.

7. Revise what you wrote: When you write anything, always read it, summarize it, and then finalize it.

8. Make every effort: Make every effort to mention what you are going to write in your paper. That means always have a good start. Try to mention everything in the introduction—what is the need for a particular research paper. Polish your work with good writing skills and always give an evaluator what he wants. Make backups: When you are going to do any important thing like making a research paper, you should always have backup copies of it either on your computer or on paper. This protects you from losing any portion of your important data.

9. Produce good diagrams of your own: Always try to include good charts or diagrams in your paper to improve quality. Using several unnecessary diagrams will degrade the quality of your paper by creating a hodgepodge. So always try to include diagrams which were made by you to improve the readability of your paper. Use of direct quotes: When you do research relevant to literature, history, or current affairs, then use of quotes becomes essential, but if the study is relevant to science, use of quotes is not preferable.

10. Use proper verb tense: Use proper verb tenses in your paper. Use past tense to present those events that have happened. Use present tense to indicate events that are going on. Use future tense to indicate events that will happen in the future. Use of wrong tenses will confuse the evaluator. Avoid sentences that are incomplete.

11. Pick a good study spot: Always try to pick a spot for your research which is quiet. Not every spot is good for studying.

12. Know what you know: Always try to know what you know by making objectives, otherwise you will be confused and unable to achieve your target.

13. Use good grammar: Always use good grammar and words that will have a positive impact on the evaluator; use of good vocabulary does not mean using tough words which the evaluator has to find in a dictionary. Do not fragment sentences. Eliminate one-word sentences. Do not ever use a big word when a smaller one would suffice.

Verbs have to be in agreement with their subjects. In a research paper, do not start sentences with conjunctions or finish them with prepositions. When writing formally, it is advisable to never split an infinitive because someone will (wrongly) complain. Avoid clichés like a disease. Always shun irritating alliteration. Use language which is simple and straightforward. Put together a neat summary.

14. Arrangement of information: Each section of the main body should start with an opening sentence, and there should be a changeover at the end of the section. Give only valid and powerful arguments for your topic. You may also maintain your arguments with records.

15. Never start at the last minute: Always allow enough time for research work. Leaving everything to the last minute will degrade your paper and spoil your work.

16. Multitasking in research is not good: Doing several things at the same time is a bad habit in the case of research activity. Research is an area where everything has a particular time slot. Divide your research work into parts, and do a particular part in a particular time slot.

17. Never copy others' work: Never copy others' work and give it your name because if the evaluator has seen it anywhere, you will be in trouble. Take proper rest and food: No matter how many hours you spend on your research activity, if you are not taking care of your health, then all your efforts will have been in vain. For quality research, take proper rest and food.

18. Go to seminars: Attend seminars if the topic is relevant to your research area. Utilize all your resources.

19. Refresh your mind after intervals: Try to give your mind a rest by listening to soft music or sleeping in intervals. This will also improve your memory. Acquire colleagues: Always try to acquire colleagues. No matter how sharp you are, if you acquire colleagues, they can give you ideas which will be helpful to your research.

20. Think technically: Always think technically. If anything happens, search for its reasons, benefits, and demerits. Think and then print: When you go to print your paper, check that tables are not split, headings are not detached from their descriptions, and page sequence is maintained.



21. Adding unnecessary information: Do not add unnecessary information like "I have used MS Excel to draw graphs." Irrelevant and inappropriate material is superfluous. Foreign terminology and phrases are not apropos. One should never take a broad view. Analogy is like feathers on a snake. Use words properly, regardless of how others use them. Remove quotations. Puns are for kids, not grunt readers. Never oversimplify: When adding material to your research paper, never go for oversimplification; this will definitely irritate the evaluator. Be specific. Never use rhythmic redundancies. Contractions shouldn't be used in a research paper. Comparisons are as terrible as clichés. Give up ampersands, abbreviations, and so on. Remove commas that are not necessary. Parenthetical words should be between brackets or commas. Understatement is always the best way to put forward earth-shaking thoughts. Give a detailed literary review.

22. Report concluded results: Use concluded results. From raw data, filter the results, and then conclude your studies based on measurements and observations taken. An appropriate number of decimal places should be used. Parenthetical remarks are prohibited here. Proofread carefully at the final stage. At the end, give an outline to your arguments. Spot perspectives of further study of the subject. Justify your conclusion at the bottom sufficiently, which will probably include examples.

23. Upon conclusion: Once you have concluded your research, the next most important step is to present your findings. Presentation is extremely important as it is the definite medium through which your research is going to be in print for the rest of the crowd. Care should be taken to categorize your thoughts well and present them in a logical and neat manner. A good quality research paper format is essential because it serves to highlight your research paper and bring to light all necessary aspects of your research.

INFORMAL GUIDELINES OF RESEARCH PAPER WRITING

Key points to remember:

- Submit all work in its final form.
- Write your paper in the form which is presented in the guidelines using the template.
- Please note the criteria peer reviewers will use for grading the final paper.

Final points:

One purpose of organizing a research paper is to let people interpret your efforts selectively. The journal requires the following sections, submitted in the order listed, with each section starting on a new page:

The introduction: This will be compiled from reference matter and reflect the design processes or outline of basis that directed you to make a study. As you carry out the process of study, the method and process section will be constructed like that. The results segment will show related statistics in nearly sequential order and direct reviewers to similar intellectual paths throughout the data that you gathered to carry out your study.

The discussion section:

This will provide understanding of the data and projections as to the implications of the results. The use of good quality references throughout the paper will give the effort trustworthiness by representing an alertness to prior workings.

Writing a research paper is not an easy job, no matter how trouble-free the actual research or concept. Practice, excellent preparation, and controlled record-keeping are the only means to make straightforward progression.

General style:

Specific editorial column necessities for compliance of a manuscript will always take over from directions in these general guidelines.

To make a paper clear: Adhere to recommended page limits.

Mistakes to avoid:

- Insertion of a title at the foot of a page with subsequent text on the next page.
- Separating a table, chart, or figure—confine each to a single page.
- Submitting a manuscript with pages out of sequence.
- In every section of your document, use standard writing style, including articles ("a" and "the").
- Keep paying attention to the topic of the paper.



- Use paragraphs to split each significant point (excluding the abstract).
- Align the primary line of each section.
- Present your points in sound order.
- Use present tense to report well-accepted matters.
- Use past tense to describe specific results.
- Do not use familiar wording; don't address the reviewer directly. Don't use slang or superlatives.
- Avoid use of extra pictures—include only those figures essential to presenting results.

Title page:

Choose a revealing title. It should be short and include the name(s) and address(es) of all authors. It should not have acronyms or abbreviations or exceed two printed lines.

Abstract: This summary should be two hundred words or less. It should clearly and briefly explain the key findings reported in the manuscript and must have precise statistics. It should not have acronyms or abbreviations. It should be logical in itself. Do not cite references at this point.

An abstract is a brief, distinct paragraph summary of finished work or work in development. In a minute or less, a reviewer can be taught the foundation behind the study, common approaches to the problem, relevant results, and significant conclusions or new questions.

Write your summary when your paper is completed because how can you write the summary of anything which is not yet written? Wealth of terminology is very essential in abstract. Use comprehensive sentences, and do not sacrifice readability for brevity; you can maintain it succinctly by phrasing sentences so that they provide more than a lone rationale. The author can at this moment go straight to shortening the outcome. Sum up the study with the subsequent elements in any summary. Try to limit the initial two items to no more than one line each.

Reason for writing the article—theory, overall issue, purpose.

- Fundamental goal.
- To-the-point depiction of the research.
- Consequences, including definite statistics—if the consequences are quantitative in nature, account for this; results of any numerical analysis should be reported. Significant conclusions or questions that emerge from the research.

Approach:

- Single section and succinct.
- An outline of the job done is always written in past tense.
- Concentrate on shortening results—limit background information to a verdict or two.
- Exact spelling, clarity of sentences and phrases, and appropriate reporting of quantities (proper units, important statistics) are just as significant in an abstract as they are anywhere else.

Introduction:

The introduction should "introduce" the manuscript. The reviewer should be presented with sufficient background information to be capable of comprehending and calculating the purpose of your study without having to refer to other works. The basis for the study should be offered. Give the most important references, but avoid making a comprehensive appraisal of the topic. Describe the problem visibly. If the problem is not acknowledged in a logical, reasonable way, the reviewer will give no attention to your results. Speak in common terms about techniques used to explain the problem, if needed, but do not present any particulars about the protocols here.

The following approach can create a valuable beginning:

- Explain the value (significance) of the study.
- Defend the model—why did you employ this particular system or method? What is its compensation? Remark upon its appropriateness from an abstract point of view as well as pointing out sensible reasons for using it.
- Present a justification. State your particular theory(-ies) or aim(s), and describe the logic that led you to choose them.
- Briefly explain the study's tentative purpose and how it meets the declared objectives.



Approach:

Use past tense except for when referring to recognized facts. After all, the manuscript will be submitted after the entire job is done. Sort out your thoughts; manufacture one key point for every section. If you make the four points listed above, you will need at least four paragraphs. Present surrounding information only when it is necessary to support a situation. The reviewer does not desire to read everything you know about a topic. Shape the theory specifically—do not take a broad view.

As always, give awareness to spelling, simplicity, and correctness of sentences and phrases.

Procedures (methods and materials):

This part is supposed to be the easiest to carve if you have good skills. A soundly written procedures segment allows a capable scientist to replicate your results. Present precise information about your supplies. The suppliers and clarity of reagents can be helpful bits of information. Present methods in sequential order, but linked methodologies can be grouped as a segment. Be concise when relating the protocols. Attempt to give the least amount of information that would permit another capable scientist to replicate your outcome, but be cautious that vital information is integrated. The use of subheadings is suggested and ought to be synchronized with the results section.

When a technique is used that has been well-described in another section, mention the specific item describing the way, but draw the basic principle while stating the situation. The purpose is to show all particular resources and broad procedures so that another person may use some or all of the methods in one more study or referee the scientific value of your work. It is not to be a step-by-step report of the whole thing you did, nor is a methods section a set of orders.

Materials:

Materials may be reported in part of a section or else they may be recognized along with your measures.

Methods:

- Report the method and not the particulars of each process that engaged the same methodology.
- Describe the method entirely.
- To be succinct, present methods under headings dedicated to specific dealings or groups of measures.
- Simplify—detail how procedures were completed, not how they were performed on a particular day.
- If well-known procedures were used, account for the procedure by name, possibly with a reference, and that's all.

Approach:

It is embarrassing to use vigorous voice when documenting methods without using first person, which would focus the reviewer's interest on the researcher rather than the job. As a result, when writing up the methods, most authors use third person passive voice.

Use standard style in this and every other part of the paper—avoid familiar lists, and use full sentences.

What to keep away from:

- Resources and methods are not a set of information.
- Skip all descriptive information and surroundings—save it for the argument.
- Leave out information that is immaterial to a third party.

Results:

The principle of a results segment is to present and demonstrate your conclusion. Create this part as entirely objective details of the outcome, and save all understanding for the discussion.

The page length of this segment is set by the sum and types of data to be reported. Use statistics and tables, if suitable, to present consequences most efficiently.

You must clearly differentiate material which would usually be incorporated in a study editorial from any unprocessed data or additional appendix matter that would not be available. In fact, such matters should not be submitted at all except if requested by the instructor.



Content:

- Sum up your conclusions in text and demonstrate them, if suitable, with figures and tables.
- In the manuscript, explain each of your consequences, and point the reader to remarks that are most appropriate.
- Present a background, such as by describing the question that was addressed by creation of an exacting study.
- Explain results of control experiments and give remarks that are not accessible in a prescribed figure or table, if appropriate.
- Examine your data, then prepare the analyzed (transformed) data in the form of a figure (graph), table, or manuscript.

What to stay away from:

- Do not discuss or infer your outcome, report surrounding information, or try to explain anything.
- Do not include raw data or intermediate calculations in a research manuscript.
- Do not present similar data more than once.
- A manuscript should complement any figures or tables, not duplicate information.
- Never confuse figures with tables—there is a difference.

Approach:

As always, use past tense when you submit your results, and put the whole thing in a reasonable order.

Put figures and tables, appropriately numbered, in order at the end of the report.

If you desire, you may place your figures and tables properly within the text of your results section.

Figures and tables:

If you put figures and tables at the end of some details, make certain that they are visibly distinguished from any attached appendix materials, such as raw facts. Whatever the position, each table must be titled, numbered one after the other, and include a heading. All figures and tables must be divided from the text.

Discussion:

The discussion is expected to be the trickiest segment to write. A lot of papers submitted to the journal are discarded based on problems with the discussion. There is no rule for how long an argument should be.

Position your understanding of the outcome visibly to lead the reviewer through your conclusions, and then finish the paper with a summing up of the implications of the study. The purpose here is to offer an understanding of your results and support all of your conclusions, using facts from your research and generally accepted information, if suitable. The implication of results should be fully described.

Infer your data in the conversation in suitable depth. This means that when you clarify an observable fact, you must explain mechanisms that may account for the observation. If your results vary from your prospect, make clear why that may have happened. If your results agree, then explain the theory that the proof supported. It is never suitable to just state that the data approved the prospect, and let it drop at that. Make a decision as to whether each premise is supported or discarded or if you cannot make a conclusion with assurance. Do not just dismiss a study or part of a study as "uncertain."

Research papers are not acknowledged if the work is imperfect. Draw what conclusions you can based upon the results that you have, and take care of the study as a finished work.

- You may propose future guidelines, such as how an experiment might be personalized to accomplish a new idea.
- Give details of all of your remarks as much as possible, focusing on mechanisms.
- Make a decision as to whether the tentative design sufficiently addressed the theory and whether or not it was correctly restricted. Try to present substitute explanations if they are sensible alternatives.
- One piece of research will not counter an overall question, so maintain the large picture in mind. Where do you go next? The best studies unlock new avenues of study. What questions remain?
- Recommendations for detailed papers will offer supplementary suggestions.



Approach:

When you refer to information, differentiate data generated by your own studies from other available information. Present work done by specific persons (including you) in past tense.

Describe generally acknowledged facts and main beliefs in present tense.

THE ADMINISTRATION RULES

Administration Rules to Be Strictly Followed before Submitting Your Research Paper to Global Journals Inc.

Please read the following rules and regulations carefully before submitting your research paper to Global Journals Inc. to avoid rejection.

Segment draft and final research paper: You have to strictly follow the template of a research paper, failing which your paper may get rejected. You are expected to write each part of the paper wholly on your own. The peer reviewers need to identify your own perspective of the concepts in your own terms. Please do not extract straight from any other source, and do not rephrase someone else's analysis. Do not allow anyone else to proofread your manuscript.

Written material: You may discuss this with your guides and key sources. Do not copy anyone else's paper, even if this is only imitation, otherwise it will be rejected on the grounds of plagiarism, which is illegal. Various methods to avoid plagiarism are strictly applied by us to every paper, and, if found guilty, you may be blacklisted, which could affect your career adversely. To guard yourself and others from possible illegal use, please do not permit anyone to use or even read your paper and file.



CRITERION FOR GRADING A RESEARCH PAPER (COMPILATION)
BY GLOBAL JOURNALS

Please note that following table is only a Grading of "Paper Compilation" and not on "Performed/Stated Research" whose grading solely depends on Individual Assigned Peer Reviewer and Editorial Board Member. These can be available only on request and after decision of Paper. This report will be the property of Global Journals.

Topics	Grades		
	A-B	C-D	E-F
<i>Abstract</i>	Clear and concise with appropriate content, Correct format. 200 words or below	Unclear summary and no specific data, Incorrect form Above 200 words	No specific data with ambiguous information Above 250 words
<i>Introduction</i>	Containing all background details with clear goal and appropriate details, flow specification, no grammar and spelling mistake, well organized sentence and paragraph, reference cited	Unclear and confusing data, appropriate format, grammar and spelling errors with unorganized matter	Out of place depth and content, hazy format
<i>Methods and Procedures</i>	Clear and to the point with well arranged paragraph, precision and accuracy of facts and figures, well organized subheads	Difficult to comprehend with embarrassed text, too much explanation but completed	Incorrect and unorganized structure with hazy meaning
<i>Result</i>	Well organized, Clear and specific, Correct units with precision, correct data, well structuring of paragraph, no grammar and spelling mistake	Complete and embarrassed text, difficult to comprehend	Irregular format with wrong facts and figures
<i>Discussion</i>	Well organized, meaningful specification, sound conclusion, logical and concise explanation, highly structured paragraph reference cited	Wordy, unclear conclusion, spurious	Conclusion is not cited, unorganized, difficult to comprehend
<i>References</i>	Complete and correct format, well organized	Beside the point, Incomplete	Wrong format and structuring



INDEX

A

Accomplished · 48, 49
Aeronautical · 7, 16

E

Elettrotekkabel · 5

M

Mandalay · 68, 70, 77, 85

N

Nandgaonkar · 45

P

Polycrystalline · 72
Polynomials · 9

S

Stipulate · 4

T

Tomasovic · 30

V

Vulnerable · 20, 58, 63

W

Waveguide · 47, 49

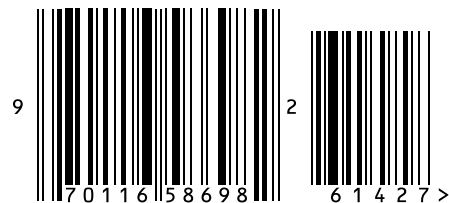


save our planet



Global Journal of Researches in Engineering

Visit us on the Web at www.GlobalJournals.org | www.EngineeringResearch.org
or email us at helpdesk@globaljournals.org



ISSN 9755861

© Global Journals